A Cost Model for the Manufacture of Bipolar Plates using Micro Milling

Erich C. Essmann

Thesis presented in partial fulfilment of the requirements for the degree of Masters of Industrial Engineering at Stellenbosch University.

Study leader: Mr Theuns Dirkse van Schalkwyk

March 201H

Declaration

I, the undersigned, hereby declare that the work contained in this thesis is my own original work and that I have not previously in its entirety or in part submitted it at any university for a degree.

……………………….. ……………………

Erich C. Essmann Date

Synopsis

In a move towards cleaner and more sustainable energy systems, hydrogen as an energy carrier and hydrogen fuel cells as energy converters are receiving increasing global attention. Considering the vital role that platinum plays in the operation of hydrogen fuels cells, South Africa stands to gain enormously as the world's leading platinum group metals supplier. Therefore, in order to benefit across the whole value chain, it is imperative to develop the capability to manufacture hydrogen fuel cell stacks locally.

This project addresses this imperative, in part, by building a framework to evaluate the manufacturing performance of one of the more costly components of the hydrogen fuel cell stack. More specifically, this project builds a cost evaluation model (or cost model) for the manufacture of bipolar plates using micro milling. In essence, the model characterises manufacturing cost (and time) as a function of relevant inputs.

The model endeavours to be flexible in accommodating relevant contributing cost drivers such as tool life and manufacturing time. Moreover, the model lays the groundwork, from a micro milling perspective, for a comparison of different manufacturing methods for bipolar plates.

The approach taken in building the cost model is a fundamental one, owing to the lack of historical cost data for this particular process. As such, manufacturing knowledge and experimentation are used to build the cost model in a structured way.

The process followed in building the cost model begins with the formulation of the cost components by reviewing relevant examples from literature. Thereafter, two main cost drivers are comprehensively addressed. Tool life is characterised experimentally as a function of cutting parameters and manufacturing time is characterised as a function of relevant inputs. The work is then synthesized into a coherent cost model.

Following the completion of the cost model, analysis is done to find the near-optimal combination of machine cutting parameters. Further, analysis is done to quantify the sensitivity of manufacturing cost to design changes and production volumes. This attempts to demonstrate how typical managerial issues can be addressed using the cost model format.

The value of this work must be seen in terms of its practical contribution. That is, its contribution to the development of the capability to manufacture hydrogen fuel cells locally. By understanding the effect of relevant input factors on manufacturing cost, 'upstream' design and development activities can be integrated with 'downstream' manufacturing activities. Therefore, this project supports the development of manufacturing capability by providing a mechanism to control cost throughout the process.

Opsomming

In die soeke na skoner, meer volhoubare energie bronne word die fokus op waterstof, as energie draer, en waterstof brandstofselle, as energie omskakelaars, al meer verskerp. Deur die sleutelrol van platinum in die werking van waterstof brandstofselle in ag te neem, word Suid-Afrika, as die wêreld se grootste platinum verskaffer, in `n uitstekende posisie geplaas om voordeel te trek uit hierdie geleentheid. Om dus as land voordeel te trek uit die proses in geheel, is dit van kardinale belang om die vermoë te ontwikkel om waterstof brandstofsel stapels op eie bodem te vervaardig.

Hierdie projek adresseer gedeeltelik hierdie noodsaaklikheid, deur `n raamwerk te bou wat die vervaardigingsoptrede van een van die meer duursame komponente van die waterstof brandstofsel stapel evalueer. Meer spesifiek, bou hierdie projek `n koste evaluerings model (of koste model) vir die vervaardiging van bipolêre plate deur die gebruik van mikro-masjienering. In wese kenmerk hierdie model vervaardigings kostes (en tyd) as `n funksie van relevante insette.

Hierdie model poog om buigsaam te wees met die in ag neming van relevante bydraende kostedrywers soos buitelleeftyd en vervaardigingstyd. Daarbenewens lê hierdie model die grondwerk, vanuit `n mikro masjienerings oogpunt, vir die vergelyking van verskillende vervaardingings metodes vir bipolêre plate.

Die benadering wat gevolg word in die bou van die koste model is fundamenteel as gevolg van die gebrek van historiese data vir hierdie spesifieke proses. As sodanig word vervaardigings kennis en eksperimentering gebruik om die koste model in `n gestruktueerde wyse te bou.

Die proses gevolg in die bou van die koste model begin met die formulering van die koste komponente deur die hersiening van relevante voorbeelde vanuit die literatuur. Daarna word twee hoof koste drywers deeglik geadresseer. Buitelleeftyd word ekperimenteel gekenmerk as funksie van masjieneringsparameters en vervaardigingstyd word gekenmerk as `n funksie van relevante insette. Die werk word dan gesintetiseer in `n samehangende koste model.

Wat volg op die voltooiing van die koste model is `n analise om die optimale kombinasie masjieneringsparameters te vind. Daaropvolgens word analises gedoen om die sensitiwiteit van vervaardigingskoste onderworpe aan ontwerpsveranderings en produksie volumes te kwantisfiseer. Dit poog om te demostreer hoe tipiese bestuursprobleem geadresseer kan word deur die koste model formaat te gebruik.

Die waarde van hierdie werk moet in die lig van die praktiese bydrae daarvan gesien word, menende, die bydrae tot die ontwikkeling van die vermoë om waterstof brandstofselle in Suid-Afrika te vervaardig. Deur die effek van relevante inset faktore op vervaardigingskoste te verstaan, kan ‘stroom-op’ ontwerp en ontwikkelings aktiwiteite geïntegreer word met ‘stroom-af’ vervaardigings

aktiwiteite. Dus, hierdie projek ondersteun die ontwikkeling van vervaardigingsvermoëns deur `n meganisme te voorsien om kostes oor die omvang van die proses te beheer.

Acknowledgements

First and foremost, I would like to thank Mr. Theuns Dirkse van Schalkwyk, for his continued guidance, enthusiasm and technical assistance throughout this work.

I would like to thank Mrs. Tanya Lane-Visser for her technical assistance in part of this work.

I would like to thank Prof. Anton Basson and Mr. Juan Atkinson for their contribution to this work and the opportunity to tackle this project.

I would like to thank Miss Alexa van Butzelaar for her patience and support throughout this project, as well as my family and friends for their encouragement.

Finally, I would like to give a special thanks to my late father, whose love and encouragement still endure today.

Table of Contents

LIST OF FIGURES

LIST OF TABLES

Glossary

Bipolar Plate	A conductive plate that allows fuel cells to be connected in series to form 'stacks'.
Combined Heat and Power	The use of hydrogen fuel cell stacks (in this case) to simultaneously generate both heat and electricity.
Cost Model	An arrangement of data, assumptions and equations that allow the translation of physical resources and characteristics into cost.
Cutting Parameters	Parameters that fully characterise the mechanics of the material removal process. These include cutting speed, feed per tooth and axial depth of cut.
Cutting Speed	In this case 'cutting speed' refers to the velocity of the cutting edge relative to the stationary equipment, not the workpiece.
Depth of Cut	Also known as 'axial depth of cut,' this is the linear distance that an end mill penetrates the workpiece measured from the tip of the shaft.
Design of Experiments	The design of controlled, information gathering experiments.
Feed Per Tooth	The distance that the cutting edge penetrates the workpiece per tooth pass. Also known as the uncut chip thickness.
Hydrogen Economy	A proposed method of energy delivery via hydrogen.
Hydrogen Fuel Cells	An energy conversion devise for converting the chemical energy from hydrogen into electrical energy through a chemical reaction with oxygen. Hydrogen fuel cells are typically grouped to form 'stacks'.
Micro Milling	The milling of components with two of more feature dimensions in the sub-millimetre range.

Nomenclature

a	Rate of cooling in the simulated annealing process
α	The axial distance from the centre in the Central Composite Design
ACR	The annual capital recovery *(R/year)*
AP	The total annual production *(plates/year)*
AP_{mach}	The annual production per machine per year *(plates/machine-year)*
b	Number of teeth/flutes on an end mill
C	Empirically determined constant from Taylor's tool life model
$C_{CM\ major}$	The cost associated with manufacturing the major micro channels *(R/plate)*
$C_{Equipment}$	The cost contribution per plate towards repaying the initial equipment cost *(R/plate)*
C_{Import}	The cost per plate to import *(R/plate)*
CL	Cutting length *(mm/tool)*
C_{Labour}	Labour cost per plate *(R/plate)*
$C_{MajorTool}$	The cost per tool used to machine the major micro channels *(R/tool)*
$C_{MajorTooling}$	The cost of all tools used to machine the major micro channels *(R/plate)*
$C_{Material}$	Material cost per plate *(R/plate)*
$C_{MinorTool}$	The cost per tool used to machine the minor micro channels *(R/tool)*
$C_{MinorTooling}$	The cost of all tools used to machine the minor micro channels *(R/plate)*
$C_{Overheads}$	The cost contribution per plate towards repaying the annual overheads *(R/plate)*. This excludes the initial cost of equipment.
$C_{PeripheralTool}$	The cost per tool used to machine the outline and peripheral features *(R/tool)*
$C_{PeripheralTooling}$	The cost of all tools used to machine the outline and peripheral features *(R/plate)*
C_{plate}	The basic cost per plate as priced by 'Schunk' *(R/plate)*
CT	Cutting Time *(min/tool)*
$C_{Tooling}$	Total tooling cost per plate *(R/plate)*. This includes the cost of tools used to machine major micro channels, minor micro channels, outline and peripheral features
C_{Unit}	Total manufacturing cost per plate *(R/plate)*
d	Axial depth of cut *(mm)*
D	Tool diameter *(mm)*
D^*	The tool diameter for diameters other than *0.7mm (mm)*
D_{major}	The diameter of the tool used to machine the major micro channels *(mm)*

d_{major}	The depth of cut used to machine the major micro channels *(mm)* (This is also the depth the channels)
D_{minor}	The diameter of the tool used to machine the minor micro channels *(mm)*
d_{minor}	The depth of cut used to machine the minor micro channels *(mm)* (This is also the depth the channels)
$D_{peripherals}$	The diameter of the tool used to machine the outline and peripheral features *(mm)*
F	Number of 2-level full factorial points in the Central Composite Experimental Design
F_R	Feed rate *(mm/min)*
$F_{R\ Max}$	The maximum feed rate achievable by the machine *(mm/min)*
$F_{R\ Max\_X\ Axis}$	Maximum achievable feed rate *(mm/min)* in the X axis direction
$F_{R\ Max\_Y\ Axis}$	Maximum achievable feed rate *(mm/min)* in the Y axis direction
$F_{R\ Peripheral}$	The feed rate used to machine the outline and peripheral features *(mm/min)*
f_t	Feed per tooth *(µm)*
$f_{t\ major}$	The feed per tooth used to machine the major micro channels *(µm)*
$f_{t\ minor}$	The feed per tooth used to machine the minor micro channels *(µm)*
$f_{t\ peripheral}$	The feed per tooth used to machine the peripheral features and outline *(µm)*
i	The effective annual interest rate of the loan for the equipment purchase *(%)*
IV	The initial value of equipment *(R)*
k	Iteration counter in the simulated annealing algorithm
k_e	Number of experimental factors
k_{lim}	The maximum number of iterations in the simulated annealing process
L_{ch}	The average length of channels *(mm)*
$L_{ch\ major}$	The average length of major micro channels *(min)*
$L_{ch\ minor}$	The average length of minor micro channels *(min)*
L_F	Length of one side of the flow field area *(mm)*
$L_{outline}$	The length of the plate outline *(mm)*
$L_{peripheral}$	The effective cutting length of the peripheral features *(mm)*
LR	The hourly rate per machine operator *(R/hour)*
L_T	Tool life *(mm^3/tool)*
$L_{T\ Peripheral}$	The tool life of tools used to machine the outline and peripheral features *(min/tool)*
$L_{T\ taylor}$	Tool life according to Taylor's tool life model *(min/tool)*
L_T*	Tool life adjusted for diameters other than *0.7mm (mm^3)*
n	Rotational velocity *(rev/min)*

N	Number of plates machined at a time
n_c	Number of centre runs in the Central Composite Experimental Design
N_{ch}	The number of channels
$N_{ch\ major}$	The number of major micro channels
$N_{ch\ minor}$	The number of minor micro channels
N_{mach}	The number of machines
$N_{mach/worker}$	The number of machines operated per worker at a time
n_{Max}	The maximum rotational velocity achievable by the machine *(rev/min)*
n_T	Empirically determined constant from Taylor's tool life model
n_{years}	The expected number of years of operation of the equipment or program
P	The probability of accepting a 'worse' solution over a 'better' solution in the simulated annealing process
Rd	The maximum half range noise in the simulated annealing process
S	Scenario for machining procedure
SV	The salvage value of the equipment of n_{years} *(R)*
t	Variable controlling the maximum half-range noise in the tweaking process as it forms part of the simulated annealing process
T_0	Variable storing the initial 'temperature' in the simulated annealing process
T_{CM}	Time to machine channels *(min/plate)*. This does not refer to any specific type of channel but rather the generic equation
$T_{CM\ major}$	Time associated with machining the major micro channels *(min/plate)*
$T_{CM\ minor}$	Time associated with machining the minor micro channels *(min/plate)*
$T_{PM\ outline}$	Time associated with machining the plate outline *(min/plate)*
$T_{PM\ peripheral\ features}$	Time associated with machining the plate peripheral features *(min/plate)*
T_{fix}	Time to fix the blank plate to the worktable *(min/plate)*. This is a function of the number of plates at a time (N)
T_{flip}	Time to flip the blank plate on the worktable (min/plate). This is a function of the number of plates at a time (N)
T_{ins}	Time to inspect a machined plate for quality purposes *(min/plate)*
T_k	Variable storing the current 'temperature' in the simulated annealing process
T_M	The total machining time for one plate *(min/plate)*. This specifically refers to time spent machining only.
T_O	The total annual overheads other than the initial cost of equipment *(R/year)*
T_p	The total manufacturing time per plate *(min/plate)*

T_{PM}	The time to machine the periphery *(min)* (This can refer to either the peripheral features or the outline depending on the context)
T_{refxyz}	Time to reference the tool to the workpiece for the x, y and z-axes *(min)*
T_{remove}	Time to remove the machined plate from the worktable *(min/plate)*. This is a function of the number of plates at a time *(N)*
T_S	Setup Time per plate *(min/plate)*
T_{sp}	Time to set the machine parameters, namely feed rate, rotational velocity and depth of cut *(min)*
T_{tc}	Time to change the tool *(min)*
u	Machine utilisation *(%)*
u_{max}	Maximum machine utilisation *(%)*
v	Cutting speed *(m/min)*
v_{major}	The cutting speed use to machine the major micro channels *(m/min)*
v_{minor}	The cutting speed use to machine the minor micro channels *(m/min)*
VMR	Volume of material removed *(mm^3/tool)*
$v_{peripheral}$	The cutting speed use to machine the outline and peripheral features *(m/min)*
W_L	Width of the land gap *(mm)* - width between channels
wp	The width of the plate *(mm)*
x	Variable to control 'T_k' in the simulated annealing process
Z	The number of tools used per plate *(tools/plate)*
Z_{Major}	The number of tools per plate used to machine the major micro channels *(tools/plate)*
Z_{Minor}	The number of tools per plate used to machine the minor micro channels *(tools/plate)*
$Z_{Peripheral}$	The number of tools per plate used to machine the outline and peripheral features *(tools/plate)*

1. Introduction

The term 'hydrogen economy' denotes a proposed system of energy delivery via hydrogen. Hydrogen shows much potential as a fuel for motive power, energy requirements for buildings and the like, despite the fact that it does not occur abundantly in nature. It is, therefore, intended to be used as an energy carrier (like electricity) rather than as a primary source of energy (like fossil fuels). Proponents of a hydrogen economy argue that this would remedy some of the negative effects of using hydrocarbon fuels, where carbon dioxide and other pollutants are released at the point of use.

HySA (2009), state that the use of hydrogen as an energy carrier combined with fuel cell technology shows much promise as a sustainable energy system for the production of electricity. Therefore, following the global trend for cleaner and more sustainable energy systems, hydrogen fuel cell technology is enjoying increasing research interest, both locally and abroad.

Local (South African) interest in hydrogen fuel cell research is driven by this country's strategically advantageous position in the budding hydrogen economy. Hydrogen and other fuel cells use platinum as a catalyst to promote the chemical reactions at work. Without platinum, the reactions would be severely inhibited and the usefulness of hydrogen fuel cell technology effectively negated. This fact makes platinum, and the availability thereof, a key driver in the development of this technology.

Platinum is a rare mineral with known reserves in only five countries in the world. Of these five countries, South Africa is the leading supplier, having approximately 80% of the world's known platinum reserves. This effectively places South Africa in the driver's seat of the global move towards a hydrogen economy by being able to control the supply of platinum.

In order to fully capitalise on this advantageous position, South Africa needs to be able to control, or partly control, the complete hydrogen fuel cell value chain. This not only includes the supply of raw materials, but also the manufacturing of the hydrogen fuel cell stacks themselves. Therefore, the development of the capability to manufacture hydrogen fuel cell stacks has been identified as a strategic objective for South Africa by the Department of Science and Technology (DST). This objective is encapsulated by the National Hydrogen and Fuel Cells Technologies Research, Development and Innovation Strategy.

The cost to manufacture a fuel cell stack is largely comprised of the cost to manufacture the bipolar plates contained within that stack. This is because bipolar plates account for most of the mass and volume in a stack. Therefore, the question of how to manufacture fuel cell stacks cost effectively is largely addressed by the ability to manufacture bipolar plates cost effectively.

As part of the development of the capability to manufacture hydrogen fuel cell stacks locally, the correct manufacturing method for bipolar plates needs to be selected. Currently, two methods stand out as potentially feasible, each with their own advantages and disadvantages. These methods are compression moulding and micro milling.

At this point, it should be clarified. Bipolar plates cannot be made using micro milling alone, because micro milling is a material removal process. Rather, this scenario involves sourcing the blank plates and machining the plate features locally. These plates would be sourced from Schunk Kohlenstofftechnik GmbH in Heuchelheim, Germany. This is because the material supplied by Schunk shows the right combination of chemical and physical properties for the purpose. Further, these blank plates are manufactured by Schunk using compression moulding.

An intuitive question to ask then is, if these blank plates need to be compression moulded by Schunk before the features are machined, would it not be easier simply to compression mould the plates with the features in already? The answer to this is not so simple, however, when considering the following:

- Schunk has already established compression moulding capacity and can make use of economies of scale because they supply worldwide.
- Schunk already has the 'recipe' according to which the plates are made and from which they would naturally be reluctant to part. Compression moulding the complete bipolar plates locally would require the development of this 'recipe'.
- There are some complications that arise when compression moulding bipolar plate features. These complications are born from the small size of the features.
- Finally, compression moulding the complete bipolar plate requires the use of a far more complex (and expensive) mould.

Following the argument above, the problem statement can be expressed as follows:

> *The need exists to be able to compare these methods in terms of overall manufacturing performance. More specifically, these methods need to be compared in terms of total manufacturing time and cost. Moreover, the comparison to be made must be dynamic. This means that a number of factors need to be taken into account such as production volumes, design features, etc. Each of these factors, if altered, could potentially change the result of the comparison and, therefore, need to be built into the comparison model.*

This project partly addresses the need, expressed above, to be able to compare manufacturing methods. This is done by considering the manufacturing performance of one method, namely micro milling. More specifically, the purpose of this project is to build a performance evaluation

framework, which allows micro milling to be compared to other manufacturing methods. The purpose of this project can be encapsulated by the following objectives:

- The primary objective is to build a flexible framework to be able to evaluate manufacturing performance (especially cost) for the micro milling of bipolar plates. This framework must accommodate typical cost drivers in micro milling, such as tool life and machining time. In addition, this framework must account for bipolar plate design parameters.
- The secondary objective of this project is to support a comparison of manufacturing methods by performing the necessary analysis from a micro milling perspective.

The approach taken in fulfilling the objectives, stated above, is to build a manufacturing cost model for the micro milling of bipolar plates. A cost model allows manufacturing cost to be evaluated for certain input values. The number and validity of these input parameters goes a long way to characterising the usefulness of a model. The more input variables, the more flexible it is. On the other hand, too many variables can make the model awkward and difficult to use. The approach taken for the purpose of this model is to find a good balance in this regard. This approach is divided into three high level stages, namely the literature review, cost model development and analysis and conclusions. This is represented by **Figure 1** below, which serves to illustrate the outline of the remainder of this document. Each high level stage is made up of relevant sections of this document, as indicated by the figure.

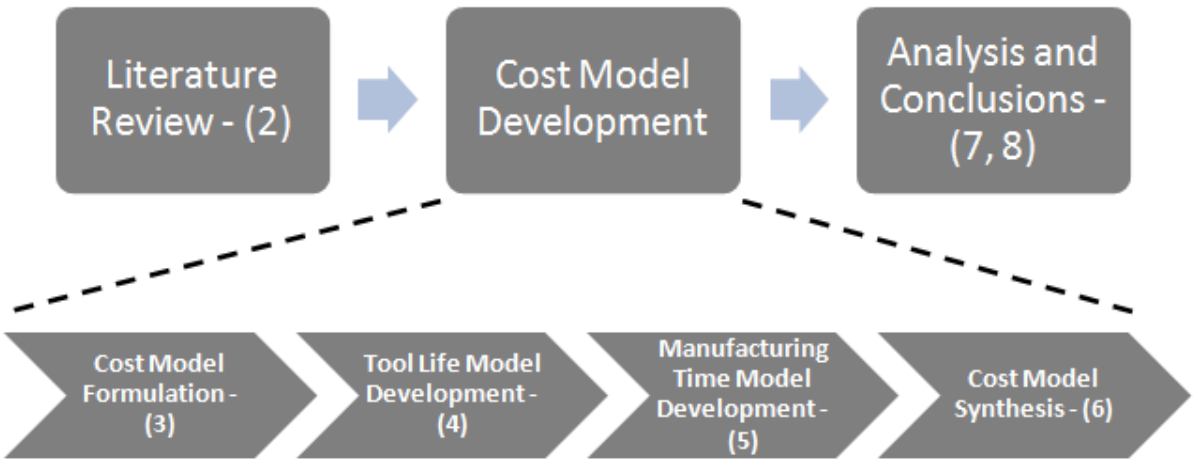

Figure 1 – Document Outline

The first high level stage of this document is encapsulated by **Section 2**, which presents a literature review of the relevant academic and industry related fields of interest. It begins by presenting a general business case for hydrogen fuel cells in South Africa. Thereafter, some general theory of the operation of hydrogen fuel cells is presented. Following this, the concepts surrounding the operation and manufacture of bipolar plates are presented. More specifically, bipolar plate material, design and manufacturing considerations are presented to give the reader an understanding of the

complexity of the bipolar plate paradigm. This section concludes with a discussion of micro milling. Micro milling is introduced in the context of micro manufacturing, the broader term for manufacturing micro components. Further, in order to facilitate an understanding of micro milling, it needs to be differentiated from conventional milling. This section does just that. After which, a general business case for micro milling is presented.

The second high level stage of this document forms the 'meat' of this project in that it consists of the cost model development sections. These are discussed presently.

Section 3 sees the high level formulation of the eventual cost model. That is, the cost categories are defined. These categories are later modelled to form the cost model. The approach taken in defining these cost categories is two-fold. Firstly, a review of typical cost breakdowns found in literature is done and, secondly, this review is used as a guideline in defining the cost categories. The benefit of doing this is that an understanding is gained of how the breakdown structure affects the final cost prediction.

Section 4 sees the modelling of one of the major cost drivers in all micro milling operations, namely tool life. In this section, tool life is characterised as a function of cutting parameters. The goal of this section is to quantify tool life and not to understand the mechanics of the cutting process. Therefore, the approach taken is to model tool life, statistically.

Section 5 sees the modelling of another major cost driver. This cost driver is not unique to micro milling. Rather, it applies to all manufacturing operations. Manufacturing time is modelled as a function of numerous related input parameters. The approach in modelling manufacturing time is not empirical because no established manufacturing process or historical time data exists. It is, however, logical to think that a manufacturing time model should be based on a manufacturing process. To overcome this dilemma, a hypothetical manufacturing process was envisaged upon which the time model is based.

Section 6 sees the coming together of the previous models. The tool life and manufacturing time models of Sections 4 and 5 respectively are synthesised, using the framework defined in Section 3. This results in an integrated cost model. More specifically, each cost category/component defined in Section 3 is modelled using the tool life and manufacturing time 'sub-models' of Sections 4 and 5. Further, with a complete cost model in place, an initial cost estimate is generated by inputting typical parameter values.

The final high level stage has to do with the analysis of the previously developed cost model as well as the conclusions that can be drawn from this analysis. As such, this stage takes a reflective look at the work done previously and considers the lessons to be learned. The sections constituting this stage are discussed presently.

Section 7 comes after the complete cost model has been developed and an initial cost estimate obtained. This section then addresses issues related to optimising and analysing the model. Since the cutting parameters influence the machining time and cost; and since these parameters are easily adjustable, they are considered first. Near-optimal solutions for machining time and cost are obtained by finding the right combination of cutting parameters. This is done by means of an optimisation algorithm. Thereafter, the effect of key input parameters on manufacturing cost is quantified. This analysis provides an indication of the sensitivity of manufacturing cost to these parameters.

Section 8 completes this project by taking a holistic view of the work done and its contribution to the development of the capability to manufacture hydrogen fuel cells locally.

2. Literature Review

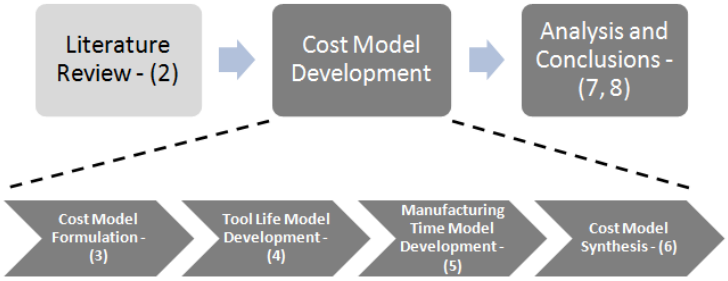

The scope of this project has its roots in two seemingly unrelated fields, namely micro manufacturing and hydrogen fuel cell technology. In addition, the scope focuses on specific topics within these fields. That is, micro milling within micro manufacturing and bipolar plates within hydrogen fuel cell technology.

One way of thinking about this project is that it has a narrow scope with a broad background. In order to facilitate understanding it is necessary to provide a background into each topic. This requires covering broad aspects of hydrogen fuel cell technology and micro manufacturing. This literature review attempts to do just that. Despite this, however, the focus of this literature review is still on the more specific topics, namely micro milling and bipolar plate manufacturing. Further, an emphasis is placed on the subject matter directly related to this project.

2.1 Hydrogen Fuel Cells – A Sustainable Energy System

In a global move toward environmental protection, governments are focusing on the development of sustainable energy systems as a means to reduce their country's carbon footprint and ensure the security of their energy supply. This comes in the midst of unrelenting international politics concerning the supply of oil, as highlighted by the volatile oil price.

One sustainable energy system involves the use of hydrogen as an energy carrier, which combined with fuel cell technology, shows much promise as a means of electricity production (HySA 2009). Fuel Cell Markets (2002), have identified several advantages to the use of fuel cells (including the hydrogen type) in a variety of applications. The following advantages provide strategic reasoning for the pursuit and continued development of hydrogen fuel cells as a technology for the future:

- **High Efficiency** – Since fuel cells convert fuel into energy using minimal steps, they are able to achieve much higher conversion efficiencies. Some fuel cells can achieve combined electrical and thermal efficiencies of up to 90% when used for Combined Heat and Power (CHP) purposes. Fuel cells vehicles can also be up to 2 to 3 times more efficient than internal combustion engine vehicles (Fuel Cell Markets 2002).
- **Reliability and Maintenance** – Fuel cells contain far fewer moving parts when compared to internal combustion engines. This means that fewer maintenance procedures are required such as oil changes etc.
- **Low Emissions** – Hydrogen Proton Exchange Membrane (PEM) fuel cells produce only water (H_2O) as a by-product of the reaction. Other fuel cells also have significantly reduced emissions because no combustion occurs in the reaction, unlike internal combustion engines.
- **Reduced Noise and Vibration** – Fuel cells generate smaller vibrations than a combustion engine, which has the effect of reduced noise.
- **Distributed Generation and Combined Heat and Power** – Traditional energy infrastructure produces large amounts of heat that is not used effectively. In fact, a coal-fired power station can have efficiencies as low as 30% because most of the heat is lost via cooling towers. Further, the electricity is produced at a central location and transmitted to points of use resulting in additional losses in the form of transmission losses. Further still, and somewhat ironically, this electricity is often used to generate more heat at the point of use. Fuel cells, on the other hand, have the ability to generate electricity and heat at the point of use. This localised heat can be used for traditional heating applications, resulting in electrical and thermal efficiencies of up to 90%. This is known as Combined Heat and Power (CHP).

- **Hydrogen Production** – Hydrogen can be produced by a variety of processes such as electrolysis. In addition, the use of renewable energy in the electrolysis can make hydrogen a very low emission fuel.
- **Hydrogen Safety** – Hydrogen has been used in a variety of industries such as hospitals, welding and glass making for some time and has an excellent safety record in terms of industrial accidents. Hydrogen is also non-polluting and non-hazardous to the environment.

2.1.1 A General Business Case for Hydrogen Fuel Cells in South Africa

Hydrogen and other fuel cells use platinum as a catalyst to promote the chemical reactions at work. Without platinum, the reactions would be severely inhibited and the usefulness of hydrogen fuel cell technology effectively negated. This fact makes platinum, and the availability thereof, a key driver in the development of hydrogen fuel cells.

Platinum is a rare mineral with known reserves in only five countries in the world. Of these five countries, South Africa is the leading supplier with 80% of the worlds known platinum reserves. This places South Africa at the focal point in the world's intensifying research efforts towards a 'hydrogen economy' (HySA 2009).

In the recent media (March 2011), Joel Netshitenzhe, director of Mapungubwe Institute for Strategic Reflection (Mistra), stated that South Africa could benefit greatly from tapping into the potential hydrogen economy. He said further that South Africa should not just export its raw materials and wait for the rest of the world to benefit from the use thereof. Instead, South Africa needs to become the epicentre of fuel cell manufacturing (Prinsloo 2011).

Aside from holding a dominant position in terms of platinum reserves, HySA (2011), has identified several other drivers behind South Africa's participation in the budding 'hydrogen economy'. These are:

- The potential socio-economic benefits that could result from the value added to platinum reserves.
- South Africa's leading technological capability of high temperature gas cooled nuclear reactors such as the Pebble Bed Modular Reactor technology. This technology is key in industrial scale generation of heat that, in turn, is used in thermal electrolysis to produce hydrogen.
- South Africa's leading position in the gasification of coal to liquid fuels technology.
- The opportunities to build a substantial knowledge base in an emerging technology, and in so doing, create socio-economic opportunities for the entire economy.

2.1.1.1 Formation of Hydrogen South Africa (HySA)

In the context of the general business case described above, the Department of Science and Technology (DST) developed the National Hydrogen and Fuel Cells Technologies Research, Development and Innovation Strategy. This 15-year program was approved by Cabinet in May 2007 and officially launched in September 2008. Hydrogen South Africa (HySA) was formed in 2008 as the result of this national strategy.

An initial effort has been made towards implementing HySA by establishing three Centres of Competence, namely **HySA Systems**, **HySA Catalyst** and **HySA Infrastructure**. Each Centre carries a unique responsibility but all three operate under a common vision. This vision is to foster proactive innovation and develop the human resources required to undertake competitive research and development activities in the field of hydrogen and fuel cell technologies (HySA 2009). For the purpose of this literature study, only HySA Systems will be discussed in further detail as it relates to the theme of this project.

2.1.1.2 HySA Systems

HySA Systems is a Technology Validation and Systems Integration Competence Centre for hydrogen and fuel cell technology. It is their long-term goal to develop key components for hydrogen and fuel cell technologies and systems for specific applications, and facilitate the export of new technology from South Africa to international markets (HySA Systems 2009).

This long-term goal is supported by their main objective, which is to perform technology validation and systems integration in four key programmes. These include:

- Combined Heat and Power
- Portable Power
- Hydrogen Fuel Vehicles
- Human Capital Development

For the purpose of this literature study, only the Combined Heat and Power programme will be discussed in detail because it relates to the theme of this project.

2.1.1.3 Combined Heat and Power (CHP)

CHP is a method of cogeneration where electricity and heat are generated and used simultaneously. Essentially, it is a means of recycling thermal energy. When electricity is generated in hydrogen (and other) fuel cells, heat is produced as a by-product. This heat can either be discarded, as is the case with most energy applications, or it can be used for other heating purposes such as the heating of water or a building. In this way, the thermal energy is recycled.

HySA Systems have identified Combined Heat and Power as a key programme because fuel cells, based on these systems, offer several benefits. These include high efficiency, low emissions and a decentralised power and heat supply for buildings and industries. HySA Systems (2009), says that there is considerable interest in the installation of CHP systems in domestic properties, as well as larger scale community and industrial heating applications. This is supported by the fact that CHP systems can operate from existing natural gas distribution networks, using a reformer to convert methane to hydrogen and, thereby, minimising additional infrastructure costs.

In addition, there is synergy between high temperature fuel cells (120 - 180°C) and the complexity of the gas reforming process. High temperature fuel cells tolerate higher impurity levels in the fuel, thereby, affording a simpler reforming process (HySA Systems 2009).

The approach taken by HySA Systems with the development of CHP systems and components is bi-directional. Firstly, a system orientated top-down approach is taken by clearly defining the system and the subsequent components. Secondly, it is also necessary to adopt a material orientated bottom-up approach. This is because new technology brings the introduction of new materials.

HySA Systems (2009), say that their CHP key programme will focus on:

- Modelling and design of complete CHP-systems based on High Temperature Proton Exchange Membrane (HT PEM) fuel cells.
- Developing Membrane Electrode Assemblies (MEA's) suitable for HT PEMFC using CHP-systems.
- Developing and testing HT PEM fuel cell stacks (up to 2 kW).
- The specification and testing of power conditioning for CHP-systems, including testing of secondary batteries.

The link between the key program focuses listed above and the work done for the purpose of this project should be noted here. The work done in this project aligns with '*developing and testing of HT PEM fuel cell stacks.*' In terms of the generic development process, cost models play a vital role. They allow 'downstream' production activities to be linked to 'upstream' design activities. Essentially, cost models characterise the expected manufacturing cost as a function of relevant design parameters. This allows organisations to make intelligent design and production decisions regarding the final cost of the product.

The role of cost models in the generic development process speaks to the purpose of this project. That is, this project endeavours to allow HySA Systems to make intelligent decisions with respect to developing the capability to manufacture hydrogen fuel cells locally.

2.1.1.4 High-Temperature Proton-Exchange Membrane (HT PEM) Fuel Cells

HT PEM fuel cells can operate at temperatures between 120 and 180°C. As stated above, there is synergy between the use of HT PEM fuels cells and CHP systems that stems from the inherent benefits of HT PEM fuel cells. These are (McConnel 2009):

- More efficient use of thermal energy or by-product heat created from the electrochemical reaction
- Reduction of components for cooling, water management and purifications in plants
- Increased tolerance to carbon monoxide (CO) and sulphur impurities in the fuel, which allows for the use of reformate fuels rather than the use of pure hydrogen

McConnel (2009), says that this combination of benefits will result in a significant competitive advantage for commercial PEM fuel cell systems.

2.1.2 The Basics of Hydrogen Fuel Cell Operation

The basic principle of hydrogen fuel cells was first demonstrated in 1839 by William Grove. Essentially, water and hydrogen were electrolysed by passing a small electric current through them using a power supply. After some time the power supply was replaced with an ammeter. This allowed the electrolysis to be reversed by recombining the hydrogen and oxygen to produce a small electric current. **Figure 2** below, courtesy of Larminie and Dicks (2002), illustrates the concept.

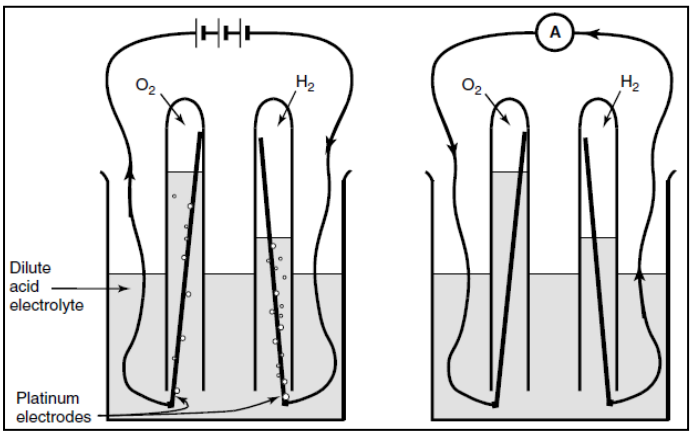

Figure 2 – The Electrolysis Principle

A simple, yet analogous way of thinking about the process is to imagine the hydrogen being 'burnt' under reaction with oxygen. However, instead of heat energy being emitted, electric current is conducted between the electrodes.

2.1.3 Proton Exchange Membrane (PEM) Fuel Cells

The PEM fuel cell was first developed by General Electric in the 1960's to be used by NASA on their first manned space vehicles. The basic operation of the PEM fuel cell is the same as that of the first acid electrolyte fuel cells. The defining feature of a PEM fuel cell is the electrolyte, which is made from a thin layer of an ion conductive polymer, known as the proton exchange membrane. This membrane is the heart of the PEM fuel cell in that it allows hydrogen protons to pass through it while at the same time blocking electrons. This effectively forces the electrons to flow through the external circuit and in so doing creates the electrical energy generated from the cell.

The process of generating electrical energy using PEM fuel cell is illustrated in **Figure 3** below, courtesy of Larminie and Dicks (2002). Hydrogen (H_2) is distributed over an anode (negative terminal), which in contact with a platinum catalyst, is broken down into a proton (H^+) and electron (e^-), according to the following formula:

$$2H_2 \rightarrow 4H^+ + 4e^- \qquad \textbf{(1)}$$

From here, the protons are allowed through the membrane while the electrons are forced to travel through the external electrical circuit. At the same time, but on the opposite side of the electrolyte membrane, oxygen is distributed over the cathode (positively charged terminal). Here, the hydrogen protons (H^+) coming from the anode via the membrane, and the electrons, also coming from the anode but via the external circuit are combined with the oxygen to form water (H_2O). This happens according to the following formula.

$$O_2 + 4H^+ + 4e^- \rightarrow 2H_2O \qquad \textbf{(2)}$$

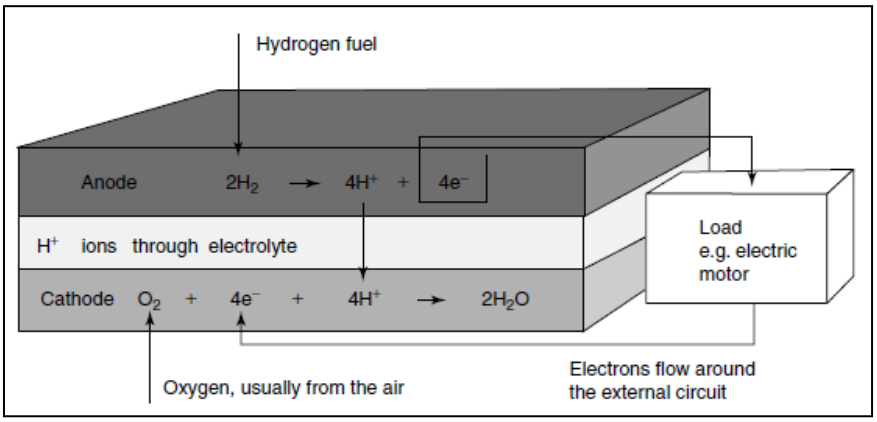

Figure 3 – Proton Exchange Membrane Fuel Cell (PEMFC) Operation

The assembly described above (electrode/membrane/electrode) is commonly known as a Membrane Electrode Assembly (MEA).

2.2 Bipolar Plates

Each Membrane Electrode Assembly (MEA), as described previously can only generate about 0.7 volts when drawing a useful current according to Larminie and Dicks (2002). Therefore, in order to generate an appropriate voltage it is necessary to join several MEA's in series. An obvious way of doing this is simply to connect the anode of one MEA to the cathode of the next via an electrical conductor. According to Larminie and Dicks (2002), the problem with this is that the electrons have to flow across the face of the electrode as they try to pass through the small contact area of the electrical conductor. This then results in a small but significant voltage drop.

A better way of connecting electrodes in series is to use bipolar plates. Bipolar plates derive their name from the fact that they are in contact with the positive electrode of one MEA and the negative of another at the same time, hence 'bipolar'.

Bipolar plates have two main purposes. Firstly, they must make a good electrical connection between the electrodes of MEA's in series. This is achieved by the increased contact area with which the bipolar plate touches the electrodes and the low electrical resistance of the material used. Secondly and simultaneously, the bipolar plates must distribute gasses evenly over the surface of the electrodes without mixing them. That is, oxygen over the cathode and hydrogen over the anode. This is achieved with the use of channels that control the direction of flow. These channels are collectively known as the flow field. A simple design for a bipolar plate is shown in **Figure 4** below.

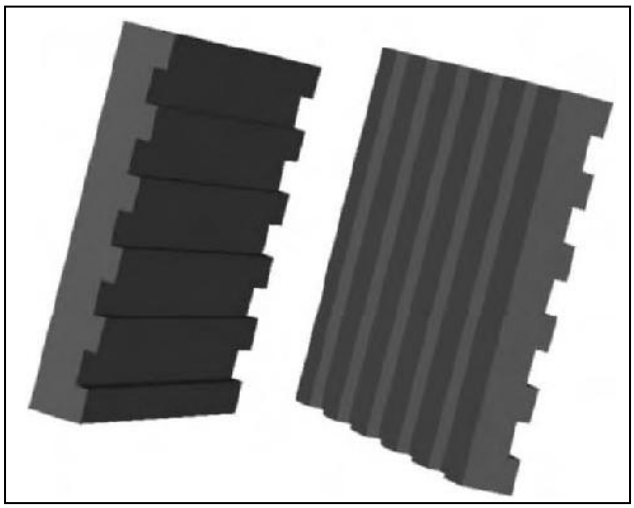

Figure 4 – Simple Bipolar Plates

The two main, but not only, purposes of a bipolar plate i.e. to provide a good electrical connection between electrodes and to distribute gas evenly over the surface of each electrode are both necessary and conflicting functions. Larminie and Dicks (2002), discuss their conflicting relationship.

The total contact area between the plates and the electrode should be as large as possible to allow minimal electrical resistance between them. However, this would reduce the flow of gas over the surface of the plates by limiting the number or width of gas channels. Another way to achieve low electrical resistance is to increase the number of contact points between the plate and the electrode. However, this makes the plates more complex and expensive to manufacture.

In addition, the bipolar plates should be as thin as possible to ensure minimal electrical resistance. However, this limits the depth of gas channels and in effect the ability to pump the gas around the cell especially considering that this should be done at a high volumetric flow rate.

It stands to reason that there is a natural trade-off between the electrical resistance and the ability to distribute gas evenly over the surface of the electrode. This trade-off marks one of the complexities of bipolar plate design and manufacture.

2.2.1 Bipolar Plate Material Considerations

In addition to the two main purposes of bipolar plates Hermann, et al. (2005), have identified several others. These are to:

- Carry heat out of the active areas
- Prevent leaks of either the reactant or the coolant
- Assist with water management

The material from which these plates are made is an important consideration. The material must have the mechanical and chemical properties required to support the various functions of the plates. Hermann, et al. (2005), have described these material properties. It must have:

- Low electrical resistance
- High thermal conductivity
- Low gas permeability to prevent reactant loss
- High corrosion resistance because the plate is in a highly corrosive environment
- Good strength as the plates give the stack its strength
- Low weight because the plates contribute significantly to the total weight of the stack

Furthermore, the plates must be manufactured inexpensively to ensure the economic feasibility of hydrogen fuel cell technology. This is because bipolar plates are a significant component in a fuel cell stack, accounting for up to 80% of the weight and 45% of the cost in PEM fuel cells (Tsuchiya and Kobayashi 2004).

The multiple material properties required for bipolar plates has brought to light a variety of potential materials (Hermann, et al 2005). For the purpose of this literature study, the most common

categories of bipolar plate materials are discussed along with their relevant advantages and disadvantages.

2.2.1.1 Non-porous Graphite

Both natural and synthetic graphite have traditionally been the most commonly used material for bipolar plates. This is owing to the chemical stability of graphite, which allows it to survive in the highly acidic fuel cell environment. The low resistivity of this material has also made it an attractive alternative. However, the high cost and low mechanical strength of pure graphite make it an impractical material for economic production.

2.2.1.2 Non-coated Metals

According to Hermann, et al. (2005), stainless steels are the only materials to have received serious attention in this category. This is mainly due to their relatively high strength, high chemical stability, low gas permeability and wide range of alloy choices. Further, stainless steels are good candidates in terms of manufacturability, especially for mass production. There are concerns, however, with the extent of corrosion as well as the contact resistance of the surface passivation film, common to stainless steels.

2.2.1.3 Coated Metals

The addition of a coated protective layer to base metals makes them an attractive alternative for the use in bipolar plates. The protective layer deters corrosion in the highly acidic environment. Aluminium, stainless steel, titanium and nickel have been considered as base metals for this type of bipolar plate, according to Hermann, et al. (2005).

The coating used must be conductive and must completely cover the base metal. In addition, the coefficient of thermal expansion of the base metal and the coating must be approximately equal. This is to avoid unequal expansion between the two, which leads to the formation of micro-pores and micro-cracks. Two types of coatings, namely carbon-based and metal-based are considered for this purpose.

2.2.1.4 Polymer Composites

Composites are lightweight and can be moulded into any shape. These characteristics make them an appealing alternative material for PEM fuel cell stacks. Composite bipolar plates are either metal- or carbon (graphite)-based.

Metal-based composites, especially those containing stainless steel, graphite and polycarbonate plastic provide a good combination of material properties. Impermeability is provided by the

stainless steel and polycarbonate, allowing the graphite to be porous and less time consuming and expensive to make. Further, each component of the composite provides a desirable property. The stainless steel provides rigidity while the polycarbonate provides chemical resistance and allows the plate to be moulded. The graphite, further, resists corrosion (Hermann, et al. 2005).

Carbon or graphite-based composites show promise as technically and economically feasible materials for bipolar plates. Middleman, et al. (2003), say that graphite filled polymer composites can offer a combination of inexpensive material and economic processing. Graphite based composites are made using either thermoplastic or thermosetting resins with fillers and with or without fibre reinforcement. Middleman, et al. (2003), described composite materials as having excellent properties and potential for economical mass production. Further, Cho, et al. (2004), have developed graphite composites whose long-term performance is comparable to that of non-porous graphite plates. In addition, these composites have none of the disadvantages of non-porous graphite. Specifically, graphite composites have good mechanical strength and are economically feasible.

It stands to reason, from the arguments presented above, that graphite-polymer composite materials show a good balance between performance and manufacturability. A unique material has been identified that is investigated exclusively for the purpose of this project. This is the FU 4369 HT graphite-polymer composite, which is solely produced by Schunk Kohlenstofftechnik GmbH in Heuchelheim, Germany. This material exhibits a strong combination of the material characteristics required, as detailed in Appendix A.

2.2.2 Bipolar Plate Flow Field Design Types

Li and Sabir (2005), say that apart from the development of low cost, lightweight materials and efficient fabrication methods, one of the major barriers to the large-scale commercialisation of fuel cells is the design of the bipolar plate flow fields. This is because the design of the flow field significantly affects the performance of the fuel cells in terms of energy efficiency and power density. Up to 50% increase in the output power density has been reported by the correct distribution of gas via flow fields alone (Watkins, et al. 1992). Three of the more common flow field designs are the parallel, serpentine and serpentine parallel designs. These will be discussed briefly for the purpose of this literature study.

2.2.2.1 Parallel Flow Fields

A typical parallel flow field design is shown in **Figure 5** below. The figure also shows a part of the cross-sectional view of this design (Pellegri and Spaziante 1980).

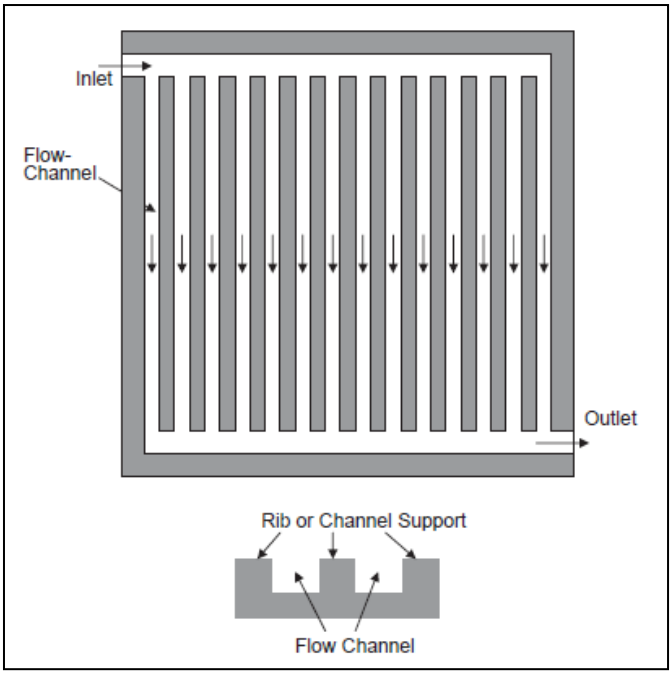

Figure 5 – Parallel Flow Field Design

Li and Sabir (2005), mention two main problems that occur with this type of design. These are as follows. When air is used as the oxidant, low and unstable cell voltages occur after some time. This is attributed to poor cell water management in the cathode. As the cell is operated for an extended period, water formed at the cathode tends to accumulate in the flow channels, clinging to the floor and sides of the channels. These water droplets formed in the channels require increased force to remove. Further, the distribution of water droplets between channels is not even, preventing gas from flowing evenly through the channels. Consequently, stagnant areas arise where water is allowed to accumulate resulting in little or no gas passing through. The result of this poor water management is poor cell performance.

Another problem associated with parallel flow field designs is the small pressure drop that occurs along the length of the channels. This results from the short channel length and lack of directional changes. Consequently, the pressure drop in the stack distribution manifold and piping systems are comparatively large. This then results in a non-uniform distribution of reactant gasses between cells in the stack. Usually, the first few cells in the stack have greater reactant gas flow than the latter cells.

2.2.2.2 Serpentine Flow Fields

In order to resolve the problem of cell water management of the parallel flow field design, Watkins, et al. (1991), proposed a flow field design with one continuous channel running in a serpentine pattern. The design has an inlet at one end and an outlet at the other. This is known as the serpentine flow field design, illustrated in **Figure 6** below.

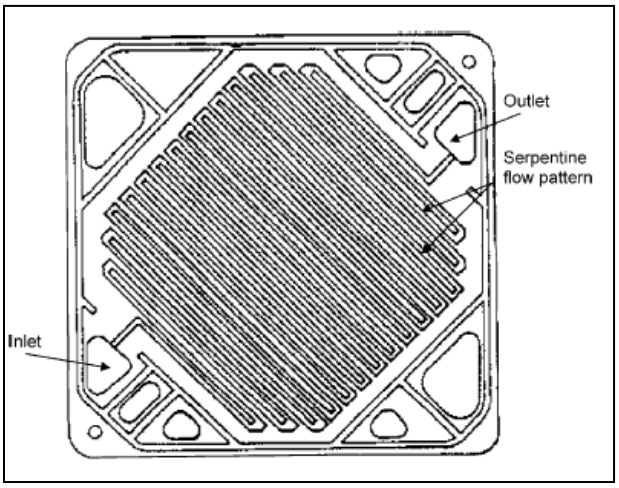

Figure 6 – Serpentine Flow Field Design

The serpentine flow field forces all of the reactant gas to flow through a single channel that traverses the entire active area of the corresponding electrode. This effectively eliminates areas of stagnation because no water is allowed to accumulate. However, one problem with this design is pointed out by Li and Sabir (2005). The relatively long flow path resulting from the use of only one channel creates a large pressure drop and a significant concentration gradient from the inlet to the outlet. When air is used as a reactant, the power required to pressurise the air sufficiently for the large pressure drop, can be as much as 30% of the output power of the stack. This consequently, significantly diminishes the efficiency of the stack.

2.2.2.3 Serpentine Parallel Flow Fields

In order to overcome the difficulties with the serpentine flow field design Watkins et al. (1992) proposed the use of several continuous and separate channels running in a serpentine pattern. This is illustrated in **Figure 7** below and is known as the serpentine parallel flow field design.

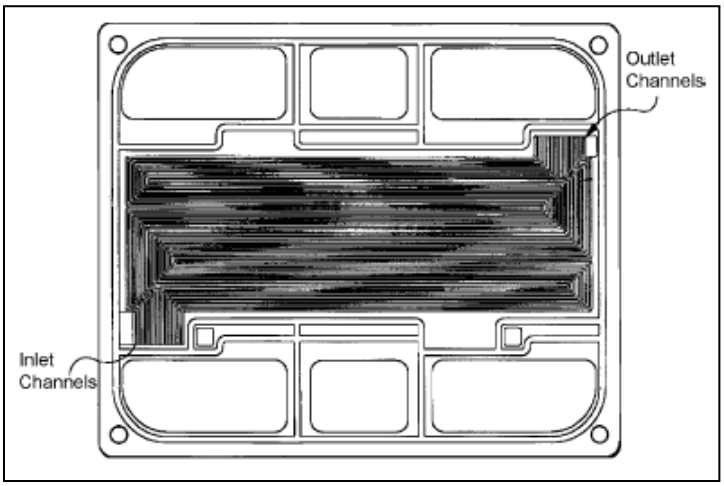

Figure 7 – Serpentine Parallel Flow Field Design

Watkins, et al. (1992), pointed out that this design would limit the pressure drop from the inlet to the outlet and thus minimise the power required to pressurise the reactant gas. Further, this design ensures sufficient water removal by gas through the channels and thereby, prevents the formation of stagnant areas on the cathode surface. Watkins, et al. (1992), reported a 50% increase in output power from a cell stack when the serpentine design is replaced by the serpentine parallel design under the same experimental conditions.

2.2.3 Bipolar Plate Manufacturing Methods

Numerous methods exist for the manufacturing of bipolar plates in general. However, most methods are material specific. That is, a method that is used for processing one material is not necessarily feasible for processing another. The scope of this discussion is limited to graphite-polymer specific methods as they are applicable to this project.

2.2.3.1 Compression Moulding

Groover (2007), describes compression moulding as an old and widely used process for moulding thermosetting plastics and thermoplastics. The difference between thermoplastics and thermosetting plastics is as follows. Thermoplastics are heated and cured by cooling. If the part were to be reheated, it would lose its shape. Thermosetting plastics are also heated and cured to form their desired shape. Once cured however, the molecular structure is changed in such a way that parts will maintain their desired shape even upon reheating. Groover (2007), describes the compression moulding process for thermosetting plastics as follows.

The compression moulding process consists of four main stages. Firstly, a precise amount of moulding compound, called the charge, is loaded into the bottom half of a heated mould. Secondly, the top half of the mould is brought together with the bottom. This compresses the charge, forcing it to conform to the shape of the mould cavity. Next, the charge is heated by means of a hot mould to polymerise the material. This cures it into a solidified part. Finally, the mould halves are opened and the part is removed by means of the knock-out pin. This process is illustrated in **Figure 8** below, courtesy of Groover (2007).

In the case where a thermoplastic binder is used, the mould has to be cooled to a temperature below the melting temperature on the binder before the part can be removed. Middleman et al. (2003), state that this can require cycle times of up to 15 minutes; too long for economic mass production. This will depend on cooling conditions though. However, if a thermosetting plastic binder is used, only a few minutes are required for the material to cure.

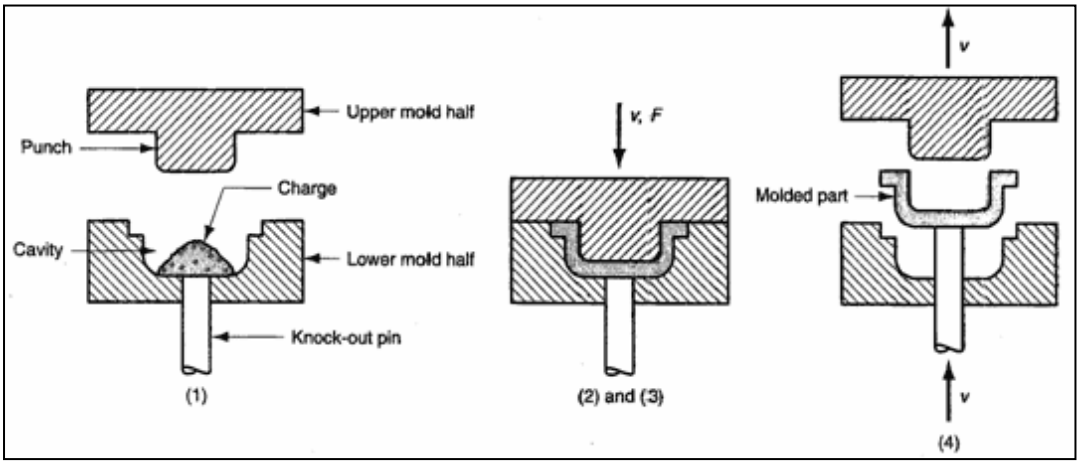

Figure 8 – Compression Moulding Process

It stands to reason that using thermosetting plastics as the binder in graphite-polymer composites is most appropriate for the manufacture of bipolar plates. Not only are the cycle times shorter, but in the high temperature environment of HT PEM fuel cells, thermosetting plastics are able to maintain their shape better.

2.2.3.2 Injection Moulding

Injection moulding is another method that has been considered for the manufacture of graphite polymer composite bipolar plates. Groover (2007), describes injection moulding as a process in which a polymer is heated to a plastic state and forced to flow under high pressure into a mould cavity, where it solidifies. The moulded item is then removed from the cavity. Middleman, et al. (2003), say that injection moulding of bipolar plates has the advantages of automated production, short cycle times and accurate sizes. However, there is difficulty in applying this process to a conductive compound. Some of the drawbacks include excessive mould wear, limited size to thickness ratio and poor electrical conductivity of the resulting bipolar plates (Middleman, et al. 2003).

2.2.3.3 Machining

Machining or more specifically, micro machining is another alternative for the manufacture of bipolar plates. Micro machining has inherent benefits that make it an attractive manufacturing method for the production of bipolar plates as well as other parts with micro features. The section following provides an in depth discussion of the aspects of micro machining and its applicability to the manufacture of bipolar plates.

2.3 Micro Machining

This section is intended to describe aspects of micro machining in general as well as its relation to the manufacture of bipolar plates. General background is given in terms of how micro milling, a specific form of machining, fits into the broader theme of micro manufacturing. After which, a discussion is presented of issues that separate micro machining from its macro machining equivalent. Finally, a general business case is presented for micro machining which is intended to clarify the motivation for the assessment of this method as a possible way of manufacturing bipolar plates.

2.3.1 Micro Manufacturing and Micro Components

"The miniaturisation of machine components is seen as a requirement of future technological developments."

Chae, et al. (2005)

Coetzee, et al. (2007), define micro-manufacturing as the fabrication of micro-systems whose outer dimensions are measured in millimetres or centimetres and whose inner surfaces are configured with features that have dimensions measured in micrometers. More specifically micro-systems are made up of components that exhibit the following attributes:

- They are about 10 µm to 10 mm in size
- They contain complex 3D geometries
- They use a variety of engineering materials
- They have very high relative accuracies (typically between the range of 10^{-3} to10^{-5}) where relative accuracy is defined as $\frac{Tolerance}{Feature\ Size}$

The above attributes refer essentially to small components that have even smaller features. More recently, however, the definition of a micro component has expanded to include larger components that have micro sized features. Qin (2010), describes micro manufacturing as the set of methods, technologies, equipment, organisational strategies and systems for the manufacture of products and/or features that have at least two dimensions that are within the sub-millimetre range. This definition includes not only small components, but also larger components that have features within the sub-millimetre range.

It is often difficult to visualise the size of objects or features without having a relatable frame of reference. **Figure 9**, courtesy of Coetzee, et al. (2007), indicates the relative scale of the different 'worlds', in terms of size. This is included to put the term 'micro' into perspective.

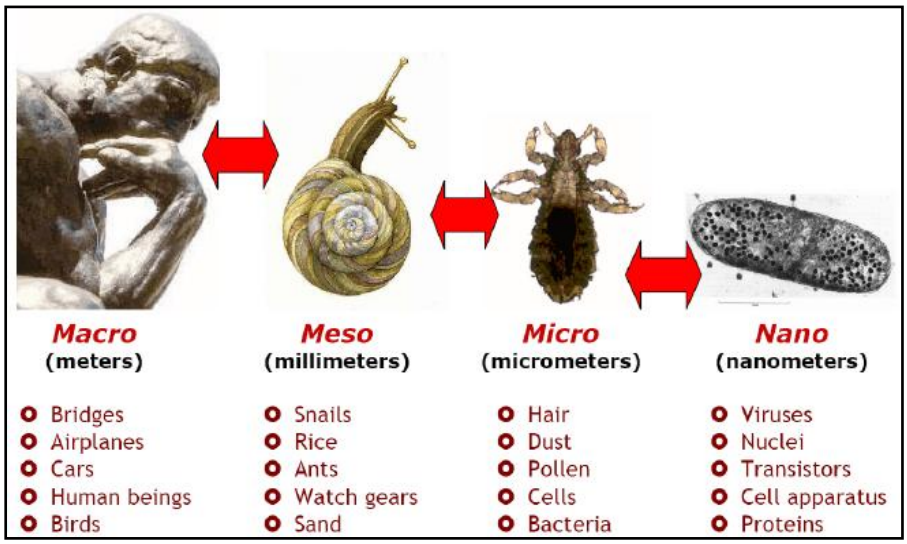

Figure 9 – Perspectives of Different Size 'Worlds'

Micro manufacturing technologies will have a significant impact on virtually all industrial sectors in the future. Using a variety of materials, components and base technologies, micro manufacturing will add functionality and, therefore, value to miniaturised systems. Highly accurate miniaturised components are experiencing an ever increasing demand in industries such as the aerospace, biomedical, electronics, environmental, communications and automotive, according to Chae, et al. (2005). This is because these components carry the inherent benefits of a smaller carbon footprint, lower power consumption and a higher heat transfer rate. The latter is attributed to a higher surface-to-volume ratio than their macro equivalents. These benefits allow micro-components to form part of highly intelligent and functional miniaturised systems, which will be able to perform unparalleled tasks or add new capabilities to traditional materials, machines, and systems (Coetzee, et al. 2007).

Ehmann, et al. (2004), describe micro manufacturing in terms of a world perspective as an **enabling, disruptive, transforming** and **strategic** technology.

It is an **enabling** technology for the broad exploitation of nano science because it bridges the gap between the nano and the macro worlds. Nanotechnologies are widely regarded to be the drivers for the next generation of products. In order to exploit these technologies for the purpose of commercial application, it is necessary to bridge the gap between the 'nano' and the 'macro' worlds. This is where the application of micro manufacturing technologies will play a vital role in providing the infrastructure for this purpose. It is, therefore, important that the nano- and micro- technologies be developed in parallel.

Micro manufacturing is a **disruptive** technology that will change our thinking as to how, when and where products are manufactured. Coetzee, et al. (2007), state that South Africa is typically at a

disadvantage when competing in global manufacturing markets because of our geographic location. Micro manufacturing could change the paradigm of products being manufactured on location. Instead, it is conceivable that products could be manufactured en route to the intended location (on a ship for example) because of the reduced size of the manufacturing equipment.

Further, micro manufacturing is a **transforming** technology that will redistribute manufacturing capability to the masses. This is because micro manufacturing can change the manufacturing paradigm from a centralised one to a decentralised one, where everyone can be a manufacturer. Coetzee, et al. (2007), suggest that this could revolutionise the manufacturing paradigm and redistribute the wealth.

Finally, micro manufacturing is a **strategic** technology that will enhance the competitive advantage of a country by providing:

- Reduced capital investment requirements
- Reduced space and energy requirements
- Increased productivity
- Increased portability

This has obvious benefits for South Africa in light of a weak Rand and an increasing energy demand. In addition, it is worth noting that the increased portability of micro manufacturing equipment stands to overcome the geographic disadvantage of South Africa's location.

2.3.1.1 Applications of Micro Manufacturing

Coetzee, et al. (2007), have indicated several markets together with typical applications within each, as given by **Table 1**.

Table 1 – Markets and Applications of Micro Manufacturing

Market	Typical Applications
Automotive	• Lubricants • Sensors • Gyroscopes and Accelerometers • Engine Management • Security
Aerospace	• Smart Materials • Adaptors • Sensors • Health and Monitoring Systems
Textile and Clothes	• Garment Health Monitoring • Micro Coatings
Energy	• Micro fuel cell • Micro Combustion Engines • Solar Cells • Advanced Batteries • Wind Energy • Hydrogen Fuel Cell
Electronics	• Displays • Printer Heads • Auto ID Systems • RF Modules • Optical switches • Micro mirrors
Life Sciences	• Implantable systems • Micro fluidics • Lab on chip • Hearing aids Diagnostic systems • Smart pills • Drug Delivery
Process Technology	• Sensors (Pressure, Temperature) • Food quality sensors • Micro robotics

2.3.1.2 Comparison of Micro Manufacturing Processes

Micro component manufacturing requires highly accurate and repeatable methods with even more accurate and repeatable measurement techniques. Several common methods of manufacturing micro components are based on semi-conductor processing techniques. This involves the photo etching of silicon materials through chemical and dry processes and usually occurs in large batch production (Chae, et al. 2005). The advantage of using silicon as the base material is that electronic components can be incorporated into the micro-device during manufacture (Liow 2009), allowing a number of electronic components to be manufactured in this way. These components make up the foundation of modern computer technology.

The environmental effect, however, of using silicon as a base material for the manufacture of micro-components has been calculated by Williams et al. (2002). They showed that a 2g, 32MB DRAM uses 1600g of secondary fossil fuel, 72g of chemical inputs, 32g of water and 700g of gases. In terms of energy, it takes 41MJ to produce a 32MB DRAM, which during a lifetime of 4 years at 3 hours per day uses only 15MJ. This high energy-intensity and amount of processing material used during manufacture is attributed to the highly organised structure of the DRAM.

According to Liow (2009), there has recently been a shift from the exclusive use of silicon in micro-devices to the use of glass, metals, ceramics and elastomers. These materials have a long history in the manufacturing industry when it comes to macro products and devices. Despite this, the use of these materials in micro component manufacturing brings with it a need for alternative manufacturing methods. These methods include, among others, machining, laser machining, focused ion beam (FIB), electro-discharge machining (EDM) and LIGA (Lithography, Electroplating and Moulding). Liow (2009), gives a short summary of these technologies in terms of minimum feature size, achievable tolerances, material removal rates and applicable materials. This is shown in **Figure 10** below.

Machining method	Minimum feature	Tolerance	Material removal rates	Materials
Mechanical micromachining	10 μm	1 μm	High	Any
Focused Ion Beam/2D & 3D [6]	100 nm	10 nm	Very low	Tool steels, non-ferrous, plastics
Excimer laser/2D or 3D	6 μm	0.1–1 μm	High	Polymers, ceramics, some metals
Femto-second laser/2D or 3D [7]	1 μm	0.5 μm	Low	Any
Micro-EDM (Sinker or Wire)/2D or 3D	10 μm	1 μm	Very high	Conductive material
LIGA/2D	0.01	0.02	Depends on process	Electroformable: copper, nickel, permalloy
Diamond milling and micromachining [8]	10	1	High	Not suitable for ferrous materials

Figure 10 – Comparison of Micro Manufacturing Processes

The methods indicated above are capable of producing high precision micro-components, but have limited usefulness in terms of production due to their high initial start-up costs, poor productivity

and material limitations. It can be argued that the broad commercialisation of micro-systems is inhibited by these drawbacks and the inability to manufacture small batch sizes cost effectively. This provides a gap in the micro manufacturing field for the application of micro machining.

The use of micro machining to manufacture micro components is motivated by the same reasoning for the use of conventional machining to manufacture macro components. That is, micro machining is a flexible manufacturing technique that can accommodate individual parts, as opposed to large batch sizes, and does not require expensive or time-consuming setups. Qin (2010), says that micro machining brings much potential to the fabrication of miniature and micro-products/components with arbitrary geometry.

2.3.2 Micro Milling – What is it?

Groover (2007), defines conventional milling as a machining operation in which a workpiece is fed past a rotating cylindrical tool with multiple cutting edges. Perhaps the defining characteristic of milling as compared to other machining processes is that the axis of rotation is perpendicular to the direction of the feed, as shown in **Figure 11** below, courtesy of eFunda Inc. (2010).

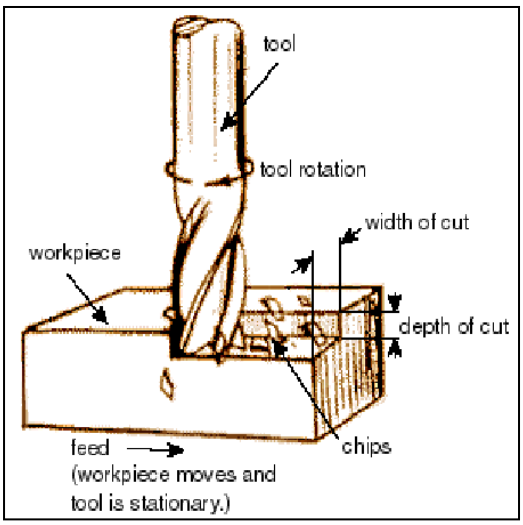

Figure 11 – Basic Milling

In principle, micro milling is the same as conventional milling in that the surface of the workpiece is mechanically removed using a cutting tool. Where micro milling differs from conventional milling is in the size of the cutting tools and resulting part features. Micro milling is used to make components with features in the sub-millimetre range. **Figure 12** below shows an example of a typical micro component with complex three-dimensional geometry, courtesy of PhysOrg.com™ (2008).

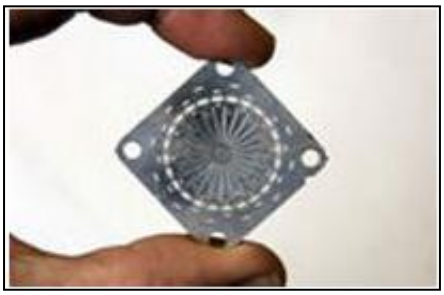

Figure 12 – Example of Micro Milling Component

Apart from the smaller size of component features and machining tools, micro milling differentiates itself from conventional milling in terms of the mechanics of the process. This comes because of the scaling down of the material removal process to the extent that traditional cutting models no longer apply. This provides reasoning for the classification of micro milling as a separate manufacturing method and not simply a scaled down version of conventional milling.

2.3.3 Micro versus Conventional Machining – Differentiating Issues

Micro cutting operations are characterised by a number of issues that set them apart from conventional cutting operations. These issues are brought about by the miniaturisation of the components and machine tools. As a result, there is a need for a fresh approach to understanding machining operations at this level. This section discusses these issues.

2.3.3.1 Chip Formation and Minimum Chip Thickness

In conventional machining, the feed per tooth is generally larger than the cutting tool edge radius. Therefore, conventional chip formation models are based on the assumption that cutting tools completely remove the surface of the work part and generate chips.

This assumption is not applicable in the case of micro machining. The small feed per tooth and edge radius of the tool cause a large negative rake angle. This has the effect of ploughing, rough surface formation and elastic recovery of the work part. Liu, et al. (2004), confirmed this by demonstrating that there is elastic deformation of the work piece during machining.

The notion behind minimum chip thickness is that the feed per tooth, or uncut chip thickness, must be greater than a critical chip thickness to ensure chip formation. **Figure 13** illustrates this concept courtesy of Chae, et al (2005).

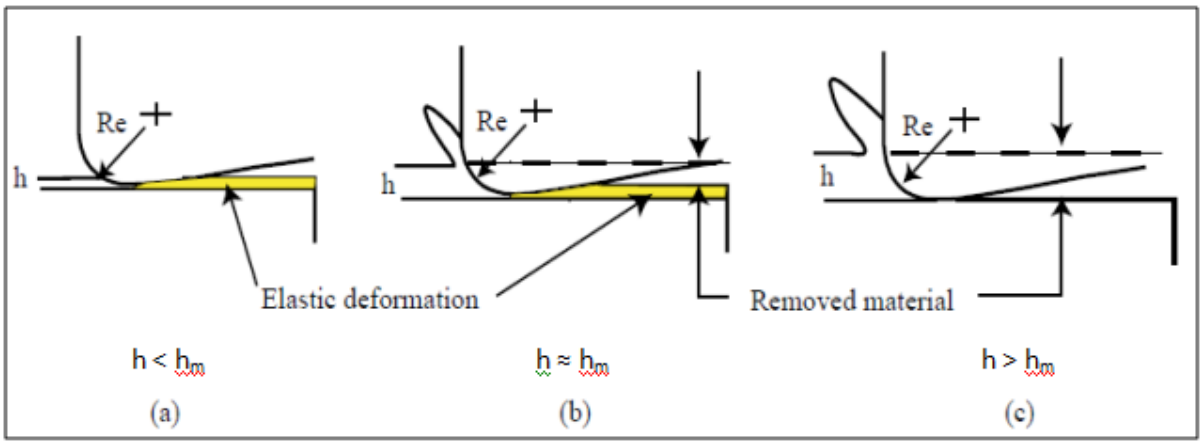

Figure 13 - The Minimum Chip Thickness Effect in Micro Milling

When the uncut chip thickness (h) is less than the minimum chip thickness (h_m) elastic deformation occurs and no chip is formed or material removed, as shown in (a). As the uncut chip thickness becomes approximately equal to the minimum chip thickness, as shown in (b), chips are formed by the shearing of the work part material with some elastic deformation still occurring. However, when the uncut chip thickness is sufficiently larger than the minimum chip thickness, the entire depth of cut is removed with little or no elastic deformation occurring.

In mechanical micro machining, it is important to consider the minimum chip thickness effect before proceeding with the cutting process. This is because chip formation and the effectiveness of the process are influenced by this effect. Failure to set the feed per tooth sufficiently above the minimum chip thickness will result in intermittent cutting where a chip is not formed during every tooth pass but rather intermittently. This causes increased friction between the tool and the workpiece as well as excessive cutting forces; both of which lead to accelerated tool wear.

2.3.3.2 Cutting Forces and Specific Cutting Energies

In micro milling, the size of the cutting edge radius (Re in **Figure 13**) is comparable to that of the uncut chip thickness. So, in contrast to conventional machining (where a sharp edge cutting model may be used), chip shear in micro machining occurs along the rounded tool edge (Matsubabara, et al. 2000). As a result, cutting has a large negative rake angle, which increases the magnitude of ploughing and shearing forces. Following this, a relatively large amount of material has to be plastically deformed for a relatively small amount of material to be removed, resulting in increased specific cutting energy (Shaw 1995).

This leads to the conclusion that cutting forces in conventional machining are quite different from those in micro machining, although both consist of mainly ploughing and shearing forces. Altintas (2000), conducted a preliminary experiment where micro cutting forces were predicted according to a conventional sharp edge-cutting model and then compared to the experimental results. It was

concluded that the dynamic component, which is mainly due to shearing forces is similar to the predicted conventional cutting force when the chip thickness is greater than the minimum chip thickness. However, the static offset forces indicate that ploughing forces cannot be fully expressed by conventional cutting models, as shown in **Figure 14**, courtesy of Chae, et al. (2005).

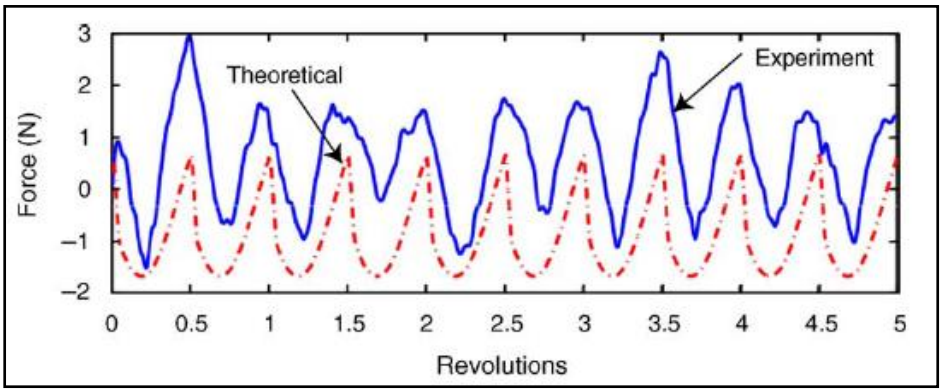

Figure 14 – Cutting Forces in Micro Milling

2.3.3.3 Tool wear and surface roughness

Some limiting factors, in terms of studying the tool wear of micro end mills, are the measurement equipment available and the criterion used to quantify the wear. Since micro tool dimensions are small, it is difficult to measure precisely any wear characteristics on the tool itself. Li, et al. (2007), propose that surface roughness of the machined part be the criterion for characterising tool wear. Their experiments indicated that the variation in surface roughness as machining progresses is strongly related to tool wear progression, validating the assumption that tool wear can be characterised in this way.

Although surface roughness in conventional milling is well understood, this is not the case in micro milling. Surface roughness in conventional milling is traditionally characterised by the feed rate and tool geometry. However, Li, et al. (2007), argue that this approach is no longer accurate for micro milling. They state that micro tool geometry, minimum chip thickness as well as the effect of tool wear play an important role in surface roughness generation. They studied the effects of tool wear, minimum chip thickness and micro tool geometry on surface roughness in micro end milling with the following important conclusions:

- The effect of tool wear on surface roughness was found to be significant. In some instances, the surface roughness coefficient (Ra) can increase several times as tool wear progresses for fixed cutting parameters.
- The cutting velocity and material removal volume are significant contributing factors in tool deterioration. A higher cutting speed results in more rapid tool wear, which in turn causes a faster deterioration of the surface roughness.

- Minimum chip thickness significantly affects surface roughness in micro milling. This is especially true as the feed rate is decreased and the feed per tooth is approximately equal to or less than the minimum chip thickness.

Further, Rahman, et al. (2001), studied the failure mechanisms and factors that affect the micro milling of pure copper. They speculated on the differences that the effect of tool wear had on the cutting forces in conventional and micro milling. A small wear of one cutting edge of a conventional cutter may increase the cutting forces by a few percent. In the case of micro milling, an even smaller amount of wear may eliminate half of one cutting edge, resulting in easily double the cutting force on the other cutting edge. The speculation was validated during their experiments, which showed that cutting forces increased with time as tool wear progressed. In addition, they concluded that for the machining of pure copper, the helix angle and depth of cut play an important role in the life of the tool.

2.3.3.4 Tool Life Theory

The commercialisation of micro milling is inhibited by, among other aspects, a limited understanding of the cutting mechanics. One reason for this is that without a deep understanding of the cutting mechanics, it is impossible to formalise a uniform tool life theory. That is, a tool life theory that characterises tool life in terms of cutting parameters and cutting conditions.

What makes this consideration even more pertinent is the fact that micro end mills are relatively costly and fragile in comparison with conventional end mills, due to their slender and minute nature. Mayor and Sodermann (2009), say that with low material removal rates and the relatively large amounts of material removal required in the production of micro parts, tool costs could easily become a dominant cost driver. Several researchers have attempted to model tool life in terms of cutting parameters with varying results.

Sreeram, et al. (2006), recognised the costly nature of micro end mills and attempted to optimise the cutting parameters by making use of a genetic algorithm. The objective of the optimisation model was to minimise unit production costs by maximising tool life. Their results showed that the optimum value for depth of cut was higher than that given by the tool manufacturer.

Prakash, et al. (2002), developed an empirical tool life model using a 1 mm diameter tool to machine copper under dry cutting conditions. In this study, axial depth of cut, cutting speed and feed rate are considered. It was found that only axial depth of cut and cutting speed are relevant to the progression of flank wear; while feed rate had no influence.

Filiz, et al. (2007), on the other hand came to a different conclusion. They studied tool life on a 254 µm diameter tool. Their results showed that tool life depends highly on feed rate due to the

minimum chip thickness effect. That is, faster feed rates led to reduced wear relative to slower feed rates.

While previous studies have considered the characterisation of tool life by cutting parameters under dry conditions, Mayor and Sodermann (2009), have attempted to do the same under flood like application of cutting fluid. In general, it was found that this significantly improved tool life in high aspect-ratio full-slot micro milling. In their study, feed rate and axial depth of cut were varied during experimentation while the spindle speed was kept constant. The tool life was measured until complete tool failure. A noteworthy aspect of this study is that they recognised that the definition of tool life is also important. That is, tool life can be defined in terms of cutting time, cutting distance or volume of material removed. It was found that the preferred parameter values for improved tool life actually depend on the measure used to quantify it. They found that if either cutting distance or cutting time is utilized then a shallower axial depth of cut results in improved life. On the other hand, if the volume of material removed is used as the measurement, then there is a point in the cutting parameter space that results in a local optimum tool life.

In general, there seems to be a lack of consistency in the results of researchers who have attempted to characterise tool life in terms of cutting parameters. This suggests that no uniform model exists as yet. As a result, it is necessary to build a tool life model that is specific to the problem at hand.

The conundrum of having to build specific tool life models for each problem speaks to the work done in this project. That is, a specific tool life model is developed in Section 4, which characterises tool life as a function of cutting parameters for the micro milling of bipolar plates.

An interesting phenomenon has been seen in micro milling that is related to the axial depth of cut and tool life. In conventional end milling, an increase in the depth of cut increases the resultant cutting force necessary for material removal. This increase in cutting force increases the rate at which the cutting edge wears resulting in more rapid tool failure and reduced tool life. Zaman, et al. (2004), have suggested that the opposite could be true for micro end milling, up to a certain extent. They found that the tool life of micro end mills was greater for a larger depth of cut, as long as the depth of cut remained below that of the diameter of the tool. This can be explained geometrically by considering **Figure 15** below, courtesy of Sreeram, et al. (2006).

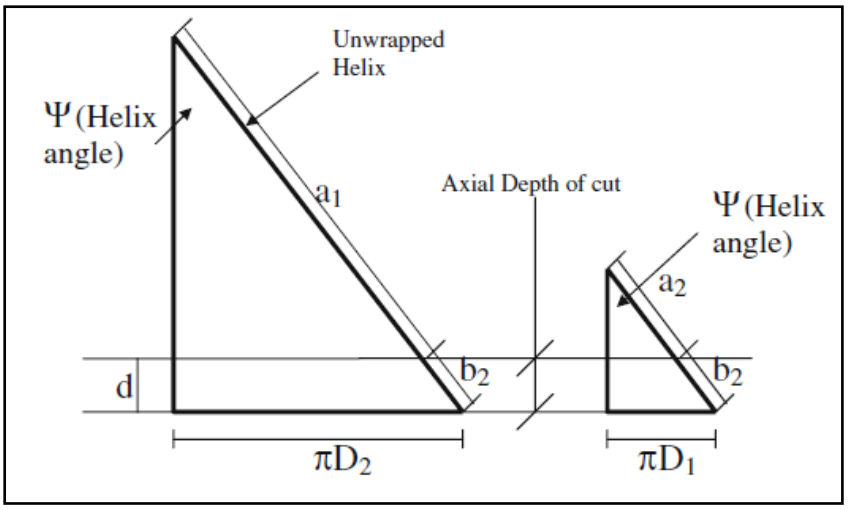

Figure 15 – Ratio of Depth of Cut to Tool Diameter in Conventional and Micro Milling

The ratio of depth of cut to the tool diameter is relatively higher in micro end milling than in conventional milling. The figure above shows the unwrapped helix face (or cutting edge) for both conventional (left) and micro (right) end milling. In addition, the amount of helix face engaged at any time is indicated for a certain depth of cut. In the figure, d is the axial depth of cut, $a_1 + b_2$ is the unwrapped helix face for a conventional end mill (diameter D_2) and $a_2 + b_2$ is the unwrapped helix face of a micro end mill (diameter D_1). It can be seen that,

$$\frac{b_2}{a_1 + b_2} < \frac{b_2}{a_2 + b_2} \quad \textbf{(3)}$$

since $a_1 > a_2$. Therefore, the proportion of the helix face that is engaged for a certain depth of cut is relatively more in micro milling than in conventional milling. This results in less idle distance traversed by the cutting edge for one rotation of the tool leading to reduced intensity on the cutting edge against the workpiece (Zaman, et al. 2004).

This increase in tool life for an increased axial depth of cut is only up to a certain extent. According to Sreeram, et al. (2006), this phenomenon is only applicable while the axial depth of cut is below that of the tool diameter, beyond which the cutting force becomes too great, resulting in tool failure.

Synergies are found between this theory and the results obtained in this project. This is detailed in Section 0.

2.3.4 A General Business Case for Micro Milling

Mechanical machining, on the macro level, has proven to be a highly flexible and effective way of manufacturing a variety of three dimensional geometries. It is this characteristic of conventional machining that creates the rationale behind micro machining, as a technically and economically feasible technique for manufacturing micro components. According to Chae, et al. (2005), the

motivation for micro machining comes from the translation of knowledge and competency from the macro machining environment.

Micro machining carries with it several inherent benefits over other micro fabrication techniques. Chae, et al. (2005), list a few as follows:

- It does not require very expensive or time-consuming set-ups, unlike lithographic methods.
- The process can accommodate individual components and is not limited to large batch sizes because making use of economies of scale is not as important. This provides the flexibility in production, which is a useful characteristic in modern day production facilities.
- The possibility exists for monitoring the quality of components in process.
- It is capable of fabricating three dimensional free-form surfaces, which is especially important for the manufacture of micro injection and micro compression moulds.
- It is capable of processing a variety of materials such as metallic alloys, composites, polymers and ceramics.

2.3.4.1 Energy Savings

Perhaps the most notable advantage of micro machining over other micro manufacturing and macro machining methods is that of a reduced carbon footprint, resulting from the reduced power consumption during the process. Liow (2009), conducted a study of the energy used with the machining of a simple T-junction to highlight the energy efficiencies that can be achieved with micro machines that are designed specifically for machining micro devices. The study involved a performance comparison of a general-purpose CNC milling machine and a prototype micro-milling facility. Four T-junctions were machined in a single stainless steel plate by each machine. Each T-junction had dimensions 2cm by 1cm with channel dimensions of 100 µm and 50 µm in width and depth respectively. The results of the study showed that the general-purpose CNC machine used approximately 800 times more electrical energy to carry out the machining operations.

Interestingly, the percentage of energy used by the spindles of the micro mill and general-purpose mill, as compared to the total used by each machine, were 19.7% and 70.8% respectively. This indicates that the general-purpose machine consumes the bulk of its energy in the spindle, even when only a fraction of the available torque is required. This then suggests that the general-purpose CNC milling machine was totally oversized for this particular operation.

2.3.4.2 Further Strategic Reasons

Dirkse van Schalkwyk and Dimitrov (2007), developed a techno-economic model; combining accuracy, repeatability and energy use associated with micro milling. This was done in an attempt to build a general business case for micro machining in the automobile industry in South Africa. The

model showed indications of clear financial advantages of micro machining over the use of conventional machines, especially for finishing operations.

Further, Dirkse van Schalkwyk and Dimitrov (2007), suggest possible strategic reasons for investing in micro machining. These include:

- Smaller business sizes or lower throughput
- More affordable start-ups
- The ability to change technology more frequently
- Lower maintenance and insurance costs
- Reduced floor space requirements

3. Cost Model Formulation

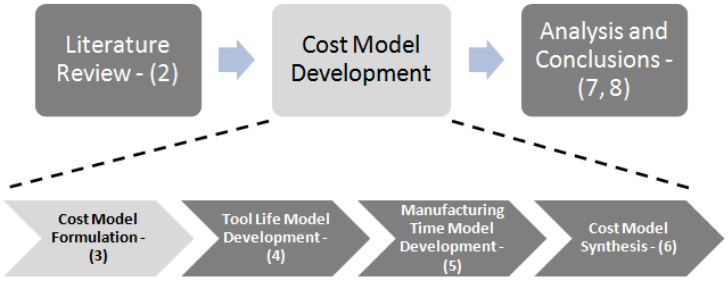

Cost Modelling, as defined by the Society of Cost Estimating Analysts (SCES), is a compilation of cost estimating logic that aggregates cost estimating details into a total cost estimate. Stated differently, cost modelling is an ordered arrangement of data, assumptions and equations that permit the translation of physical resources or characteristics into costs. Curran, et al. (2004), summarise this definition by describing cost modelling as a set of equations, logic, programs and input formats that specify the problem. That is, this set of equations and logic characterise the cost to manufacture a component or product.

Cost models are typically used early in the product development cycle, when product specific cost data is not yet available. Rather, cost data for similar products or processes are typically used to build the cost model. These models, otherwise known as cost estimating models, allow organisations to make intelligent design and production decisions regarding the final cost of the product. Crow (2000), describes the role of cost modelling in a simplified product development process shown in **Figure 16** below.

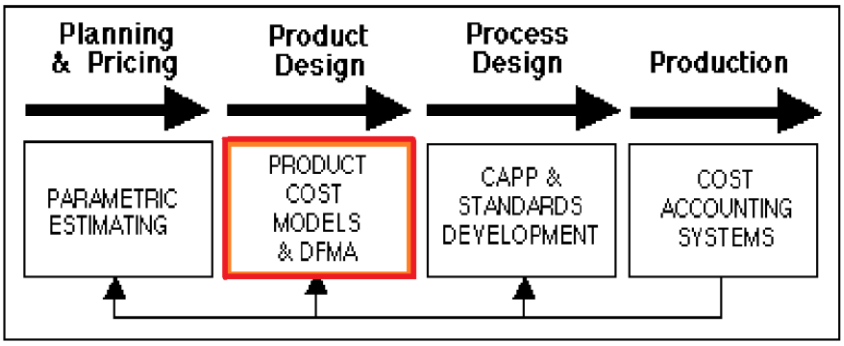

Figure 16 – Cost Modelling in the Product Development Process

The need for cost models stems from the three widely recognised measures of product effectiveness. That is, product cost, quality and time to market. Together, these three measures determine the effectiveness of a product in meeting customer demands and contribute significantly to the commercial success of the product. In many companies, product costs are an afterthought, with the primary focus being on quality or time to market. This approach may be fine for some

companies in the short term, however, in highly competitive markets, this approach is certainly not sustainable (Crow 2000).

Traditional ideas about the nature of cost, state that cost is determined in the production stage. However, over the last few decades, there has been a paradigm shift in the understanding of cost, especially in terms of when cost is incurred, as opposed to when cost is committed. **Figure 17**, courtesy of Giebel (2010), illustrates this concept. It presents an overview of the nature of cost in terms of when it is committed versus when it is incurred over the product life. It can be seen that as much as 80% of total product cost is already committed in the design stage. Similarly, only a small fraction of the total product cost is actually accrued at this time. **Figure 17** does not reflect all situations precisely, but rather serves to illustrate the general case.

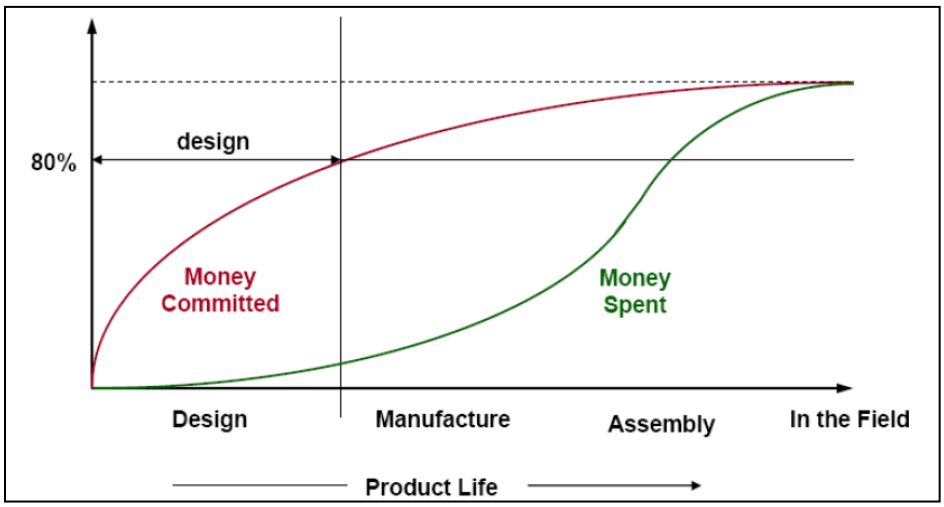

Figure 17 – The Nature of Cost

From the figure above, it is intuitive that the greatest potential to influence final product cost is in the early stages of product development i.e. the design stage. The design decisions made early in the product development cycle can be used to identify drivers and reduce costs related to manufacturing, assembly and distribution.

Engineers are responsible for the decisions made in the product design stage. As such, there is an increasing realisation in industry that engineers, and not financial experts, are responsible for final product cost. This notion is supported by Curran, et al. (2004). They state that engineers create the potential for cost.

Following this, the need is presented to be able to integrate cost into the decision making process. Cost models provide a means of doing this by modelling 'downstream' costs in terms of 'upstream' design variables. These enable design engineers to understand the influence of design decisions on the eventual product cost. Crow (2000), says that a product cost model or life cycle cost model

provides an objective basis for evaluating design alternatives from a very early stage in the development cycle. Therefore, cost models can be used to evaluate design alternatives early in the product development process.

Schreve, et al. (1999), corroborate this by describing an important characteristic of cost models. They say that cost models can be used by designers to do trade-off studies. That is, designers can compare the effect of design variables on one or more design objectives such as performance or cost. Schreve, et al. (1999), mention another important characteristic of cost models. Cost models help designers to consider each step in the manufacturing of their product systematically. The process of building a cost model is, therefore, an assessment of the manufacturability of the design. Further, cost estimates can be seen as a quantitative manufacturability analysis.

Cost models are used to integrate 'upstream' design activities with 'downstream' production activities. Typically, this is done using either the Design-For-Cost (DFC) or the Design-To-Cost (DTC) approach.

DFC can be thought of as a forward-feeding engineering process that uses process information during design. This approach is directly aligned with concurrent engineering (Curran, et al. 2004).

DTC, on the other hand, is a more management driven process. This makes use of target costing to arrive at a cost objective. The product is then designed to meet the cost objective. Crow (2000), describes DTC as a management strategy and supporting methodologies to achieve an affordable product. This is done by treating target cost as an independent design parameter that needs to be achieved during the development of a product.

Whether the approach taken to cost integration is DTC or DFC, it still forms part of the concurrent engineering methodology. Groover (2008), describes concurrent engineering as an approach used in product development in which the functions of design, manufacturing and other are integrated to reduce the time to market. Essentially, concurrent engineering requires input from various business functions (not only design) in the product development stage. This ensures that issues, which would normally only be addressed much later in the product development cycle, are identified and addressed early leading to a reduced time to market. Another benefit of concurrent engineering, in the context of cost modelling, is that cost drivers are identified and quantified early in the product development cycle, allowing greater cost control and higher potential for achieving cost targets.

3.1 Review of Typical Manufacturing Cost Breakdowns

Product cost is made up of a number of cost categories. The breakdown or categorisation of costs is not necessarily the same for all product costs. Typical product cost categories for machined products include, but are not limited to:

- Material cost
- Tool cost
- Tool replacement cost
- Setup cost
- Handling cost
- Labour cost

The above categories are not mutually exclusive. That is, a cost incurred may fall into one or more of the above categories. Therefore, care must be taken in defining cost categories. There is no one correct way to do this. Each alternative breakdown serves to highlight individual cost drivers. The purpose of this section is to review typical cost breakdowns found in literature and use these as a guideline in defining the breakdown for this cost model.

3.1.1 Cost Model of Boothroyd, et al. (2002)

As part of the broad methodology known as Design for Manufacture and Assembly (DFMA), Boothroyd, et al. (2002), devised a methodology for developing cost models of machined components. They recognised the need for designers to know the magnitude of the effects of design decisions on manufacturing costs. The approach taken with this methodology is to find a compromise between traditional detailed cost estimating and over-simplified volumetric approaches. Cost categories as defined by this methodology are described below.

- **Material cost** refers to cost of raw materials from which the component is made. Boothroyd, et al. (2002), state that this cost can account for more than 50% of the total cost. Therefore, this should be estimated with great care.
- **Machine loading and unloading cost** accounts for the cost incurred when parts are loaded and unloaded from the machine. These costs are driven by the time taken and cost rates to do so.
- **Other non-productive costs** account for the time taken to position the tool, set the cutting parameters, engage feed and withdraw the tool after operation. These times together comprise the setup time of the workpiece.

- **Handling cost** accounts for the time taken to move batches of partially machined workpieces between machines.
- **Machining cost** accounts for the cost incurred during the period between when the machine is engaged and disengaged. Boothroyd, et al. (2002), point out that the tool would not be cutting for the whole of this time. As such, allowances should be made for tool approach times.
- **Tool replacement cost** accounts for two items. These are the cost of machine idle time while the operator replaces the tool and the cost of providing a new cutting edge or tool.

The DFMA cost estimating model concentrates on direct costs. That is, the costs that are directly attributable to the product. No allowance is made for indirect or overhead costs such as production or corporate overheads that account for the salary of the administration staff, the cost of the machine, etc. It could be argued that this model is sufficient as a design evaluation tool because direct costs are the most influenced by design decisions. However, referring specifically to machine costs, the author believes that it is unwise to omit this. This is because the machine cost becomes a significant contributor when evaluating alternative manufacturing methods.

3.1.2 Cost Model of Sreeram, et al. (2006)

Sreeram, et al. (2006), recognised that tool life is a significant cost driver in micro milling operations and that cutting parameters are strong influencers of tool life. Following this, they built a machining cost model and applied a genetic algorithm to find the near-optimal combination of cutting parameters, which resulted in lowest unit cost. Their unit cost model was made up of the following cost categories:

- **Cutting cost** accounts for cost of machining. This cost is driven by the cutting parameters chosen and total machining distance. Also, this cost is a function of an overhead and labour rate defined in terms of USD/hr.
- **Material cost** accounts for the cost of raw material.
- **Tool cost** accounts for the cost of tooling. This cost is a function of tool life, which is determined by the cutting parameters chosen. This cost is a key criterion in their optimisation model.
- **Tool replacement cost** accounts for costs incurred during tool replacement.
- **Setup cost** is the cost incurred for the time spent setting up the machine. This is a function of the time to do so and the overhead and labour rates.

An interesting feature of this cost breakdown is seen in the allocation of overheads. Sreeram, et al. (2006), proposed a single rate, known as the overhead and labour rate that accounts for direct labour costs and for indirect overhead costs. Because overheads are indirect, the allocation base needs to be defined. In this case, they have chosen the direct labour hours as the base for apportioning overhead costs. The overheads could otherwise have been apportioned over direct machine hours or over units of production. This presents a topic with which care must be taken in developing a cost model because inappropriate definition of the overhead allocation base can lead to skewed cost estimates and, ultimately, incorrect analysis.

3.1.3 Cost Model of Lee, et al. (2007)

Lee, et al. (2007), realised the potential of hydrogen fuel cells as a promising, environmentally friendly energy source and the importance of the bipolar plate as a major cost contributor to the fuel cell. They built a cost model to evaluate the cost of manufacturing graphite composite bipolar plates using two alternative methods, namely compression moulding and machining. Their cost model consisted of the following elements:

- **Material cost** accounts for the cost of raw material. Lee, et al. (2007), present this cost element as a function of the volume of raw material used and price per unit volume.
- **Preparation cost** accounts for the time required to setup the machine. This is the equivalent of setup cost and is a function of the operators wage rate and the preparation time required.
- **Machining cost** is a function of machining time, operators wage rate and the associated indirect cost. This indirect cost is a function of machine depreciation and other overhead costs associated with the machine such as maintenance.
- **Tool cost** accounts for the cost of tooling and is a function of tool life.

An interesting feature of this cost model is the way in which overheads are allocated. Overheads or, more specifically, production overheads are apportioned over machine hours as opposed to labour hours (which are not necessarily the same). This is another commonly accepted allocation base for overhead costs.

3.1.4 Direct Costs versus Indirect Costs

Where direct costs can be directly linked to a product, indirect costs cannot. This means that indirect costs must be allocated using some pre-defined base. This is known as cost allocation. Steward, et al. (1995), describe cost allocation as the interpretation of cost and its categorisation in order to arrive at a reasonable distribution of those costs. The traditional approach to allocating overheads is to use volume-based allocation. Typical volume-based allocation bases include the following:

- Labour hours – In this case, the overhead rate is calculated according to:

$$\text{Overhead Rate} = \frac{Total\ Overheads}{Total\ Labour\ hours} \quad \textbf{(4)}$$

  The overhead cost per unit would then be calculated as the number of direct labour hours × the overhead rate.

- Machine hours – Similarly, machine-hours could be used as the overhead allocation base.
- Units of Production – Alternatively, overheads can be directly allocated per unit production according to:

$$Overhead\ Rate = \frac{Total\ Overheads}{Total\ Production\ Units} \quad \textbf{(5)}$$

  This type of overhead rate is known as a 'blanket' rate and is only appropriate when a company produces only one product (Gowthorpe 2005).

Allocating overhead costs according to volume-based methods could lead to incorrect conclusions if the wrong allocation base is defined. This is because these methods imply that indirect costs are proportional to direct costs (Curran, et al. 2004). This is not always the case, especially considering the trend in industry to make increasing use of automated equipment. Automation of the production line implies higher indirect costs (more expensive equipment) and lower direct costs (less labour intensive). Therefore, it is becoming increasingly important to generate accurate estimates of indirect costs.

A more detailed allocation method that addresses this need is Activity Based Costing (ABC). This method assumes that costs are caused by activities and that products consume those activities. In other words, activities drive costs. Gowthorpe (2005), argues that the application of ABC can result in significant improvement in the quality of information, and consequently, better control and planning of production. Gowthorpe (2005), also states that ABC requires a considerably more complex system because a great deal of information has to be collected and administered. As a result, the system is difficult and costly to implement.

Considering the above argument, it stands to reason that ABC may not be the correct allocation method for this cost model. This is because ABC requires substantial historical data, which is not available for this purpose. In addition, machining is still labour intensive because it is difficult to automate such a process. This implies that direct costs still strongly outweigh indirect costs in this regard. This negates the need for accurate estimates of indirect costs and places the emphasis on direct costs, as is highlighted by the example cost breakdowns in the sections above.

3.2 The Manufacturing Cost Model

A common characteristic of the cost breakdowns presented above is the emphasis placed on estimating direct costs accurately. One logical reason for this is that direct costs account for the lion's share of final unit cost. Another is that direct costs are the most influenced by design changes.

Another commonality between the above breakdowns is the inclusion of tool cost. An inexperienced cost accountant might be inclined to assign tooling costs to production overheads, not recognising the significant contribution of tooling cost and the need to allocate it to each product or component accurately. This is especially relevant in micro milling operations where tool costs are relatively high and tool life relatively low.

Yet another commonality, in the example breakdowns presented above, is the attention given to the manufacturing time. In all cases a differentiation is made between productive and non-productive times, indicating the importance of this as a cost driver in machining operations.

Based on the review of common cost breakdowns presented above and the logic behind these breakdowns, the manufacturing cost model for the purpose of this project, is defined as follows:

$$C_{Unit} = C_{Material} + C_{Labour} + C_{Tooling} + C_{Equipment} + C_{Overheads} \quad \textbf{(6)}$$

where C_{Unit} *= manufacturing cost per unit (R/plate),* $C_{Material}$ *= material cost per unit (R/plate),* $C_{Tooling}$ *= tooling cost per unit (R/plate),* $C_{Equipment}$ *= equipment cost per unit (R/plate)* and $C_{Overheads}$ *= additional overhead cost per unit (R/plate)*. An explanation and justification for each of these categories follows below.

Material cost per unit is represented by $\boldsymbol{C_{Material}}$ in the breakdown. As explained in Section 1, the cost of material, for the purpose of this cost model, is simply the cost of purchasing blank plates from Schunk Kohlenstofftechnik GmbH and importing them.

The labour cost per unit is represented by $\boldsymbol{C_{Labour}}$. It is assumed here that each plate is machined by only one worker and one machine. This simplifies the analysis, but is also a valid assumption based on the type of component. A further consideration in determining the labour cost is the number of machines operated per worker. It is not impossible for one worker to operate two or more machines, especially if the setup time is comparatively smaller than the machining time.

The tooling cost per plate is represented by $\boldsymbol{C_{Tooling}}$. This includes the cost of tools used to machine the major micro channels, minor micro channels, plate outline and the peripheral features, described in Section 3.3.

The cost of equipment, $C_{Equipment}$, accounts for the cost of machinery, workpiece holding systems, import cost, installations, etc that make up the initial capital cost. Typically, a company will not pay a lump sum amount to cover this capital cost. Rather, they will take out a loan to cover this cost and repay this loan on a monthly or annual basis. Therefore, the cost of equipment, $C_{Equipment}$, is seen as a capital recovery cost. That is, the contribution per plate towards repaying the initial capital cost. The approach taken to allocate equipment cost is to apportion the cost of equipment directly over the forecasted number of units produced. This type of overhead absorption rate is known as a 'blanket' overhead rate and is appropriate when a company produces only one product (Gowthorpe 2005). For the purpose of this project, it is assumed that this is the case.

The overhead cost per unit is represented by $C_{Overheads}$ in the above breakdown. The approach taken in defining this is similar to that of $C_{Equipment}$. That is, a blanket overhead rate is defined which describes the contribution, per unit of production, towards covering sundry overheads, excluding the cost of equipment.

Traditional cost models are based on historical data. The data is used to determine the cost estimating relationships, which characterise the estimated cost in terms of input variables. The problem with the cost model developed for the purpose of this project is that there is no historical data available. As such, an alternative approach is necessary. The approach must be to build the cost estimating relationships from fundamental engineering knowledge and experimentation.

The following two sections (Section 4 and 5) address this issue by quantifying two significant cost drivers in the manufacturing cost model. These are tool life and manufacturing time respectively. Traditionally, costs resulting from these drivers would be estimated using historical cost data for similar products or processes. However, since this is not possible for this project, these drivers are quantified by building separate tool life and manufacturing time models.

3.3 The Bipolar Plate Features

Before continuing any further, it is necessary to describe the different features of the particular bipolar plate design under study. This is necessary because the cost model is built around this design and, as such, makes reference to particular design features on numerous occasions. For confidentiality reasons, the detailed design cannot be disclosed in this document. However, the general features of the design can be illustrated.

The bipolar plate design is made up of four primary features. These are the outline, peripheral features, major micro channels and minor micro channels. The following figures are presented to give the reader a better understanding of the plate features.

Figure 18 below shows the outline of the plate design, without any other features. This shape is formed by machining along the profile of the plate.

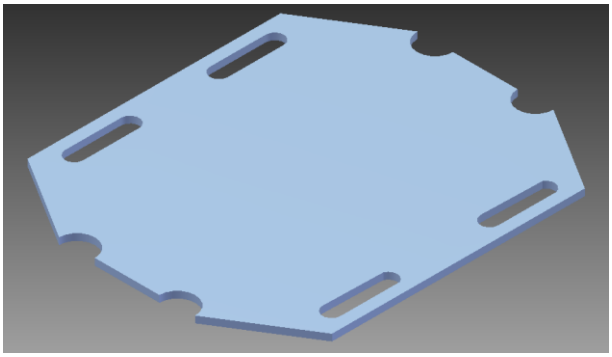

Figure 18 – Plate Outline

Figure 19 illustrates the outline of the plate as well as the peripheral features.

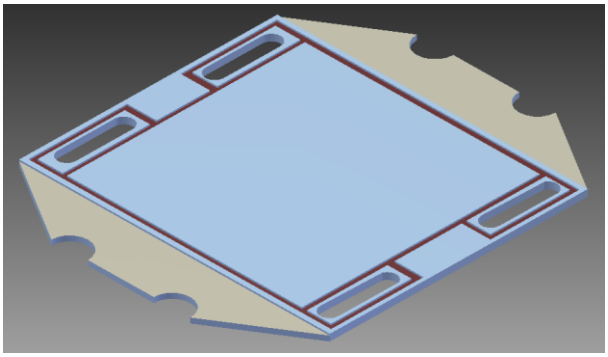

Figure 19 – Plate Outline and Peripheral Features

Figure 20 shows further progression by illustrating the major micro channels in addition to the previously mentioned features

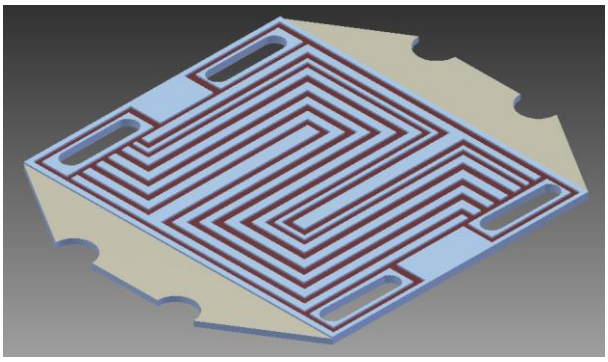

Figure 20 – Plate Outline, Peripheral Features and Major Micro Channels

Finally, **Figure 21** shows the inclusion of what is termed the minor micro channels.

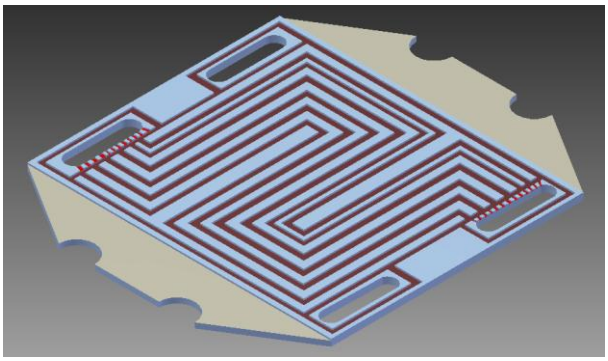

Figure 21 – Plate Outline, Peripheral Features, Major and Minor Micro Channels

4. Tool Life Model Development

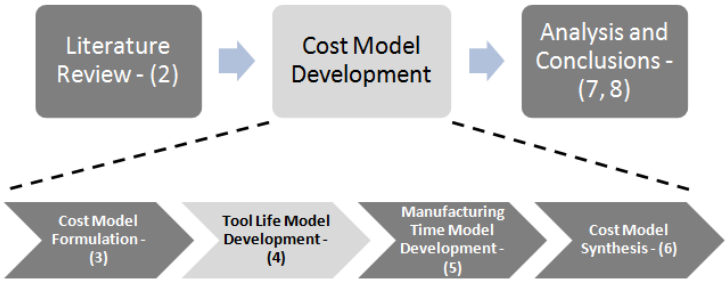

Tool life is a major cost driver in all micro machining operations. This is because micro tools are fragile in nature and, hence, prone to early failure and because they are expensive, relative to their conventional equivalents. Therefore, in order to build a useful cost model for any micro machining operation, it is first necessary to model tool life sufficiently.

This chapter describes the empirical model building process followed for this purpose. The process followed is largely based on that of Response Surface Methodology (RSM). Further, the tools and techniques contained within RSM are used as a basis for building the empirical tool life model.

In any real world product or process development, several input variables exist that potentially influence some performance measure. This performance measure is commonly known as the response. It is possible that these input (independent) variables affect the response according to a known relationship defined by the laws of physics. In this case, it is recommended to model the response in terms of the input variables using proven analytical techniques. However, in cases where the relationship between the input variables and the response is not fully understood, it is not possible to employ analytical techniques. Such cases call for the empirical approach taken by RSM and the tools contained within it.

For the purpose of this project, it is necessary to characterise the tool life in terms of the factors affecting it, such as the cutting parameters. In micro machining, not enough is understood about the mechanics of the process to sufficiently model the expected tool life using analytical techniques. Rather, an empirical approach is necessary. RSM is useful in this regard because it finds functions that approximate a response (tool life) in terms of input variables.

Taylor's Tool life Model, developed around 1900, is credited to F.W. Taylor. The model describes the relationship between cutting speed (m/min) and tool life (min) according to the following formula.

$$v{L_{T\ taylor}}^{n_T} = C \qquad \textbf{(7)}$$

where *v = cutting speed (m/min),* $L_{T\ taylor}$ *= tool life according to Taylor's model (min)* and n_T and *C* are empirically determined constants whose values depend on feed, depth of cut, work material, type of

tool and the tool life criterion used. There are two main concerns with this model in terms of its applicability to this project. These are as follows:

- The tool life is defined as the length of useful cutting time. This implies that the use of cutting length or volume of material removed is not considered as a possible definition of tool life. Literature has shown that the quality of empirical tool life models depend on the characteristic used to define tool life (Mayor and Sodermann 2009).
- Taylor's model typically uses flank wear as the criterion to measure tool wear. Further, a certain amount of wear is defined as maximum amount of wear beyond which the tool is no longer useful. The problem is that this method only recognises one possible tool failure mechanism. That is, it assumes that tools fail gradually and not catastrophically. This is not the case in micro milling because the small size and brittle nature of micro tools make them susceptible to breakage. Further elaboration on this matter is given in Section 4.2.2 on page 58.

Instead of Taylor's tool life model, a broader approach is needed to model the tool life of micro end mills. One that incorporates more than one tool failure mechanism and that allows different definitions of tool life to be compared. The remainder of this section addresses this need.

This section is divided into three main sub-sections constituting the design, execution and analysis of the tool life experiments performed. The approach taken in this section is to describe simultaneously the academic and practical aspects associated with the empirical model building process. This is done by describing the academic aspects of each technique and using the work done as an ongoing example to illustrate these concepts.

4.1 Designing the Tool Life Experiments

This section describes all the practical and academic aspects associated with designing the experiments carried out for the purpose of this project.

4.1.1 Selecting the Experimental Factors

In order to select the correct experimental input variables or factors, it is first necessary to identify factors that potentially affect the tool life. These variables are categorised and illustrated in a cause and effect diagram in **Figure 22** below.

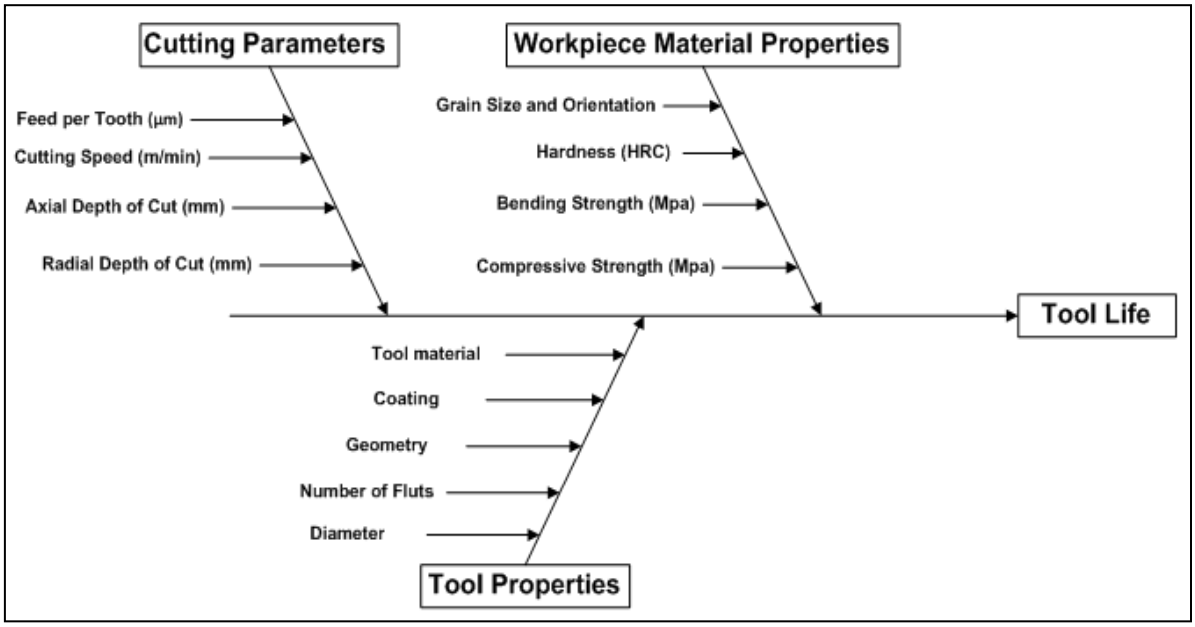

Figure 22 – Tool Life Cause and Effect Diagram

There are a number of potential factors, which may or may not influence tool life, illustrated above. To test all of these factors through experimentation would require an impossible effort in terms of the time and cost constraints of this project. In fact, a full factorial experiment at two levels using all of the factors listed above would require $2^{13} = 8192$ experiments. This amount could be reduced by using more efficiently designed experiments; however, it is the opinion of the author that this would still not bring the number of required experiments to a feasible amount.

It is clearly necessary to reduce the number of experimental factors. This could be achieved in a number of ways. Firstly, it is possible to narrow the scope of the investigation. For the purpose of this project, the work piece material has been predefined. As mentioned in section 2.2.1 on page 14, a unique material has been identified which exhibits a strong combination of the material properties needed for bipolar plates. By limiting the scope to one material (with fixed material properties), it is possible to reduce the number of experimental combinations significantly.

Further, it is possible to limit the scope of experimentation to one type and size of end mill. Consider the serpentine channels that run over the face of the bipolar plate. These channels have a fixed width and depth. Further, these channels, referred to as the major micro channels, account for approximately 80% of the total plate machining time. Therefore, they are the only bipolar plate feature considered in these experiments. For effective machining of the major micro channels, the approach must be taken to machine the width (and depth) of each channel in a single pass. Therefore, the diameter of the tool is limited to the width of the channels. It is assumed at this stage that the channel width is fixed (0.7 mm) and it is, therefore, possible to limit the scope of the experiments to one tool diameter.

Still further, the tool properties can also be simplified. Often, the ideal tool geometry and coating depends on the material being cut. There are tools, which have been specially developed for graphite machining. These tools have been designed for optimal tool life and surface finish when machining graphite and graphite composites. It is intuitive to think then that these tools would be the most economical and should thus be considered for the purpose of this project.

This is not the case, however, according to industry expert Sven Bornbaum. Mr Bornbaum is the project manager for fuel cell components at Schunk Kohlenstofftechnik GmbH. According to him, one would typically pay €100 for graphite specific micro end mills and achieve approximately 10 'bipolar plates worth' of tool life on each. On the other hand, a standard uncoated solid carbide end mills is priced at around €10 and lasts for approximately two 'bipolar plates worth' of machining. In addition, standard micro end mills can be used at the same material removal rates and achieve a similar surface finish as that of graphite specific tools.

Considering the information above, it is reasonable to limit the scope of the experiments to standard uncoated solid carbide end mills of diameter equal to that of the channel width.

Now the only experimental factors that remain are those relating to the cutting parameters. For the purpose of this project, though, it is not necessary to consider the radial depth of cut as an experimental factor. This is because all serpentine channels are formed using full emersion slot milling and, thus, the radial depth of cut remains constant at a value equal to the tool diameter.

As a result, the only experimental factors that remain are *feed per tooth (µm)*, *cutting speed (m/min)* and *axial depth of cut (mm).* Using only these experimental factors is consistent with other experimental based efforts to characterise tool life. Prakash, et al. (2002) characterised tool life in terms of *feed per tooth, cutting speed* and *depth of cut* using a *1 mm* micro end mill on pure copper. Further, Mayor and Sodermann (2009), investigated the cutting parameter space for its effect on micro end milling tool life, also on pure copper.

4.1.2 Design of Experiments (DOE)

The purpose of designing experiments is two-fold. Firstly, it is to enable the experiments to capture as much information regarding the relationship between input and response variables as possible. This includes not only first order main and interaction effects, but also, second order main effects if necessary. Secondly, the experiment must be economical. This means that it should require as few runs as possible. The efficiency of an experimental design is described by the amount of information obtained for a certain number of experimental runs. The more information and the fewer runs, the better the efficiency.

There are a number of useful experimental designs used in practice. Each of these designs has its own benefits and shortcomings. For example, a full factorial design with three levels per factor captures both first and second order main and interaction effects. This type of design has a resolution V, which is the best possible but typically requires more experimental runs than is often feasible. It should be noted here that design resolution is a measure of the degree to which certain effects are not measured independently of one another, otherwise known as confounding effects. Confounding is then an occurrence of an average change in response that cannot be attributed to any one effect in particular. On the other hand, using a Taguchi orthogonal array as an experimental design can significantly reduce the number of required runs. However, this design runs the risk of losing possible significant factor effects, through confounding. This is especially true if little is understood about the process being tested prior to experimentation.

The experimental design chosen for the purpose of this project has an additional objective, apart from being economical and capturing sufficient information. It must also result in data that are conducive to multiple linear regression analysis. In other words, it must be possible to fit an empirical function such that it is a good representation of the data. Still further it is required that the empirical function be a second order polynomial. The reason being that little is understood about the relationship between the input and response variables for this problem. As a result, it is necessary to accommodate the possibility that there is curvature in the response function i.e. it is not simply linear. As such, it is appropriate to use an experimental design that is conducive to fitting second order empirical functions. The Central Composite Design (CCD) is useful in this regard.

4.1.2.1 Central Composite Design (CCD)

The CCD is the most popular class of second-order designs, according to Myers, et al. (2009). It was first introduced by Box and Wilson in 1951 and much of the popularity of the CCD comes from the sequential nature of it.

The CCD consists of:

- *F* 2-level factorial points, where $F = 2^{k_e}$ and k_e is the number of experimental factors.
- $2k_e$ axial points and
- n_c centre runs

The sequential nature of the design is then as follows. Firstly, the *F* 2-level full factorial runs are completed. This represents a variance-optimal first order model that includes two factor interaction terms. From here, first order main effects as well as first order two factor interaction effects can be estimated from the resulting data. Thereafter the n_c centre runs are completed. These provide insight into whether or not there is non-linearity in the system. If this is the case, the $2k_e$ axial runs allow the pure quadratic terms to be estimated. Myers, et al. (2009), describe how the three components of the design play different roles.

- The *F* 2-level full factorial runs contribute significantly to the estimation of linear terms and two-factor interaction terms. In fact, these points are the sole contributors to the estimation of the interaction terms.
- The $2k_e$ axial points contribute significantly to the estimation of the second order terms (quadratic terms). Without axial points, only the sum of the second order terms could be estimated.
- The n_c centre runs also contribute to the estimation of the quadratic terms, but more importantly, provide an internal estimate of statistical error within the experiment (pure error).

4.1.2.2 Design Matrix, Geometric View and Selecting the Design Parameters

The experimental design is often represented in the form of a matrix, known as the design matrix. Each column in the design matrix represents one experimental factor. For the purpose of these experiments, three factors have been identified, namely *feed per tooth (f_t), cutting speed (v) and axial depth of cut (d).* Each row in the design matrix represents a combination of factor values to be tested, otherwise known as an experimental run. The design matrix essentially indicates the configuration of the factors at different levels as well as the sequence of experimental runs. A typical design matrix is shown below, with coded values, for a three factor Central Composite Design. Notice there are $2^3 = 8$ full factorial runs, $2x3 = 6$ axial runs and n_c centre runs.

$$D = \begin{matrix} v & f_t & d \end{matrix} \begin{bmatrix} -1 & -1 & -1 \\ 1 & -1 & -1 \\ -1 & 1 & -1 \\ 1 & 1 & -1 \\ -1 & -1 & 1 \\ 1 & -1 & 1 \\ -1 & 1 & 1 \\ 1 & 1 & 1 \\ -\alpha & 0 & 0 \\ \alpha & 0 & 0 \\ 0 & -\alpha & 0 \\ 0 & \alpha & 0 \\ 0 & 0 & -\alpha \\ 0 & 0 & \alpha \\ 0 & 0 & 0 \\ 0 & 0 & 0 \\ 0 & 0 & 0 \\ 0 & 0 & 0 \end{bmatrix}$$

8 Full Factorial Runs

6 Axial Runs

n_c Centre Runs

It is sometimes useful to represent the experimental design in geometric view. This helps to visualise the separate components of the design, namely the 2^3 full factorial runs, the *2 x 3* axial runs and the n_c centre runs. The geometric view of a CCD for $k_e = 3$ is shown in **Figure 23** below, where $x_1 = v$, $x_2 = f_t$ and $x_3 = d$.

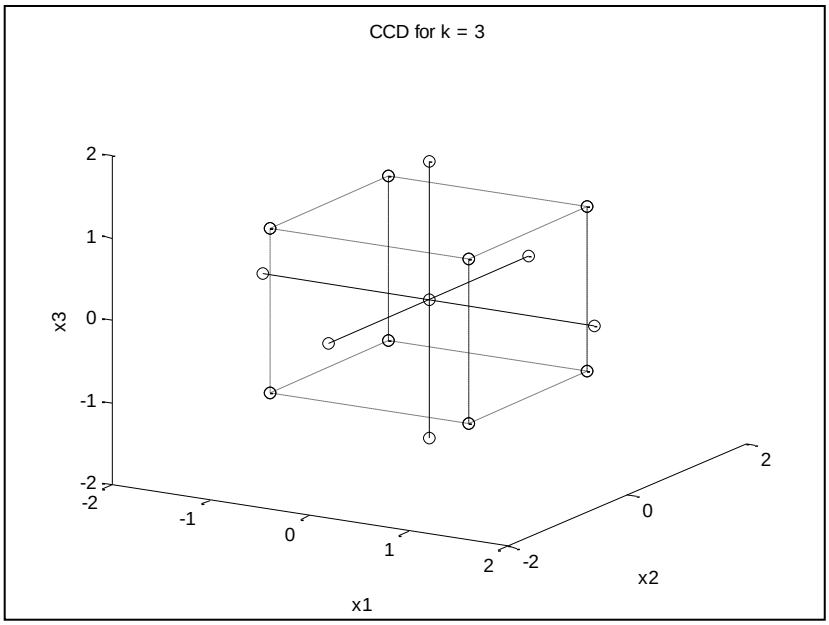

Figure 23 – Geometric View of CCD for $k_e = 3$

The flexibility of the Central Composite Design comes from the selection of the design parameters α and n_c, the axial distance from the centre and the number of centre runs respectively (Myers, et al. 2009). The selection of these parameters is closely related to design rotatability, an important

concept in Design of Experiments. Montgomery and Runger (2007), say that a rotatable design is one in which the standard deviation of the predicted response ŷ is constant at all points that are the same distance from the centre of the design. This is intended to create stability in the design in that the response is predicted with equal precision for all points that are the same distance from the centre of the design. This is despite the fact that the precision decreases with increasing distance from the centre.

A CCD may be made rotatable by the proper selection of the axial spacing α. General guidelines exist for the selection of α. Myers, et al. (2009), say that rotatability is achieved by using $\alpha = \sqrt[4]{F}$ where *F* is the number of factorial points. In the case of the tool life experiments, $F = 2^3 = 8$ factorial points, which results in $\alpha = \sqrt[4]{8} = 1.682$. Further, Myers, et al. (2009), state that the more centre runs used the better, although the recommended number for a CCD with $k_e = 3$ is 3 to 5 centre runs.

For the purpose of these experiments the design parameters of $\boldsymbol{\alpha = 1.682}$ and $\boldsymbol{n_c = 4}$ have been selected.

4.1.2.3 Selecting Experimental Factor Ranges

It is further necessary to select the range of values for each of the experimental factors. That is, an upper and lower bound for the *cutting speed*, *feed per tooth* and *depth of cut*. Before doing so, it is necessary to understand what the *region of interest* and the *region of operability* are for the situation at hand.

Verseput (2000), defines the *region of interest* as a geometric region characterised by lower and upper limits on experimental factor combinations that are of interest to the experimenter. In other words, the region of interest is the range in which the experimenter would like to test. The *region of operability*, on the other hand, describes the lower and upper limits of experimental factors that can be operationally achieved with acceptable safety and that will output a testable product. These concepts must be considered when defining the ranges for experimental factor levels.

The approach taken in defining the region of interest for the purpose of these experiments was two-phased. Firstly, the technical design of the bipolar plate was considered, taking into account the design features of the micro channels. More specifically, the *depth of cut* factor must correspond to the channel depth on the bipolar plate design. Secondly, an industry expert was consulted to identify typical ranges of *cutting speed* and *feed per tooth*. This was done because of the newness of the material used. Little is known about the machinability of the material, except by those who deal with it on a daily basis. The recommendations given by Sven Bornbaum, project manager at Schunk Kohlenstofftechnik GmbH, are listed below. These recommendations are geared towards improving

tool life while maintaining acceptable machining quality and come from the experience gained out of thousands of machined plates, according to Mr. Bornbaum. The recommendations are as follows:

- High-speed cutting is advantageous in terms of maintaining a good surface finish. This implies that the *cutting speed* parameter must be kept as high as possible.
- The *feed per tooth* parameter should be kept between 0.04 and 0.05 mm (40 and 50 µm). These are typically large values for *feed per tooth* in the micro machining realm.
- The *depth of cut* typically ranges between 0.2 and 2 mm. It can be inferred for this that typical channel depths for bipolar plates range between these values. This is because Schunk always employs the strategy to cut the channel depth (and width) in a single pass.

It is possible to make an inference from the recommendations above. A high *cutting speed* coupled with a large *feed per tooth* implies that Schunk are cutting at a high feed rate, given the relationship:

$$F_R = \frac{n \times b \times f_t}{1000} \quad \textbf{(8)}$$

where F_R *= feed rate (mm/min*), f_t *= feed per tooth, n = rotational speed (rpm*) and *b = number of teeth/flutes*. Since a high feed rate is associated with a shorter cutting time, it is reasonable to assume that Schunk selects their cutting parameters based mostly on productivity considerations. The purpose of this tool life model, however, is to characterise tool life over a broad spectrum of cutting parameters, in order to optimise total cost. This includes not only costs associated with cutting time, but also tooling costs.

The region of operability is limited to the capability of the machine used. That is, the achievable feed rates and rotational speeds are limited by the machine. Micro-machines are typically associated with high cutting speeds, because they employ high-speed spindles. Further, the small tool diameters in micro machining limit the allowable cutting force and as such, limit the achievable feed rates. Therefore, typical micro machines are not equipped to apply high feed rates.

The maximum achievable feed rate, for the purpose of these experiments, was limited by the particular micro milling machine used. It was *1654 mm/min*. This was a major consideration in the selection of cutting parameters for the purpose of these experiments.

After considering the limitations enforced by the machine, as well as the recommendations given by an industry expert, the following cutting parameter ranges were chosen.

Table 2 – Experimental Factor Ranges

Coded Values	-α	-1	0	1	α
			Natural Values		
Cutting Speed (m/min)	**47.5**	**56.621**	**70**	**83.379**	**92.5**
Feed per Tooth (µm)	**10**	**13.040**	**17.5**	**21.960**	**25**
Axial Depth of Cut (mm)	**0.2**	**0.5649**	**1.1**	**1.6351**	**2**

The specifications of the tools chosen are given in **Table 3** below

Table 3 – Tool Specifications

Specification	Description
Manufacturer	Performance Micro Tools
Type	TR Series Micro End Mills Standard Length
Part Number	TR-2-0280-S
Cutter Diameter	0.7112 mm
Tolerance on Cutter Diameter	± 0.0127 mm
Flute Length	2.1336 mm
Shank Diameter	3.175 mm
Overall Length	38.1 mm
Number of Flutes	2
Material	Solid Carbide
Price	USD 9.65

4.2 Executing the Experiments

This section describes the practical aspects involved with executing the experiments and recording the data.

4.2.1 The Physical Experimental Setup

The machine used for these experiments was the Minitech 12528 from Minitech Machine Corporation. The physical setup of this machine was relatively straightforward for this purpose. Flat blank plates, obtained from Schunk, were fixed to the worktable using mechanical clamps on two sides. This method provides sufficient clamping force and machining tolerance for this purpose. The setup is shown below.

Figure 24 – The Machine Setup

Another consideration when conducting the experiments is the matter of dust that forms during the material removal process. Graphite machining is synonymous with dust formation, and this graphite composite is no different. The dust is formed due to the brittle nature of the material and has the capacity to compromise the integrity of the experiment by accumulating in the cutting path, creating additional friction and wear as a result. Further, the graphite dust can clog the exposed moving parts of the machining and, if left unattended, can damage the machine. Still further, there is a health risk associated with inhaling the airborne dust particles. It is, therefore, of utmost importance to attach a vacuum feature that removes the dust during machining. For these experiments, a plastic pipe,

attached to a powerful portable vacuum, was used. The pipe was held in position by a wire spring system, as seen in **Figure 24**.

4.2.1.1 Generating the Cutting Path

N-Code was developed to cut one long path, ensuring that the direction of feed is always at 45°, relative to the X-axis. The cutting path is, essentially, diagonal along the worktable. This was done for an important reason. The maximum feed rate in any one axis-direction is limited by the capacity of the drive motor controlling that axis. In the case of the milling machine used, the maximum feed rate achievable by any one axis, is 1170 mm/min. This would severely limit the range of testable cutting parameters. However, by ensuring the cutting path is diagonal across the worktable, both X and Y-axis drive motors are activated simultaneously, resulting in a notably higher combined feed rate. The combined feed rate is thus:

$$F_{R\,Max} = \sqrt[2]{F^2_{R\,Max\_YAxis} + F^2_{R\,Max\_YAxis}} \qquad (9)$$

$$= \sqrt[2]{1170^2 + 1170^2} = 1654.63\ mm/min$$

where $F_{R\,Max}$ = *maximum achievable feed rate (combined),* $F_{R\,Max\_X\,Axis}$ and $F_{R\,Max\_Y\,Axis}$ are the maximum feed rates in the *X* and *Y* directions respectively. The resulting cutting path is shown in **Figure 25** below.

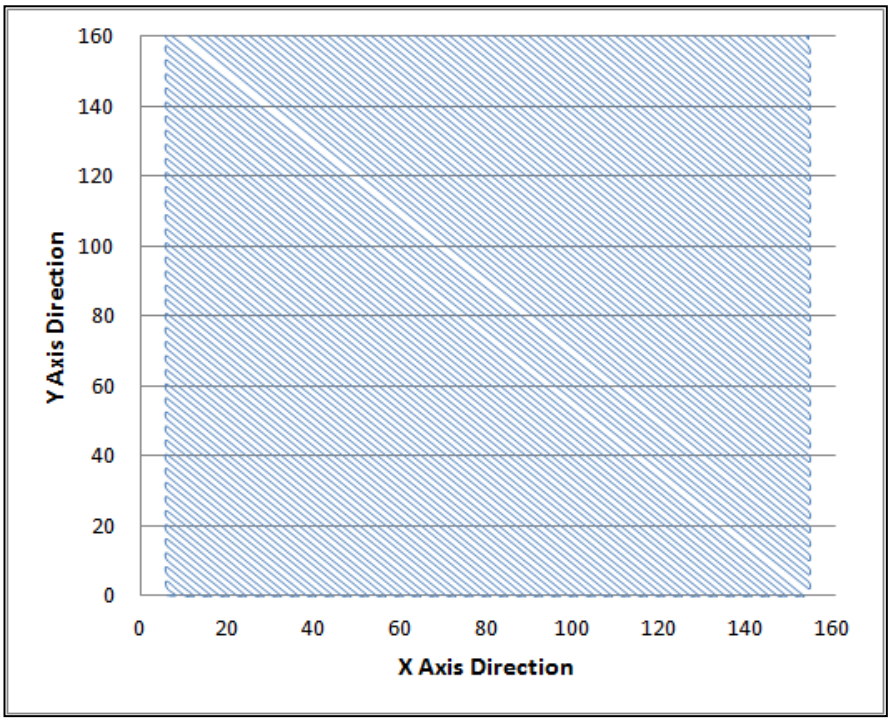

Figure 25 – Cutting Path

4.2.1.2 Setting the Machine Parameters

Another practical consideration when setting up the experiments was the setting of the machine input parameters (*feed rate* and *rotational speed*), based on the experimental factor values (*cutting speed and feed per tooth*). Both machine input parameters can be derived directly from the experimental factors according to the following formula:

$$n = \frac{v \times 1000}{\pi \times D} \quad \textbf{(10)}$$

and

$$F_R = \frac{n \times b \times f_t}{1000} \quad \textbf{(11)}$$

where, *n = rotational speed (rpm)*, *v = cutting speed (m/min)*, *D = tool diameter (mm)*, F_R *= feed rate (mm/min)*, *b = number of teeth* (= 2 for these experiments), and f_t *= feed per tooth (µm)*.

Specifying the feed rate and depth of cut is simply a matter of inserting the values into the Minitech control program. This can be done to precise values (usually up to three or four thousandths of a millimetre). However, in the case of the Minitech machine, the spindle has its own control system that is used to control the rotational speed. When used on the 'manual' setting, the rotational speed can only be adjusted in increments of 1000 rpm. This method of control was seen as too rigid for these experiments where more precise rotational speeds are required.

The spindle, however, also has the option to control the rotational speed on the 'automatic' setting. On this setting, the rotational speed is controlled via an externally supplied DC voltage. This DC voltage (0 – 9V) sets the rotational speed proportionally (1000 – 60 000 rpm). If the control voltage is monitored accurately (to two decimal places) with a multi-meter, the rotational speed can then be controlled in increments of 67 rpm. This solution, although not perfect, compared to controlling the rotational speed in increments of 1000 rpm, seemed reasonable.

4.2.2 Measuring Tool Life

In the case of tool life experiments in general, recording the data is not a simple matter of reading the results. This is largely due to the nature of tool failure and the way in which tool life is defined.

4.2.2.1 Deciding on Criteria for Tool Life

Tools typically fail or stop functioning correctly in one of two ways. Either they fail catastrophically and suddenly or they fail gradually. In this context, failure refers to the point where the tool no longer fulfils its function sufficiently.

Catastrophic failure is characterised by tool breakage. This is an extreme failure mechanism and can occur for a number of reasons. Tansel, et al. (1998), identified two main reasons for catastrophic tool failure. These are:

- Chip clogging – Chip clogging occurs when material chips (or dust) obstruct the cutting edge from further material removal. This can lead to a continuous increase in cutting force and eventually breakage. This problem can be avoided in micro milling operations by using a tool with two cutting edges. This is because cutting depth is typically small and each cutting edge is only engaged for about half a revolution for full emersion slot milling.
- Fatigue – Breakage can occur after an extended period of wear. As tool wear occurs, so the cutting edge radius increases, leading to a corresponding increase in cutting force. This is because the larger the cutting edge radius, the more force is required to mechanically remove workpiece material. This increased cutting force may then result in eventual tool breakage, although not necessarily immediately. As the tool rotates, the stress in the shaft will shift between points. This cyclical shift results in fatigue in the shaft and eventual breakage. Tansel, et al. (1998), say that this is often the reason for failure when the workpiece material is soft and brittle, such as graphite.

Gradual failure is characterised by wear to the extent that the tool no longer functions sufficiently for the purpose. Firstly, this can mean that the tool no longer produces a satisfactory surface finish or quality of cut. Secondly, in the case of micro milling, it can mean that the diameter of the tool and subsequently the channel width, no longer falls within the channel tolerance limit. This can happen as micro end mills are known to wear over the whole length of shaft immersed in the workpiece material. Owing to the small size and difficulty with visual tool inspection, the reduction of the starting diameter is often used to quantify tool wear. This is unlike conventional machining where flank and rake wear are traditionally used to quantify tool wear.

Filiz, et al. (2007), used this method during their experimental investigation of the micro machinability of copper 101 with tungsten carbide micro end mills. In order to investigate wear progression, they conducted a number of experiments in which channels of nominal depth 30 µm were machined at three different speed levels and four feed levels. They noticed considerable reduction in tool diameter and used this as an indication of tool wear. Further, instead of measuring the tool itself, they used the channel widths as the actual measure of tool wear. This is because channel widths are more easily measurable under a microscope. The Society of Manufacturing Engineers (1983), define this method of judging tool failure as size failure. That is, the occurrence of a change in dimension of the finished part by a certain amount. The convenience of this method is

that the position along the cutting path acts as a time-stamp, allowing almost continuous estimation of tool wear over time.

The method of using tool diameter reduction as a measure of tool wear in micro end milling is further validated by industry practice. Schunk also monitors the channel width to ensure that it remains within the tolerance limits specified by the design of the bipolar plate. The moment, the channel width reduces below the tolerance limit, the tool is changed.

Owing to the convenience of using the reduction in channel width as a measure of tool wear and the validation for this method found in literature and industry, this method was chosen for the purpose of these experiments. Further, it was necessary to define the point where tool wear is considered excessive.

4.2.2.2 Deciding on the Critical Amount of Tool Wear

It is intuitive to try to maximise the amount by which the tool diameter is allowed to reduce, while remaining within the channel tolerance limits. Consider the hypothetical situation where the starting tool diameter is exactly equal to the upper channel tolerance limit. Then it is possible to get a useful tool life that corresponds to a reduction in tool diameter equal to the full channel tolerance range. However, the reducing channel width is not the only consideration. There is also the matter of the quality of the machined surfaces.

The workpiece material in question has a tendency to chip on the edge of the channel ribs. This chipping increases as machining progresses, which suggests that it is related to tool wear. Consider the images shown in **Figure 26** below.

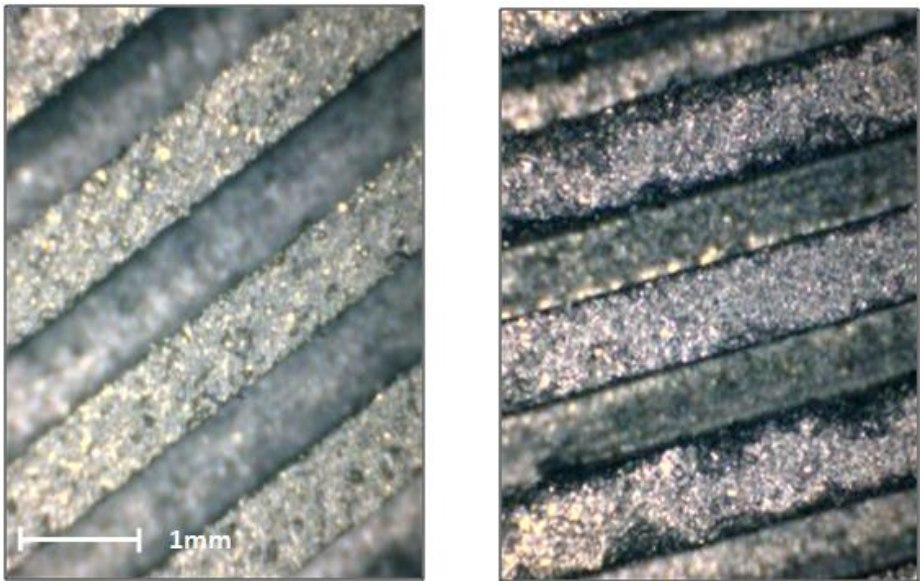

Figure 26 – Images Comparing Channels Machined with New and Worn Tools

The images above show machined channels, at a scale of approximately 18:1. The image on the left shows micro channels at the start of a cut (new tool), while the image on the right shows micro channels after approximately 16.8m of cutting (worn tool). Consider the image of the worn tool. The chipping that occurs on the edge of the channel ribs is indicative of a worn tool. It would be possible to compare a quantitative measure of the chipping to the amount of tool wear. Even though this was not done for the purpose of this project, the author is convinced that a positive correlation between tool wear and rib chipping would occur.

The evidence of chipping presented above places a constraint on the amount of tool wear, in terms of diameter reduction, that is tolerable. On the one hand, it would be advantageous to maximise the tool life by allowing as much tool wear as possible. On the other hand, allowing a tool to wear too much creates excessive surface defects, which could negatively affect the performance of the bipolar plate during operation. It was, therefore, necessary to balance these objectives when deciding on a critical amount of tool wear, beyond which the tool was considered worn and no longer useful for the purpose.

Deciding on the critical amount of wear tolerable is a subjective process, relying on good judgement rather than empirical evidence. This is because the negative effect of rib chipping on the performance of the bipolar plate is not yet quantifiable. Rib chipping reduces the contact surface between the bipolar plate and the MEA, which could reduce the electrical conductivity between the two. Further, severe chipping may allow fuel cell fluid to flow between channels, which is also possibly an undesirable effect.

Making liberal assumptions about the tolerable tool wear can compromise the integrity and usefulness of the tool life model. For this reason, a more conservative approach was taken. The tolerable wear, for the purpose of this model, was decided to be 100 µm worth of wear. In other words, the life of the tool was measured up to the point where the nominal tool diameter had reduced by 100 µm.

4.2.2.3 Recording Tool Life

As stated earlier, there are typically two ways in which tools fail. These are either catastrophically, where the tool breaks, or gradually, where the tool wears. For the purpose of these experiments, both of these failure mechanisms were considered. The tool life after each experimental run was recorded as the length of cut, up to the point where the earliest failure mechanism occurred.

In the case where the tools failed catastrophically, the tool life could easily be determined via visual inspection, based on the number and length of channels machined successfully. This is provided the tool wear had not exceeded the critical amount prior to breaking.

In the case where tools failed gradually, the measurement of tool life required more effort. Each completed plated had 153 micro channels machined into it. Further, the channels were not of equal length. It was necessary to identify the point where the tool wear was equal to the critical amount. This was done by taking several measurements of the channel widths spaced over the total cutting path. These channel widths were compared to the starting width to determine the reduction. Photographs of the channels were taken, at certain points along the cutting path, under an optical microscope with 102 times optical zoom. Measurements of the channel widths were then taken from the photographs using calibrated computer software. See below for an example of a photograph of a micro channel used for measurement.

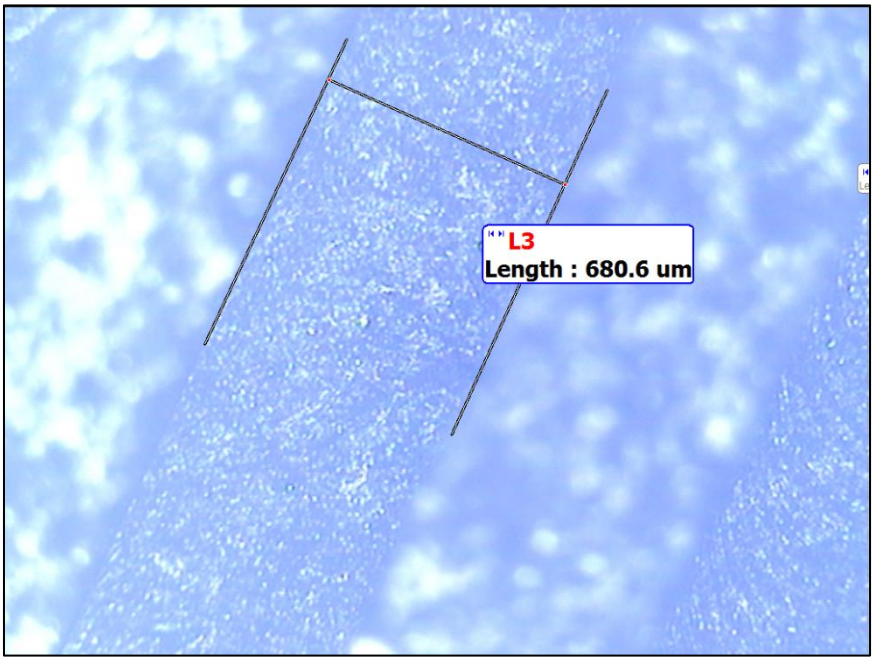

Figure 27 – Image used to Measure Channel Width

Invariably, the exact point at which the wear was 100 µm was not at the point where the photographs were taken. So, short of photographing and measuring every micro channel for every experiment, is was necessary to interpolate over the recorded wear versus cutting length to find the point of 100 µm wear.

4.2.2.4 Results

The results of the experiments are presented in the table below.

Table 4 – Experiment Results

Run	Coded Experimental Factors Values			Natural Experimental Factor Values			Machine Parameters		Tool Life (mm)
	Cutting Speed	Feed/tooth	Depth of Cut	Cutting Speed (m/min)	Feed/tooth (um)	Depth of Cut (mm)	RPM	Feed Rate (mm/min)	
1	-1	-1	-1	56.621	13.040	0.565	25342	660.941	12886.497
2	1	-1	-1	83.379	13.040	0.565	37318	973.276	5144.530
3	-1	1	-1	56.621	21.960	0.565	25342	1112.992	5570.790
4	1	1	-1	83.379	21.960	0.565	37318	1638.951	9636.601
5	-1	-1	1	56.621	13.040	1.635	25342	660.941	13466.417
6	1	-1	1	83.379	13.040	1.635	37318	973.276	15036.808
7	-1	1	1	56.621	21.960	1.635	25342	1112.992	10873.640
8	1	1	1	83.379	21.960	1.635	37318	1638.951	9713.592
9	-1.6818	0	0	47.500	17.500	1.100	21259	744.081	19410.052
10	1.6818	0	0	92.500	17.500	1.100	41400	1448.999	20902.941
11	0	-1.6818	0	70.000	10.000	1.100	31330	626.594	11237.564
12	0	1.6818	0	70.000	25.000	1.100	31330	1566.486	29299.892
13	0	0	-	70.000	17.500	0.200	31330	1096.540	7950.618
14	0	0	1.681	70.000	17.500	2.000	31330	1096.540	13739.308
15	0	0	0	70.000	17.500	1.100	31330	1096.540	17400.874
16	0	0	0	70.000	17.500	1.100	31330	1096.540	17347.656
17	0	0	0	70.000	17.500	1.100	31330	1096.540	20320.245
18	0	0	0	70.000	17.500	1.100	31330	1096.540	21211.358

4.3 Analysis of the Experimental Data

This section details all of the practical and academic aspects involved in the analysis of the experimental data. This includes a description of the statistical and other tools used for the analysis.

The purpose this tool life model is to characterise tool life in terms of cutting parameters. The relationship can be formalised as follows:

$$L_T = f(f_t, v, d) + \varepsilon \quad \textbf{(12)}$$

where f_t = *feed per tooth (μm)*, *v = cutting speed (m/min)*, *d = axial depth of cut (mm)* and ε = *statistical error on the measured response.*

For this application, as with any application of RSM, the form of the true response $f(f_t, v, d)$ is unknown and probably very complicated. It is for this reason that the term *ε* is included. It accounts for effects such as measurement error and sources of variation that are inherent in the process or system (Myers, et al. 2009). Other sources of variation, in this case, may include inconsistency in the workpiece material or cutting tools. The term *ε* is thus treated as a statistical error that follows the standard normal distribution with a mean of zero and variance of σ^2. If the expected value of *ε* is zero, then

$$E(L_T) = E\big(f(f_t, v, d)\big) + E(\varepsilon) \quad \textbf{(13)}$$
$$= f(f_t, v, d)$$

The variables *v*, f_t and *d* are known as the natural variables because they are expressed in natural units of measurement (Myers, et al. 2009). In RSM, it is sometimes convenient to work with coded variables such as x_1, x_2 and x_3, which are dimensionless with a mean of zero and the same standard deviation as the natural equivalent. Coded variables are linear transformations of their natural equivalents. The generic form of the transformation equation is

$$x_i = \frac{y_i - y_{i0}}{y_{i1} - y_{i0}} \quad \textbf{(14)}$$

where *i = 1,2,3*; y_i represents the natural equivalent of x_i and y_{i0} and y_{i1} represent the natural values at coded values of *0* and *1* respectively. It follows then that the specific transforming equations are

$$x_1 = \frac{v - 70\ m.min^{-1}}{13.3786\ m.min^{-1}} \quad \textbf{(15)}$$

$$x_2 = \frac{f_t - 17.5\ \mu m}{4.4595\ \mu m} \quad \textbf{(16)}$$

$$x_3 = \frac{d - 1.1\ mm}{0.5351432\ mm} \quad \textbf{(17)}$$

where x_1, x_2 and x_3 represent the coded variables for *cutting speed*, *feed per tooth* and *axial depth of cut* respectively. The response function can now be represented in terms of the coded variables by

$$L_T = f(x_1, x_2, x_3) \quad \textbf{(18)}$$

The true form of *f* is unknown and must, therefore, be approximated using a regression model. Either a first order or a second order regression model is used for this purpose. The second order model is most widely used for the following reasons, courtesy of (Myers, et al. 2009):

- The second order model is highly flexible because it can take on a variety of forms. For this reason, a good approximation of the true response surface can often be found.
- It is easy to estimate the regression coefficients in the second order model. The method of least squares is often used for this purpose.
- Practical experience indicates that second order models work well in solving real response world problems.

Following the argument above, a second order model is used for this purpose. The general form of a second order model is shown below.

$$L_T = \beta_0 + \sum_{j=1}^{k} \beta_j x_j + \sum_{j=1}^{k} \beta_{jj} x_j^2 + \sum_{i<j} \sum_{j=2}^{k} \beta_{ij} x_i x_j \quad \textbf{(19)}$$

The coefficients of regression (β's) are estimated using the method of least squares as it forms part of linear regression analysis. The flexibility of the second order model is demonstrated by the number of possible terms, which may or may not be included in the final model. In general, it is possible to find a good approximation of the true response by testing different combinations of terms.

It should be noted here, the close relationship between RSM and linear regression analysis. Consider the model above. The β's are a set of unknown parameters, which must be estimated to complete the model. This is done by collecting data on the system (through experimentation in this case) and using this data to estimate the parameters. Myers, et al. (2009), describe linear regression analysis as the branch of statistical analysis that uses these data to estimate the β's.

4.3.1 Multiple Linear Regression Analysis

A linear regression model can be thought of as an empirical model where some response function *Y* is related to *k* independent or regressor variables. Multiple linear regression analysis refers to the case where *k > 1*. In other words, the response variable is related to multiple regressor variables. Consider the general from of a second order regression model as shown in **Equation (19)**.

It can be seen that the shape of the response L_T is non-linear, owing to the presence of second order terms. Despite this, the model is still considered a 'linear' regression model. Montgomery and Runger (2007), say that, in general, any regression model that has linear regression coefficients (β's) is a linear regression model, regardless of the shape of the response that is generated.

The regression coefficient β_j represents the expected change in the response T_L per unit change in x_j provided that all remaining regressor variables x_i, for $i \neq j$, are held constant. In other words, β_j represents the mean effect of regressor x_j.

4.3.2 Least Square Estimates of Regression Coefficients – A Matrix Approach

The least squares estimate of parameters is used for estimating the regression coefficients. The underlying principal of least squares estimation is to determine the regression coefficients such that the residual error is minimised. Montgomery and Runger (2007), describe a useful way of estimating the regression coefficients using a matrix algebra approach. A description of this follows below. Experienced readers can skip to Section 4.3.3.

Suppose there are *k* regressor variables and *n* observations, (x_{i1}, xi_2, …, x_{ik}, y_i) for *i = 1, 2, …, n*. In addition, the model relating the regressors to the response is

$$y_i = \beta_0 + \beta_1 x_{i1} + \beta_2 x_{i2} + \ldots + \beta_k x_{ik} + \epsilon_i \quad for\ i = 1,2,\ldots,n$$

This model is a system of *n* equations and can be expressed in matrix notation as

$$\boldsymbol{y} = \boldsymbol{X\beta} + \boldsymbol{\epsilon}$$

where

$$\boldsymbol{y} = \begin{bmatrix} y_1 \\ y_2 \\ \vdots \\ y_n \end{bmatrix} \qquad \boldsymbol{X} = \begin{bmatrix} 1 & x_{11} & x_{12} & \cdots & x_{1k} \\ 1 & x_{21} & x_{22} & \cdots & x_{2k} \\ \vdots & \vdots & \vdots & & \vdots \\ 1 & x_{n1} & x_{n2} & \cdots & x_{nk} \end{bmatrix} \qquad \boldsymbol{\beta} = \begin{bmatrix} \beta_0 \\ \beta_1 \\ \vdots \\ \beta_k \end{bmatrix} \qquad \boldsymbol{\epsilon} = \begin{bmatrix} \epsilon_1 \\ \epsilon_2 \\ \vdots \\ \epsilon_n \end{bmatrix}$$

Now, the goal is to find the vector of least squares estimators $\widehat{\boldsymbol{\beta}}$ that minimises the least squares function defined as

$$L = \sum_{i=1}^{n} \epsilon_i^2 = \boldsymbol{\epsilon'\epsilon} = (\boldsymbol{y} - \boldsymbol{X\beta})'(\boldsymbol{y} - \boldsymbol{X\beta})$$

The least squares estimator $\widehat{\boldsymbol{\beta}}$ is an unbiased estimator for $\boldsymbol{\beta}$ in the equations

$$\frac{\partial L}{\partial \boldsymbol{\beta}} = \boldsymbol{0}$$

Then by taking the partial derivatives as described above, the resulting equations that must be solved are

$$\boldsymbol{X'X\widehat{\beta}} = \boldsymbol{X'y}$$

Then by manipulation, the least squares estimates of $\boldsymbol{\beta}$ are

$$\widehat{\boldsymbol{\beta}} = (\boldsymbol{X'X})^{-1}\boldsymbol{X'y}$$

Finally, the fitted regression model is given by

$$\widehat{\boldsymbol{y}} = \boldsymbol{X\widehat{\beta}}$$

4.3.3 Model Building

One of the advantages of using a second order regression model, as mentioned previously, is that it is highly flexible because it can take on a variety of forms. Consider again the general form of a second order model as presented in **Equation (19)**.

The final model, based on the general form can take on any finite combination of first order, second order and/or interaction terms. Strictly speaking, if there are *K* candidate regressor variables, then there are $2^K - 1$ possible regression equations. For this reason, a good approximation of the true response surface can often be found with a second order model.

According to Montgomery and Runger (2007), an important consideration in regression analysis involves selecting the set of regressor variables to be used in the model. This is known as variable selection. The analyst can often specify the set of variables to use; based on theoretical considerations. However, this was not the case for this project. This is because little is known about the mechanics of micro machining a graphite-composite material or the tool life implications. It is, therefore, necessary to regard all possible regression equations as candidate equations.

One approach to variable selection, as described by Montgomery and Runger (2007), is to consider all possible regressions. This requires that the analyst fit all possible regression equations involving one variable, then two variables, then three variables etc. The regressions are then evaluated according to some universal criterion and the 'best' model is selected. A commonly used criterion to evaluate the fit of a model is *adjusted* R^2 (R^2_{adj}).

4.3.4 Adjusted R^2 to Assess the Fit of the Regression Model

The coefficient of multiple determination, R^2, is a commonly used criterion to evaluate the fit of a regression model. R^2 is defined by the formula

$$R^2 = \frac{SS_R}{SS_T} = 1 - \frac{SS_E}{SS_T}$$

where SS_T, SS_R and SS_E are the t*otal,* r*egression* and e*rror sum of squares* respectively. These concepts are elaborated on in Section 4.3.7 on page 73.

The R^2 statistic is a measure of the variability accounted for by the model. However, there is a problem with using the R^2 value as a measure of the quality of fit. This is because the R^2 value always increases when an additional regressor variable is added to the model. Essentially then, the highest R^2 value will always occur when all the candidate regressor variables are incorporated. This makes it difficult to interpret the final model as well as the benefit of including each regressor variable.

It is often better to use the *adjusted* R^2 given by the formula

$$R^2_{adj} = 1 - \frac{SS_E/(n-p)}{SS_T/(n-1)}$$

Since $SS_E/(n-p)$ is the error mean square and $SS_T/(n-1)$ is constant, R^2_{adj} will only increase when a regressor variable is added, if that variable reduces the error mean square. Therefore, the model that maximises R^2_{adj} value also minimises the mean square error. The R^2_{adj} statistic essentially guards against over fitting by penalising the model for adding terms that are not useful (Montgomery and Runger 2007). The R^2_{adj} value is expected to increase each time a regressor variable is added, but only up to a point. In fact, the R^2_{adj} statistic actually tends to decrease after a while.

4.3.5 Selection of Regressor Variables in the Tool Life Model

In Section 4.1.1 on page 48, it was shown how the cutting parameters were selected as experimental factors for the tool life experimental design. These cutting parameters are *cutting speed (v), feed per tooth (f_t)* and *axial depth of cut (d).* Now, because it was decided to apply a second order model for the reasons listed in Section 4.1.2 on page 50, there are 9 candidate regressor variables. These include 3 first order main effects (*v, f_t, d)*, 3 second order main effects *(v^2, f_t^2, d^2)* and 3 interaction effects *($v*f_t$, v*d, f_t*d)*. This means that $2^9 - 1 = 511$ possible combinations of regressor variables exist. The approach taken for the purpose of the tool life model was to evaluate all of the possible regressions using the R^2_{adj} statistic. It was therefore necessary to code a short program using Matlab™ that evaluated all possible regressions in this way. The regression model with the highest R^2_{adj} value was selected as the 'best'.

When considering tool life, it is important to bring clarity to the definition. That is, the life of a tool can be defined in several ways. These are cutting length (mm), cutting time (min) or total volume of material removed (mm^3). There is some discrepancy in literature regarding the correct way to define tool life.

Mayor and Sodemann (2009), investigated the parameter space for tool life in the micro milling of copper. They concluded that the amount of variation attributed to the cutting parameters (R^2_{adj}), is highest when tool life is defined in terms of volume of material removed. They say that this suggests that cutting parameters can best be optimised when tool life is measured in terms of volume of material removed. Prakash, et al. (2002), on the other hand, were successful when modelling tool life as defined by cutting length. They developed an empirical model for the micro milling of copper using 1 mm end mills.

The disparity seen in literature provides grounds for considering various definitions of tool life when developing a tool life model. Three definitions are considers for this model. These include, volume of material removed, cutting length and cutting time.

The tool life data was originally measured and recorded in terms of *cutting length (CL)*. It is, however, easy to transform it into *volume of material removed (VMR*) and *cutting time (CT*) according to the formulae

$$VMR = CL \times d \times D \quad \textbf{(20)}$$

and

$$CT = \frac{CL}{FR} \quad \textbf{(21)}$$

where *VMR = volume of material removed (mm^3), CL = cutting length (mm), d = axial depth of cut (mm), FR = feed rate (mm/min), D = tool diameter (mm)* and *CT = cutting time (min)*. The Matlab™ program mentioned previously was used to determine the highest possible R^2_{adj} value for each definition of tool life considering all possible regression models. The results are shown in **Table 5** below.

Table 5 – Maximum Adjusted R Square for Different Definitions of Tool Life

	Tool Life		
	Cutting Length	**Volume of Material Removed**	**Cutting Time**
Maximum R^2_{adj}	0.3222	0.6330	0.5697

It is plain to see that the highest R^2_{adj} value is achieved when defining tool life in terms of volume of material removed. This suggests that a regression model using tool life defined in this way will yield the most promising results.

However, the low R^2_{adj} value is cause for concern, indicating that the initial model is not a sufficient representation of the data. A normal probability plot of the regression model resulting from the model selection is shown in **Figure 28** below.

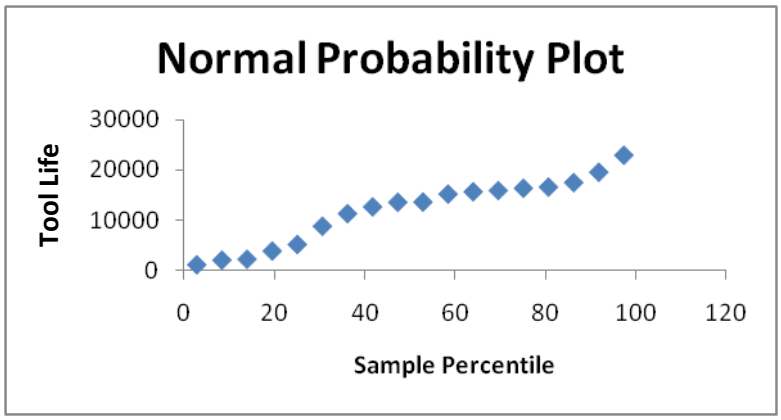

Figure 28 – Normal Probability Plot for Non-Transformed Analysis

The normal probability plot tests for the normality assumption in linear regression analysis. This is the assumption made that the data follow a normal distribution. If the normal probability plot

follows approximately a straight line, then the data are assumed normally distributed. Visual inspection of the figure above shows distinct curvature in the shape of the graph, indicating a possible violation of the normality assumption. Myers, et al. (2009), suggest that when this plot indicates a problem with the normality assumption a transformation of the response variable should be considered as a remedial measure.

Transformations are used in regression analysis for three reasons. These are, according to Myers, et al. (2009):

- To stabilise the response variance
- To make the distribution of the response variance tend more towards the normal distribution
- To improve the fit of the model to the data

Further, Myers, et al. (2009), say that transforming the response variable can be reasonably effective at accomplishing more than one of the above objectives simultaneously.

It was, therefore, decided to transform the response variable. The most commonly used transformation is to take the natural logarithm of the response variable. The new relationship between the input variables and response function can now be formalised as follows:

$$ln(L_T) = f(f_t, v, d) + \varepsilon \quad \textbf{(22)}$$

or by making L_T the subject of the formula,

$$L_T = e^{f(f_t,v,d)+\varepsilon} \quad \textbf{(23)}$$

The same procedure was followed as the one for the non-transformed analysis. The Matlab™ program mentioned previously was used to determine the highest possible R^2_{adj} value for each definition of tool life considering all possible regression models. The results are shown in **Table 6** below.

Table 6 – Maximum Adjusted R Square for Different Transformed Definitions of Tool Life

	Tool Life		
	***ln*(CL)**	***ln*(VMR)**	***ln*(CT)**
Maximum R^2_{adj}	0.3619	0.8405	0.5697

The table above indicates vastly improved results when the natural logarithm of the response variable is taken. It is reaffirming to note that the maximum R^2_{adj} value occurs when tool life is defined as the volume of material removed. This is consistent with previous analysis.

The normal probability plot of the transformed data, shown below in **Figure 29**, indicates an improved adherence to the normality assumption. This is indicated by the 'straightness' of the graph and validates the decision to transform the response variable.

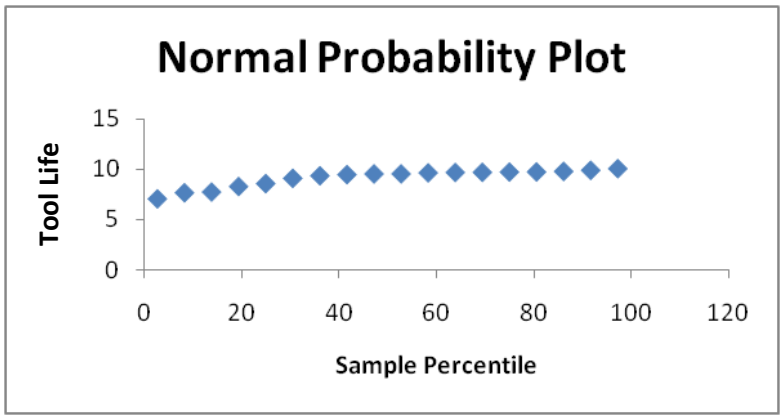

Figure 29 – Normal Probability Plot for Transformed Analysis

Further transformation of either the response or input variables is ill advised. In a situation, where the simpler-the-better further transformations will only complicate the model, making interpretations more difficult and less intuitive. It was, therefore, decided to accept the model as shown below.

4.3.6 Regression Results

The results of the regression analysis are discussed presently. Regression analysis was done using MS Excel™. This software has a useful regression analysis toolbox that is capable of handling multiple linear regression analysis. The critical regression statistics are presented in **Table 7** below.

Table 7 – Regression Summary Statistics

Regression Statistics	
Multiple R	0.9420
R^2	0.8874
R^2_{adj}	0.8405
Standard Error – $\hat{\sigma}$	0.3556
Variance – $\hat{\sigma}^2$	0.1265
Observations	18

R^2_{adj} can be interpreted as an estimate of the amount of variation in the data that is accounted for by the regression model. In the case of this model, *84.05%* of the variation in the observed data is accounted for by the model. The variance of the error term ε is estimated by $\hat{\sigma}^2$, where this is an unbiased estimator of the true variance σ^2. By unbiased estimator it is meant that $E(\hat{\sigma}^2) = \sigma^2$.

The regression results are presented in **Table 8** below.

Table 8 – Regression Results

	Coefficients	*Standard Error*	*t Stat*	*P-value*	*Lower 95%*	*Upper 95%*
Intercept	5.84236	0.50716	11.51969	0.00000	4.73735	6.94738
d	5.27527	0.77244	6.82932	0.00002	3.59226	6.95828
$\mathbf{v^2}$	-0.00035	0.00020	-1.71682	0.11169	-0.00079	0.00009
$\mathbf{f_t^2}$	-0.00506	0.00317	-1.59501	0.13669	-0.01197	0.00185
$\mathbf{d^2}$	-1.72381	0.34146	-5.04830	0.00029	-2.46780	-0.97983
$\mathbf{v*f_t}$	0.00270	0.00158	1.71410	0.11220	-0.00073	0.00614

The results above show the combination of regression terms that result in the 'best fitting' model. They indicate a strong influence from the depth of cut parameter *d*. Further, several second order terms are indicated in the model. This validates the decision to fit a second order model.

The coefficients for each term are estimated by the method of least squares as described previously. The least squares estimator is an unbiased estimator of the true regression coefficient, which is unknown.

The *t-Stat* value is a statistic used to test whether the regression coefficients are significant to the model. The hypothesis to test if an individual regression coefficient, say β_j equals a value β_{j0} is (Montgomery and Runger 2007):

$$H_0: \beta_j = \beta_{j0}$$

$$H_1: \beta_j \neq \beta_{j0}$$

The test statistic for this hypothesis is

$$T_0 = \frac{\widehat{\beta_J} - \beta_{j0}}{\sqrt{\hat{\sigma}^2 C_{jj}}} = \frac{\widehat{\beta_J} - \beta_{j0}}{se(\beta_{j0})}$$

where $se(\beta_{j0})$ is the standard error of β_{j0}. If β_{j0} is set to zero i.e. β_j is tested to see if it is equal to zero, then, in effect, β_j is tested to see if it is significant to the model. The *t-Stat* in the table above tests to see if the regression coefficients are significant to the model, by testing the hypothesis

$$H_0: \beta_j = 0$$

$$H_1: \beta_j \neq 0$$

The hypothesis is rejected if $|T_0| > t_{\alpha/2,\ n-p}$, where *n* is the number of observations and *p* is the number of parameters in the regression model. In this case, taking $\alpha = 5\%$, $t_{\alpha/2,\ n-p} = t_{0.025,\ 12} = 2.179$. It can be seen that for *3* out of the *6* regression parameters, no sufficient evidence exists to reject the null hypothesis. These parameters are v^2, f_t^2 and $v*f_t$ (notice here again the significance of terms including the *depth of cut, d*). Thus, it cannot be concluded that these parameters contribute

significantly to the model. What this implies is that those coefficients whose hypotheses tests were not rejected may be deleted from the model without reducing the quality of the fit.

This might be cause for concern; however, the test described here is only a partial or marginal test. This means that the value of the regression coefficients $\hat{\beta}_j$ depend on the presence and value of the other regressor variables x_i ($i \neq j$). For this reason, it cannot be said that the exclusion of any of the above terms would result in a better fit. Further, the combination of regression terms used above yielded the highest R^2_{adj} value out of any combination. Still further, the regression model, as a whole, passes the test for significance of regression with flying colours. A description of this follows shortly.

4.3.7 Using Analysis of Variance to Test the Significance of Regression

The Analysis of Variance (*ANOVA*) method is commonly used to test for the significance of regression, according to Myers, et al. (2009). In essence, what *ANOVA* does is divide the total variability in the response variable into meaningful components and uses this as the basis for the test. The relationship is defined as follows:

$$SS_T = SS_R + SS_E$$

where SS_T is known as the total corrected sum of squares and represents the total variability in the data. This can be broken up into the variability explained by the model (SS_R, also known as the regression sum of squares) and the residual variation that is left unexplained by the model (SS_E, known as the error sum of squares).

Now, the test for significance of regression tests whether a linear relationship exists between the response variable and a subset of regressor variables. In this case, the specific subset or combination as identified previously is tested.

The hypotheses are:

H_0: $\beta_1 = \beta_2 = \ldots = \beta_k = 0$

H_1: $\beta_j \neq 0$ *for at least one j*

If the null hypothesis H_0 is true, it implies that, at least one of the regressor variables contributes significantly to the model. In addition, if H_0 is true, then SS_R/σ^2 is a random variable that follows the chi-square distribution with k degrees of freedom, where k is the number of regressor variables. Further, SS_E/σ^2 is also a chi-square random variable with $n - p$ degrees of freedom where, n is the number of observations and $p = k + 1$. It can now be stated that the test statistic for the above hypothesis is

$$F_0 = \frac{SS_R/k}{SS_E/(n-p)} = \frac{MS_R}{MS_E}$$

where MS_R and MS_E are known as the regression and error mean squares respectively. The null hypothesis is rejected if $F_0 > f_{\alpha,k,n-p}$. The *ANOVA* results for the purpose of this regression model are presented in **Table 9** below.

Table 9 – Analysis of Variance

ANOVA					
	Degrees of Freedom	*Sum of Squares*	*Mean Squares*	F_0	*Significance F*
Regression	5	11.9589	2.3918	18.9112	0.000026
Residual	12	1.5177	0.1265		
Total	17	13.4766			

If α is chosen at 5%, then $f_{\alpha,k,n-p} = f_{0.05,\ 5,\ 12} = 3.11$. The null hypothesis is therefore rejected ($F_0 > 3.11$) at *95%* confidence and it is concluded that the response variable is linearly related to at least one regression coefficients.

The test for significance of regression is not an absolute judgement of whether or not a model is a satisfactory representation of the data. However, combined with the statistical evidence presented previously, it is the opinion of the author that the model sufficiently represents the data observed. Therefore, the model shown in the equation below is accepted for the purpose of this project. An interpretation of the model continues in the next section.

$$L_T = e^{5.842+5.275d-0.000348v^2-0.00506{f_t}^2-1.724\,d^2+0.00270vf_t} \quad \textbf{(24)}$$

The model above is only statistically valid for certain parameter ranges, presented in **Table 2**, but repeated below for convenience.

Table 10 – Experimental Factor Ranges

Experimental Factors	Minimum	Maximum
Cutting Speed (m/min)	47.5	92.5
Feed per Tooth (µm)	10	25
Axial Depth of Cut (mm)	0.2	2

4.3.8 Visual Interpretation of the Model

Interpretation of the empirical model determined, or any model for that matter, is greatly aided through visual representation. The empirical model, developed for the purpose of this project, is essentially a mathematical function that characterises tool life of a micro end mill in terms of its cutting parameters. It is, therefore, possible to generate graphs that illustrate this relationship. This function has three input variables (*cutting speed (v)*, *feed per tooth (f_t)* and *axial depth of cut (d)*) and

a response variable namely *tool life (L_T)*. This means that four variables together describe the model. Since the Cartesian axes only has three dimensions, it is necessary to hold one model variable constant when plotting the remaining variables. **Figure 30** below represents the model visually and in its entirety. Also note, a larger version of this figure is presented in Appendix D. The colours of this figure represent the associated tool life on the response surface with red being high and blue being low.

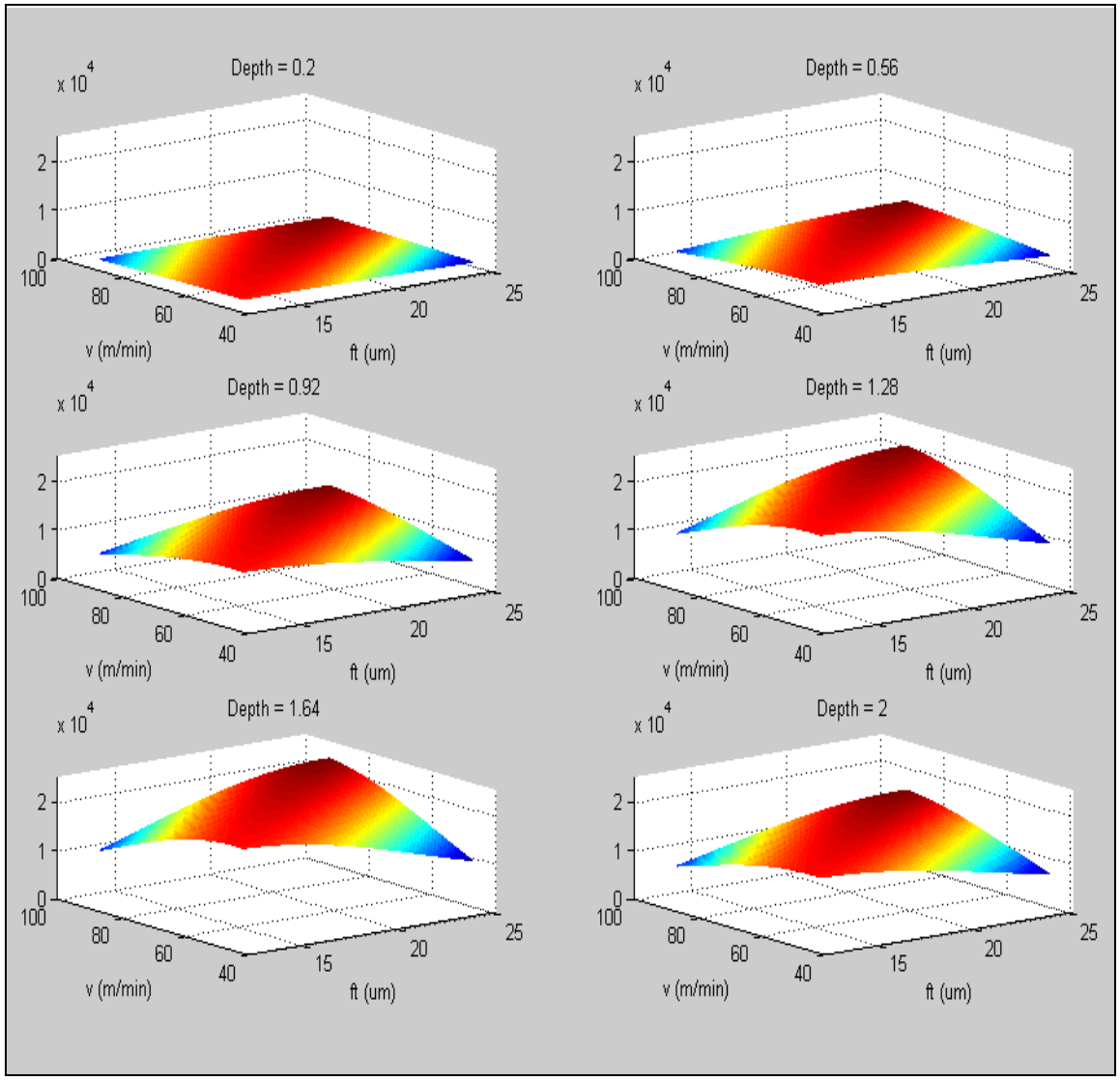

Figure 30 – Visual Representation of Tool Life Model

The figure above shows six plots. For each plot, the *depth of cut(d)* is held constant and the *tool life* is plotted (on the *z-axis* in mm^3) for the full range of *feed per tooth(f_t)* and *cutting speed (v)* on the *x* and *y* axes respectively. By full range, it is meant the range over which the parameters were tested. Further, the *depth of cut (d)*, for each graph increases from left to right and top to bottom across the figure.

There are several interpretations to be made from **Figure 30** above. These include, but are not limited to, the following:

- At low *depth of cut*, a low L_T is seen. As *depth of cut* increases from 0.2 mm to 1.64 mm, L_T increases. This is shown by the rising level of the response surface and is intuitive considering that L_T is defined as 'volume' of material removed, according to

$$L_T = CL \times d \times D$$

  where *CL = length of cut (mm)* and *D = tool diameter (mm).* Therefore, a high *depth of cut* is expected to result in a correspondingly high L_T. However, as *depth of cut* increases beyond *1.64 mm*, the model shows a counterintuitive downward trend in L_T, signifying a reduced length of cut. This phenomenon has been seen before in literature. Zaman, et al. (2004) concluded in their research that an increased depth of cut corresponds to an increased tool life, up to a certain extent. After this, a further increased depth of cut corresponds to a decreased tool life. This is unlike conventional milling.

  Interestingly, it seems as though the influence of *cutting speed* and *feed per tooth* increases as *depth of cut* is brought towards its optimum. In other words, the variation attributed to *cutting speed* and *feed per tooth* is increased as *depth of cut* tends towards its optimum. This is shown by increased curvature of the response surface as *depth of cut* tends towards its optimum.

Another way of viewing the tool life model is shown in **Figure 31** below. The concept is similar to that of **Figure 30** above, except the variables are switched. Also note, a larger version of this figure is presented in Appendix D. The meaning of the colours of this figure is similar to that of **Figure 30**.

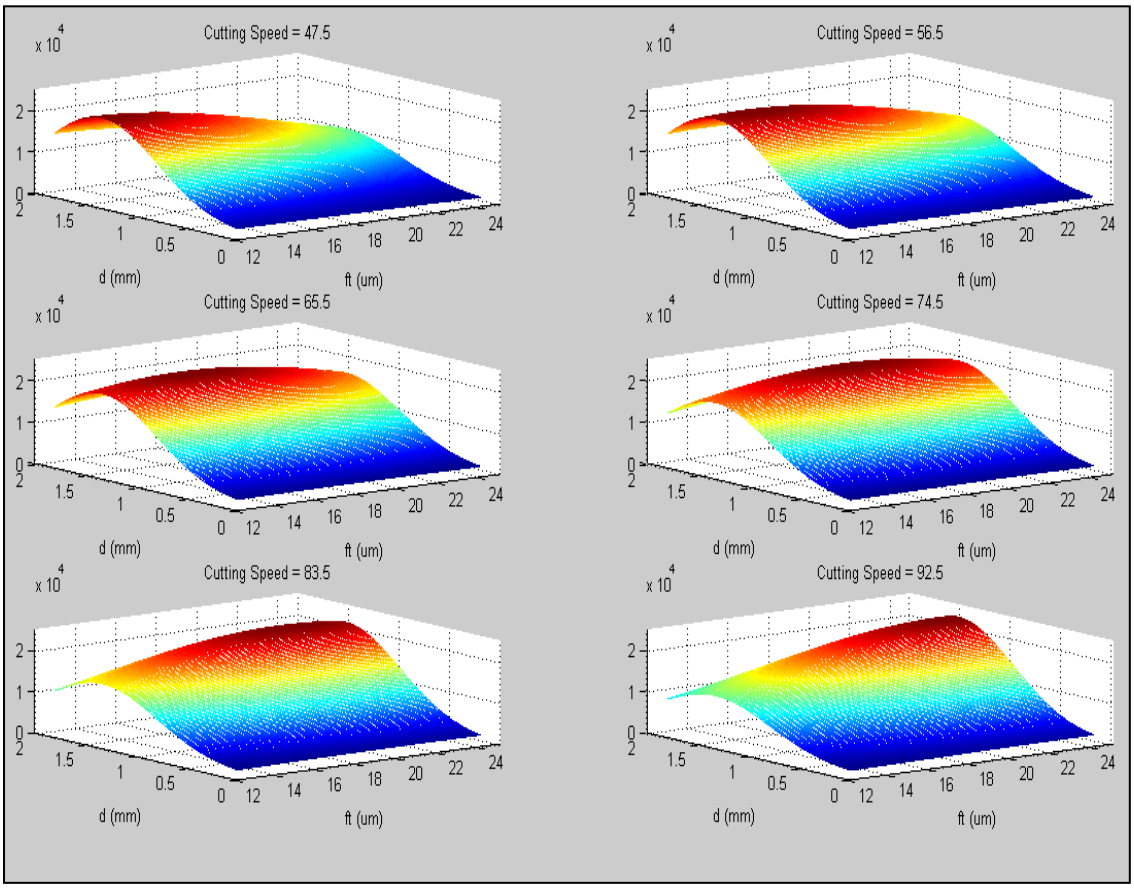

Figure 31 – Alternative Visual Representation of Tool Life Model

For each graph in the figure above, tool life is plotted against *depth of cut* and *feed per tooth* for a constant *cutting speed*. The *cutting speed* is thus varied from graph to graph. Further deductions can be made from these graphs:

- Again, it is seen that there exists an optimal tool life, which is largely governed by the *depth of cut parameter*. In other words, the *depth of cut* parameter is the main influencing parameter in achieving optimal tool life.
- Consider for each graph, as *depth of cut* tends towards the value, which results in optimum tool life, there is increased curvature in the response surface. This indicates increased variation due to *cutting speed* and *feed per tooth*, as tool life reaches its optimum for each graph.
- Another consideration made apparent by **Figure 31** above, is the importance of the combination of *cutting speed* and *feed per tooth*. Consider the changing shape of the response surface as *cutting speed* increases from graph to graph. The *depth of cut* that results in optimum tool life for each graph remains relatively constant. However, the *feed per tooth* that results in optimum tool life for each graph does not. It appears as though there is interaction between *cutting speed* and *feed per tooth* that results in optimal tool

life. At low *cutting speeds*, a low *feed per tooth* yields the best tool life, but at a high cutting speed, a high feed per tooth value yields the best tool life. Observe **Figure 32** below. The graphs show the side view of response surface plots, as in **Figure 31** above, for *cutting speed* equal to 47.5 and 92.5 on the left and right respectively. There is a noticeable change in the shape of the surface peak as it shifts from low *feed per tooth* at low *cutting speeds*; to a high *feed per tooth* at high *cutting speeds*. This effect is brought about by the inclusion of the $v*f_t$ term in the regression model.

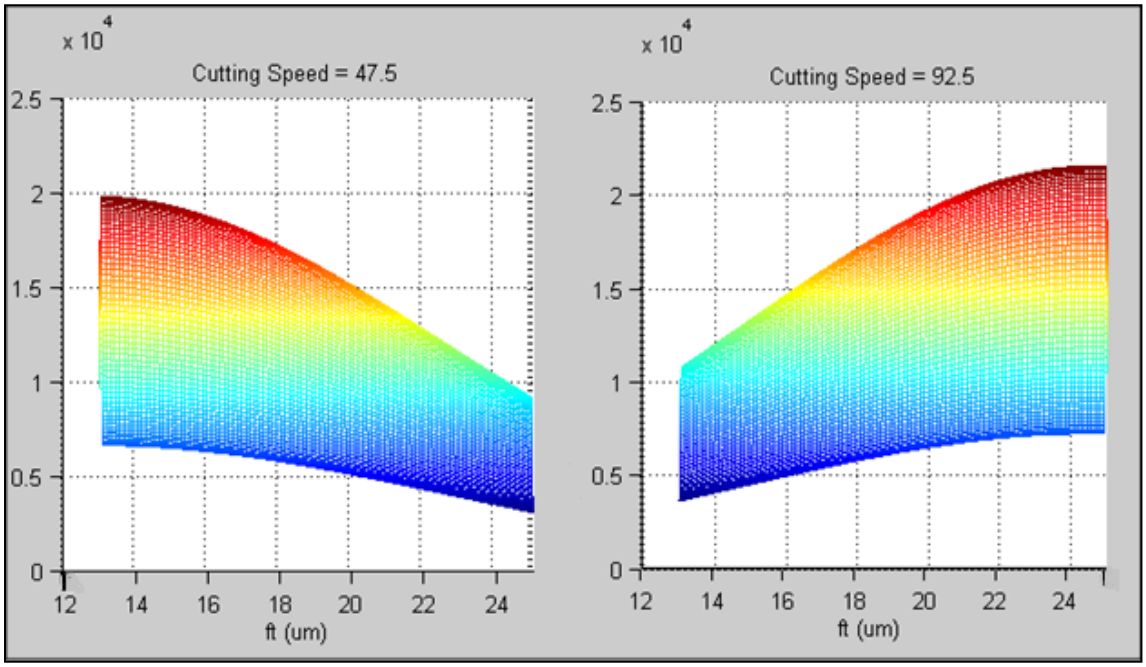

Figure 32 –Model Representation Indicating Cutting Speed and Feed per Tooth Interaction

4.4 Conclusion – Usefulness of the Tool Life Model

For the purpose of this chapter, an empirical model was developed that characterises tool life of micro end mills in terms of their cutting parameters, namely *cutting speed*, *feed per tooth* and *axial depth of cut*. This was done using an empirical model building approach that follows the Response Surface Methodology (RSM). Design of Experiments, multiple linear regression analysis and analysis of variance were the main statistical based tools used to build this model.

The initial intention of this tool life model was to predict tool life under certain operating conditions and, in so doing, be able to predict the cost of tools. The tool life model is, therefore, intended to form part of a higher-level cost model. This is not, however, the model's only use. Three main uses have been identified and are as follows:

- The tool life response can also be optimised through selection of the correct machining parameters. This could allow the user to select parameters that result in the lowest possible tooling cost.
- The tool life model essentially describes the useful life of the tool. This does not necessarily mean the life until breakage, but rather, until the tool no longer produces a satisfactory machined surface. The tool life model can be used to estimate how long a tool can be used before it no longer is able to produce quality products. This then, essentially protects the manufacturer from failing to meet the customer specified requirements.
- Finally, the model can be used to map the predicted tool life response over a particular region of interest. In other words, the tool life is described over a broad range of machining parameters. This plays an important role in the context of the high-level manufacturing cost model. It will eventually be required to optimise this cost model in terms of lowest overall manufacturing cost. It may be the case that the specific machining parameters that optimise tool cost do not necessarily optimise overall manufacturing cost. This is because overall costs include factors such as machining time cost, which are also dependant on the machining parameters.

In conclusion, some of the limitations of the model should be noted. These include, but are not limited to the following:

- The model represents the *estimated* tool life for certain cutting parameters. In other words, it does not describe the definitive relationship between the input and response variables, but rather serves to provide insight into this relationship.

- The model is bounded by the cutting parameter ranges, as determined in Section 4.1.2.3. It is possible to extrapolate the response beyond these ranges, but statistical confidence is lost in doing so.
- Finally, the model is constrained to the conditions specified in Section 4.1. That is, the model is valid for the material and micro end mills described. Validation outside these conditions requires additional experimentation.

5. Manufacturing Time Model Development

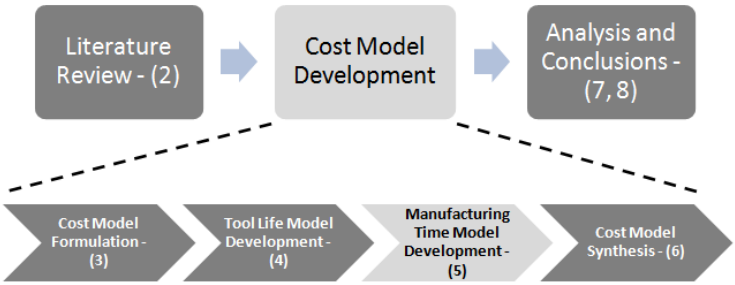

The time taken to manufacture a component is a major cost driver in any production process. Moreover, manufacturing time is important from a strategic point of view considering the fact that lead time is either an order winner or an order qualifier for any product.

In a competitive industry, the time-cost relationship is a key consideration. It might be required to know how a reduced manufacturing time will affect the associated costs or visa verse. In order to understand this relationship it is necessary to develop a detailed manufacturing time model.

The purpose of this chapter is, therefore, to develop a detailed manufacturing time model. This model is used to quantify each step in the manufacturing process and ultimately forms part of the broader manufacturing cost model. **Figure 33** illustrates the framework of the model.

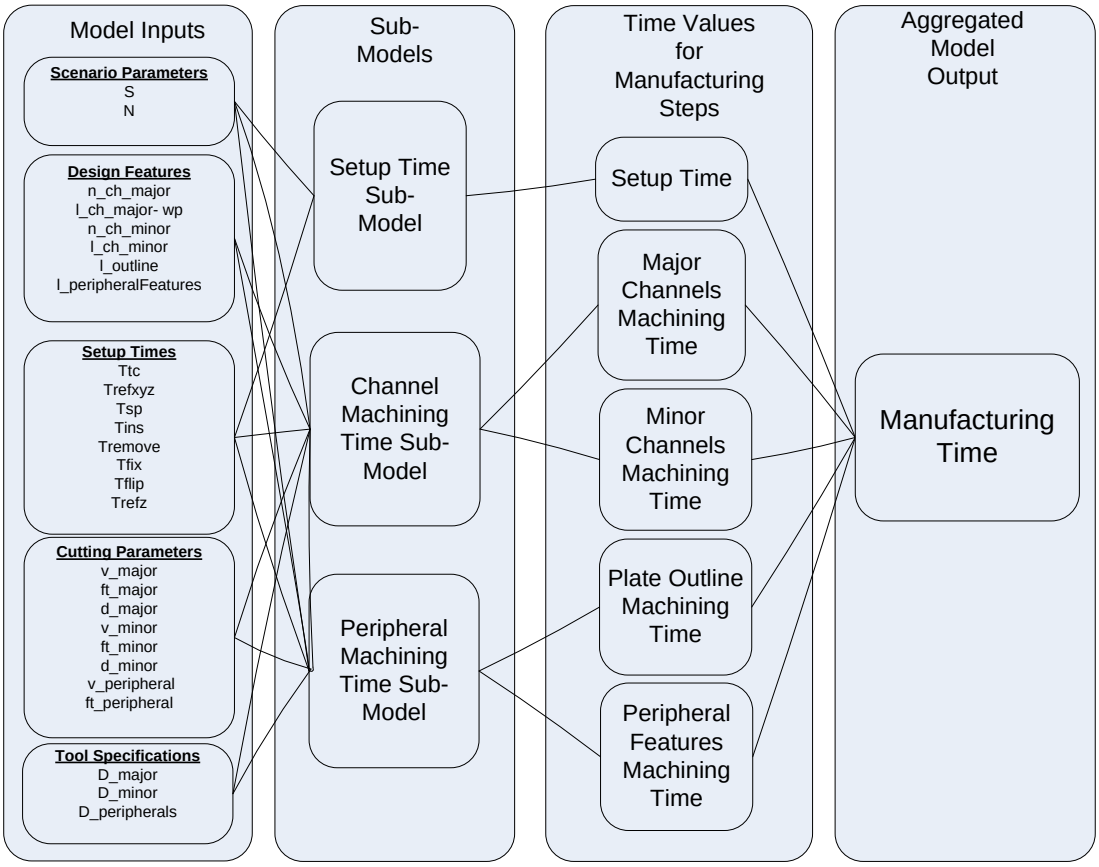

Figure 33 – Manufacturing Time Model

The manufacturing time model is made up of sub-models, each of which is used to quantify individual steps in the machining process. Consider **Figure 33**. Input parameters described in **Table 13**, are fed into their respective sub-models, from which time values for individual steps in the manufacturing process are determined. The individual time values are then aggregated to output a final manufacturing time estimate.

The approach taken in building this time model, as in the case of the broader cost model, is to incorporate flexibility into the model. Flexibility is required to be able to evaluate the effect that changing the input parameters will have on the manufacturing time and cost.

Following the logic of **Figure 33**, the manufacturing time model can be formalised as:

$$T_P = T_S + T_{CM\ major} + T_{CM\ minor} + T_{PM\ outline} + T_{PM\ peripheral\ features} \quad \textbf{(25)}$$

where T_P *= total plate manufacturing time (min/plate),* T_S *= setup time (min/plate),* $T_{CM\ major}$ *= major channel machining time (min/plate),* $T_{CM\ minor}$ *= minor channel machining time (min/plate),* $T_{PM\ outline}$ *= plate outline machining time (min/plate)* and $T_{PM\ peripheral\ features}$ *(min/plate)*.

5.1 Manufacturing Time Sub-Models

This section details the sub-models that combine to form the manufacturing time model. The inputs associated with each model are described as well as the underlying assumptions made in developing these models. It should be noted here that the manufacturing time model and sub-models are defined in terms of minutes per plate (min/plate).

5.1.1 Setup Time Sub-Model

The *Setup Time* sub-model accounts for the majority of the non-productive times associated with machining. Two alternative scenarios (*S*) are considered, each of which represents an alternative order of carrying out the manufacturing steps. Each scenario further includes the option to manufacture *N* plates at a time, where *N = 1, 2,…* . The scenarios are as follows:

- *Scenario 1 refers to the case where, for N plates, all the necessary machining for one side is completed (peripheral, major and minor channels), before the plates are flipped and the other side is completed.*
- *Scenario 2 on the other hand, refers to the case where, for N plates, the peripheral machining is carried out on both sides, then the major channel machining on both sides and finally the minor channel machining on both sides.*

Scenario 1 is characterised by less plate handling and more tool changes. This is because a tool change is necessary when changing, for example, from peripheral to channel machining or from major channel to minor channel machining.

Scenario 2 on the other hand is characterised by more plate handling and fewer tool changes. This is because plate handling is necessary when changing from machining one side to machining the other.

The reason for allowing two scenarios is to provide flexibility in the model. In the case where an automatic tool changing system is used, scenario 1 might be faster. Conversely, if a vacuum workpiece holding system is used, allowing for short plate handling times, scenario 2 might be preferable.

It should be noted here that plate handling carries with it the risk of loss of accuracy. This is because changing the position of the plate means that at least 3 degrees of freedom are lost whereas changing the tool means that only one degree of freedom is last. However, the task of re-referencing the plates after each movement is accounted for in the model.

The setup time (min/plate) is described by the following formulae:

$$T_S = \frac{5 \times T_{tc} + 6 \times N \times T_{refxyz} + 5 \times T_{sp} + N \times (T_{fix} + T_{flip} + T_{remove})}{N} + T_{ins} \quad \textbf{(26)}$$

, for S = 1

$$T_S = \frac{3 \times T_{tc} + 6 \times N \times T_{refxyz} + 3 \times T_{sp} + N \times (T_{fix} + 3 \times T_{flip} + T_{remove})}{N} + T_{ins} \quad \textbf{(27)}$$

, for S = 2

where T_S *= setup time*, T_{tc} *= tool changing time*, T_{refxyz} *= the combined x,y and z-axes referencing time*, T_{sp} *= machine parameters setting time,* T_{fix} *= plate fixing time,* T_{flip} *= plate flipping time,* T_{remove} *= plate removing time* and T_{ins} *= plate inspection time.* The numerical values in the equations above represent the number of times that the associated activity needs to be performed for that scenario. For example, **Equation (26)** above indicates that five tool changes are required in Scenario 1.

It should be noted here that it is possible for an operator to operate more than one machine at a time. If this is the case, then it is possible for the setup activities of one plate to be done in parallel with the machining activities of another plate. That is, if doing so does not delay any one of the activities. This is accounted for in the cost model synthesise of Section 6.1.2 on page 94.

5.1.2 Channel Machining Time Sub-Model

The channel machining time model is used to determine the machining time for both major ($T_{CM\ major}$) and minor channels ($T_{CM\ minor}$). The difference is seen in the values of the model input parameters. This is seen later in Section 5.2.3. The generic channel machining time model is as follows:

$$T_{CM} = \frac{(N_{ch} \times L_{ch})}{F_R} + \frac{wp \times (N-1)}{F_R \times N} + (T_{tc} + T_{refz}) \times Z \quad \textbf{(28)}$$

where T_{CM} *= channel machining time (min/plate)*, N_{ch} = number of channels on both sides of the plate, L_{ch} *= average length of channels*, F_R *= feed rate (mm/min)*, *wp = plate width (mm), N = number of plates at a time,* T_{tc} *= tool changing time,* T_{refz} *= z-axis referencing time* and *Z = tool life multiplier*.

The model above requires some explanation. The first term accounts for the actual machining time, governed by the *cumulative cutting length (mm)* and the *feed rate (*F_R *(mm/min))* according to **Equations (10)** and **(11)**, repeated here for convenience,

$$F_R = \frac{n \times f_t \times 2}{1000}$$

and

$$n = \frac{v \times 1000}{\pi \times D}$$

where *n = rotational speed (rpm), v = cutting speed (m/min),* f_t *= feed per tooth (µm)* and *D = tool diameter (mm)*.

The second term in the model above accounts for the additional non-productive travel time per plate when more than one plate is machined at a time. Non-productive travel occurs when the cutting tool is not engaged, but needs to move to a specified location to continue machining. This typically occurs at a faster feed rate known as the rapid traverse feed rate. However, for the purpose of this model, the rapid traverse feed rate is approximated by the cutting feed rate, F_R. This is because, when the cutting feed rate is chosen optimally or near optimally, it is very similar to the rapid traverse feed rate, which represents the maximum achievable feed rate of the machine.

The final term in the model accounts for additional setup time, necessary when tools fail midway through production runs. If this happens, the tool needs to be replaced (T_{tc}) and the z-axis needs to be re-referenced (T_{refz}). This term is naturally driven by the tool life accounted for by the parameter *Z,* according to

$$Z = \frac{N_{ch} \times L_{ch}}{L_T/_{d \times D}} \tag{29}$$

where N_{ch} *= number of channels,* L_{ch} *= average length of channels (mm), d = channel depth (mm), D = tool diameter (mm)* and L_T *= tool life (mm*^{3}*/tool)* as a function of *v,ft, d* (as given by **Equation (22)** in Section 4.3.7). The parameter *Z* represents the average number of tools used per plate. It might be argued that this parameter should be defined as the number of tool breakages per plate. In this case the parameter should become Z – *1* because the first tool is accounted for in the setup. However, this logic assumes that machining always starts with a new tool, which is not this case here. Rather, machining on a plate can start with tool worn by previous machining. In this event, tool failure occurs earlier relative to the progress made on the plate. For this reason, the average number of additional tool changes required per plate is accounted for by the parameter *Z* as defined in **Equation (29)**.

5.1.3 Peripheral Machining Time Sub-Model

The peripheral machining time model is used to determine the time to machine the plate outline ($T_{PM\ outline}$) as well as the peripheral features ($T_{PM\ peripheral\ features}$). This model is similar to that of the channel machining time model. There are, however, small differences, which are highlighted below. The model is as follows:

$$T_{PM} = \frac{L_{peripheral}}{F_R} + \frac{wp \times (N-1)}{F_R \times N} + (T_{tc} + T_{refz}) \times Z \tag{30}$$

where T_{PM} *= peripheral machining time (min),* $L_{peripheral}$ *= effective cutting length of peripheral machining (mm)*. The variable *Z,* similar to the channel machining time model, represents the

number of tools required per plate. In this case, however, the formulation is slightly different. More specifically,

$$Z = \frac{L_{peripheral} / F_R}{L_{T\ taylor}} \quad \textbf{(31)}$$

where $L_{T\ taylor}$ = *tool life (min)*, according to Taylor's tool life model. Peripheral tool life is given by

$$L_{T\ taylor} = \left(\frac{C}{v}\right)^{1/n_T} \quad \textbf{(32)}$$

where *v = cutting speed (m/min)* and *C* and n_T are constants. For the purpose of this model, *C* and n_T are assigned the values of *170* and *0.14* respectively as determined by Lee, et al. (2007). These values were determined by experimental analysis of the machining of a similar polymer-graphite composite material. The tool diameter used for peripheral machining is not in the micro range. Therefore, for the reasons given in Section 4, the Taylor model is applicable.

5.2 Applying the Manufacturing Time Model

For the purpose of this model, five categories of model inputs have been identified. These are scenario parameters, design features, setup times, tool specifications and cutting parameters, as shown in **Figure 33**. As stated in Section 1, the aim of this project is not only to develop a flexible cost model. Rather, this project must also provide an initial estimated time and cost for manufacturing bipolar plates using micro milling.

In order to carry out the latter, it is necessary to quantify the input parameters shown in **Figure 33**. That is, it is necessary to obtain numerical values for the input parameters under assumed operational conditions. The following operational conditions are assumed:

- Machining is done on a micro milling machine, also known as a desktop milling machine, similar to that shown in **Figure 24** on page 56.
- A vacuum workpiece holding system is used to secure the plates during machining. These systems typically provide the best results in terms of productivity and machining accuracy, according to industry expert Sven Bornbaum of Schunk Kohlenstofftechnik GmbH.
- Manual tool changes are performed by the machine operator.
- Further, referencing the machine axes is done using an electrical continuity tester. A continuity tester tests whether two points are connected electrically. Referencing is done by connecting one terminal of the continuity tester to the cutting tool and the other terminal to the plate, both of which are electrically conductive. The cutting tool is then moved manually, in very small increments, until it touches the plate. The position of the cutting tool relative to the plate is then known and the axis is referenced. This procedure is followed for each of the x, y and z-axes.

The input parameters can now be quantified for the assumed operational conditions. The remainder of this section details the approach taken in quantifying the time model input parameters as well as the results achieved.

5.2.1 Estimating Setup Times

Setup times are estimated via time studies carried out under the assumed operational conditions, listed above. It was attempted to simulate a standard pace when performing the actions. A standard pace, as defined by Freivalds (2009), is the effective rate of performance of a conscientious, self-paced, qualified employee when working neither fast nor slow and giving due consideration to the physical, mental, or visual requirements of the specific job. The average time recorded to perform each of the following activities is shown in **Table 11**. Further, averages were taken over 10

repetitions. It should be noted that exercise was performed by the author and the times recorded do not reflect those of an experienced machinist.

Table 11 – Setup Time Estimates

Setup	Average	Minimum	Maximum
Tool Change (Ttc)	0.571	0.442	0.786
Reference x,y and z-axes (Trefxyz)	2.243	1.913	2.459
Reference z-axis (Trefz)	0.773	0.671	0.876
Set Machine Parameters (Tsp)	0.396	0.336	0.517

The estimated setup times above are subject to certain assumptions concerning the operational conditions. Changing the operational conditions will require new estimates to be made. For example, the tool changing mechanism is manual, due to the technology used. However, there are technologies that allow for automatic tool changes. In the event that these technologies are used, T_{tc} will be much reduced.

Similarly, there are micro end mills that come with a plastic stopper fixed at a set distance along the shaft of the tool. Using these tools could significantly reduce, if not eliminate, the time to reference the z-axis. That is, assuming that the use of these end mills does not violate the machining accuracy requirements.

In terms of workpiece holding, the only reasonable method was to assume that a vacuum workpiece holding system is used. This is because the geometry of the plate does not allow for mechanical clamping without having to change the clamping setup for machining of different plate features (peripheral, channels). This seemed like an impractical solution in an environment that is intended to operate productively.

The times in **Table 12** represent the average recorded for fixing, flipping and removing *N* plates, where *N* = *1, 2, 3* and *4*. Averages were taken over 10 repetitions of each.

Table 12 – Workpiece Handling Time Estimates

Workpiece Handling Time Estimates (using vacuum clamping)						
	Fixing		Flipping		Removing	
# Plates, N	Average (Min – Max)	Fixing Time/plate	Average (Min – Max)	Flipping Time/plate	Average (Min – Max)	Removing Time/plate
1	0.289 (0.28 – 0.292)	0.289	0.317 (0.3 – 0.343)	0.317	0.275 (0.25 – 0.282)	0.275
2	0.424 (0.40 – 0.451)	0.296	0.461 (0.453 – 0.472)	0.314	0.350 (0.348 – 0.353)	0.258
3	0.436 (0.421 – 0.482)	0.257	0.503 (0.48 – 0.512)	0.279	0.443 (0.44 – 0.445)	0.259
4	0.378 (0.362 – 0.381)	0.220	0.464 (0.458 – 0.47)	0.241	0.376 (0.365 – 0.39)	0.219

5.2.2 Assigning Values to the remaining Model Variables

In Section 5.2.1, estimates for setup parameters are obtained using time studies under assumed operational conditions. It is still necessary, however, to assign numerical values to the remaining model input parameters. This section addresses that issue.

As shown in **Figure 33**, there are four categories of model inputs, aside from the setup time parameters, described in Section 5.2.1. These categories include scenario parameters, design features, cutting parameters and tool specifications. Assigning values to model parameters within each category is approached in a different way, depending on the nature of the category. These procedures are described below.

- Scenario parameters – The range of values for these model inputs are limited. The scenario value, S, detailed in Section 5.1.1 on page 83, can be either 1 or 2. This parameter describes the order of machining steps and is included to provide flexibility in the machining time model. The number of plates manufactured at one time, N, provides further flexibility to the time model. The optimal combination of S and N depends on the value of the setup time constants.
- Design features – These parameters are prescribed by the technical design of the bipolar plate. Further, these parameters are included in the cost model to be able to evaluate the effect of changing design features on manufacturing time and cost.

- Tool specifications – These parameters are also prescribed by the bipolar plate design. This is because the diameter of the tool used must be equal to the width of channels. This is to avoid having to perform more than one pass for each channel.
- Cutting parameters – Cutting parameters are mostly at the discretion of the machine operator. That is, the machine user chooses the feed rate and rotational velocity, which together control the feed per tooth and cutting speed. However, parameters relating to the axial depth of cut are also prescribed by the design features. This is because, the approach taken for this model is to cut the full depth of cut on the first pass. Once again, this is to avoid having to perform more than one pass.

The following fixed model parameters are applicable for the purpose of this project

Table 13 – Model Input Parameter Values

Model Input Category	Model Input	Value	Description
Design Features	$N_{ch\ major}$	23	# of major channels
	$L_{ch\ major}$	309	Average length of major channels
	wp	136	Width of the plate
	$N_{ch\ minor}$	21	# of minor channels
	$L_{ch\ minor}$	5	Average length of minor channels
	$L_{outline}$	794.67	Length of the plate outline
	$L_{peripheral}$	104.4	Effective length of peripheral features
Tool specifications	D_{major}	0.7	Diameter, major channel, micro end mill
	D_{minor}	0.5	Diameter, minor channel, micro end mill
	$D_{peripherals}$	2.5	Diameter, macro end mill
Cutting Parameters	d_{major}	0.7	Depth of cut, major channel, micro end mill
	v_{major}	70	Cutting speed, major channel, micro end mill
	v_{minor}	70	Cutting speed, minor channel, micro end mill
	$f_{t\ minor}$	15	Feed per tooth, minor channel,

Model Input Category	Model Input	Value	Description
			micro end mill
	d_{minor}	0.5	Depth of cut, minor channel, micro end mill
	$f_{t\ major}$	15	Feed per tooth, major channel, micro end mill
	$v_{peripheral}$	90.32079	Cutting speed, macro tool
	$f_{t\ peripheral}$	50	Feed per tooth, macro end mill

The values listed in the cutting parameters category, in **Table 13**, are not the only feasible or even recommended values. They are simply typical values for their respective parameters and are included here for the purpose of illustration. Further analysis on the effect of these parameters is presented in Section 7.1.

5.2.3 Manufacturing Time Model Results

Using the model input parameters described in **Table 11**, **Table 12** and **Table 13**; the following results (in minutes) are obtained for the manufacturing time model.

Table 14 – Manufacturing Time Model (S = 1, N = 1)

Time Category	Time (min/plate)	Obtained From
Setup Time (T_S)	19.209	**Equation (26)**
Major Channel Machining Time ($T_{CM\ major}$)	16.466	**Equation (28)**
Minor Channel Machining Time ($T_{CM\ minor}$)	0.189	
Outline Machining Time ($T_{PM\ outline}$)	0.701	**Equation (30)**
Peripheral Features Machining Time ($T_{PM\ peripheral\ features}$)	3.685	
Manufacturing Time (T_P)	40.250	Total

It can be seen from **Table 14** that the setup time and the major channel machining time are the two major 'time' drivers. Further, from **Equations (23)** and **(24)** it can be seen that the setup time is largely influenced by the values for S and N. **Figure 34** shows the effect that an increase in N has on the setup time, for scenario S = 1, 2.

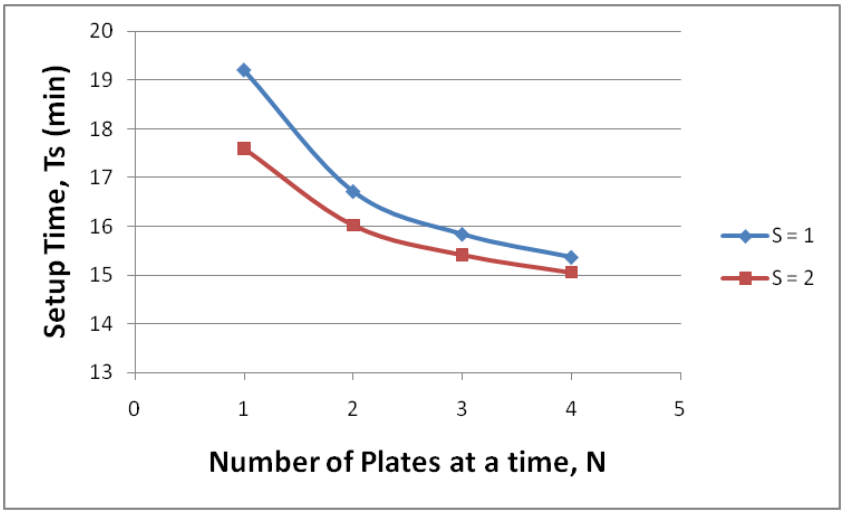

Figure 34 – Setup Time Sensitivity

The figure indicates that scenario 2 is always preferable to scenario 1, with shorter setup times per plate for N = 1, ... , 4. Recall from Section 5.1.1 on page 83, that scenario 1 is characterised by less plate handling and more tool changes whereas scenario 2 is characterised by more plate handling and fewer tool changes. This is relationship is stated formally by **Equation (26)**.

Therefore, the conclusion can be drawn that the tool changing time has more of an effect on the setup time than do the work handling times (plate fixing, flipping and removing time). The reader should bear in mind that the analysis presented in **Figure 34** is based on the setup time estimates described in Section 5.2.1 on page 87. These estimates were obtained by running time studies under assumed operational conditions. Therefore, it cannot be assumed that scenario 2 is always preferable to scenario 1. Rather, the particular machine arrangement must be taken into account. This is because the inclusion of certain equipment might change the result. For example, if an automated tool changing system were included, reducing the tool change time, scenario 1 might then be preferable.

The reader should also note here that the number of plates machined at a time, N, is constrained by the amount of travel in the x-axis of the machine. Travel is the distance that an axis can move. Micro milling machines have travel that ranges between 150 and 600 mm depending on the size (and price) of the machine.

It should also be noted that in order to accommodate additional plates on the same worktable, the workpiece holding mechanism must also be adjusted. In the case of a vacuum workpiece holding mechanism, this means that a larger and more expensive vacuum table is required.

6. Cost Model Synthesis

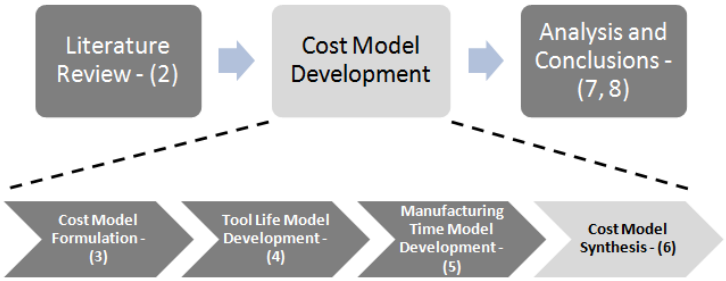

This section sees the coming together of the previous models. The tool life and manufacturing time models of Sections 4 and 5 respectively are synthesised, using the format described in Section 3, into a unified cost model. The cost model framework is represented in **Figure 35**, below. This figure illustrates the logic of the model in translating the inputs into a final cost estimate.

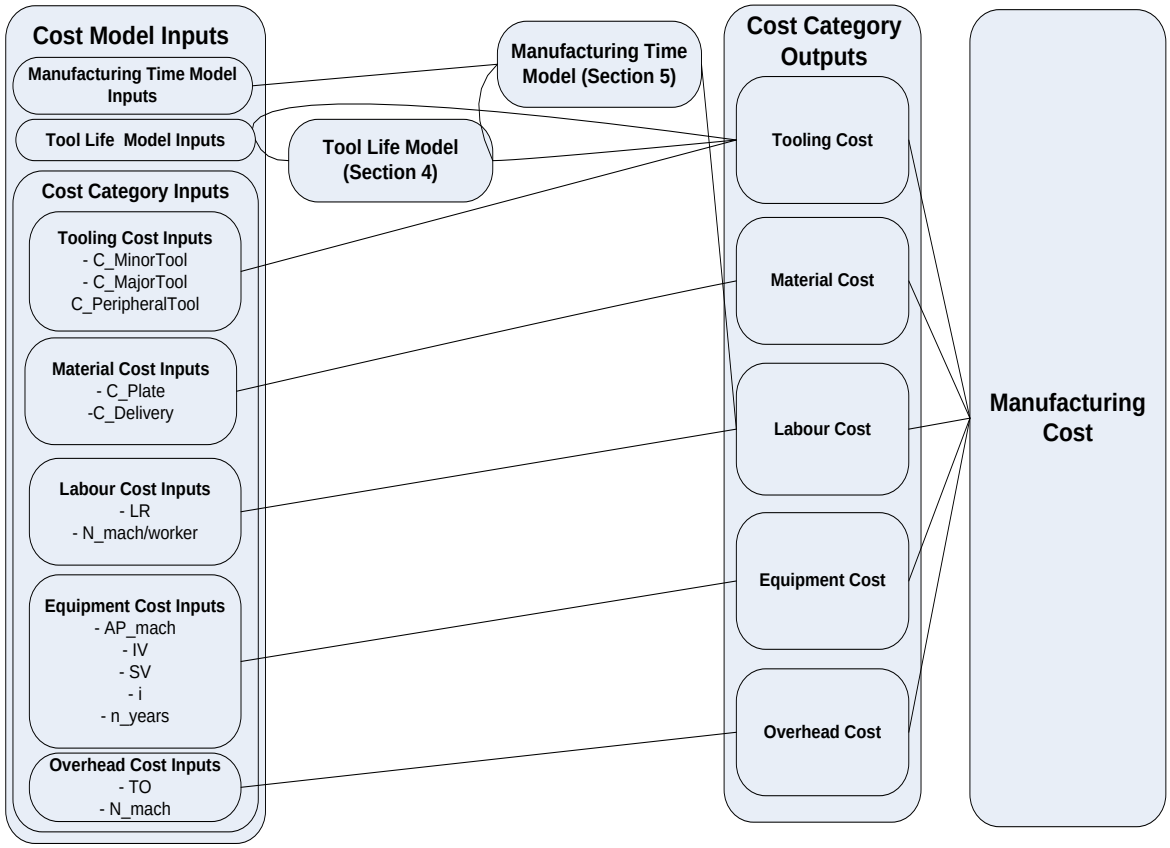

Figure 35 – Manufacturing Cost Model

6.1 Manufacturing Cost Model Components

6.1.1 Material Cost, $C_{Material}$

As explained in Section 1, the cost of material, for the purpose of this cost model, is simply the cost of purchasing blank plates from Schunk Kohlenstofftechnik GmbH and importing them. The cost of material is defined as follows:

$$C_{Material} = C_{Plate} + C_{Import} \quad \textbf{(33)}$$

where C_{Plate} *= cost per plate (R/plate)* and C_{Import} *= cost to import a plate (R/plate)*, inclusive of freight and import duties.

6.1.2 Labour Cost, C_{Labour}

It is assumed here that a plate is machined by only one operator and one machine. This simplifies the analysis, but is also a valid assumption based on the type of component. Labour cost is determined as follows:

$$C_{Labour} = \frac{T_p}{60} \times LR \times \frac{1}{N_{mach/worker}} \quad \textbf{(34)}$$

where T_p *= processing or manufacturing time (min/plate)*, LR *= operators wage rate (R/hr)* and $N_{mach/woker}$ *= the number of machines operated per worker*.

The manufacturing time, T_p, is addressed in detail in Section 5. The number of machines operated per worker, $N_{mach/woker,}$ accounts for the fact that it is possible for a skilled operator to operate more than one machine at a time. This is especially true if the setup time is relatively shorter than the machining time.

6.1.3 Tooling Cost, $C_{Tooling}$

The cost of tooling is as follows:

$$C_{Tooling} = C_{Major\ Tooling} + C_{Minor\ Tooling} + C_{Peripheral\ Tooling} \quad \textbf{(35)}$$

where $C_{Major\ Tooling}$, $C_{Minor\ Tooling}$ and $C_{Peripheral\ Tooling}$ are the costs of tooling (R/plate) to machine the major micro channels, minor micro channels and peripheral features respectively. Further,

$$C_{Major\ Tooling} = C_{Major\ Tool} \times Z_{Major} \quad \textbf{(36)}$$

$$C_{Minor\ Tooling} = C_{Minor\ Tool} \times Z_{Minor} \quad \textbf{(37)}$$

$$C_{Peripheral\ Tooling} = C_{Peripheral\ Tool} \times Z_{Peripheral} \quad \textbf{(38)}$$

where $C_{Major\ Tool}$, $C_{Minor\ Tool}$ and $C_{Peripheral\ Tool}$ are the cost per tool *(R/tool)* used to machine major micro channels, minor micro channels and peripheral features respectively. In addition, Z_{Major}, Z_{Minor} and $Z_{Peripheral}$ are the number of tools used per plate to machine the major micro channels, minor micro channels and peripheral features respectively.

The task now is to translate predicted tool life, which is done using the tool life model developed in Section 4, into an equivalent '*Z*' value representing the estimated number of tools used per plate.

6.1.3.1 Translating Major Micro Tool Life

To determine this tooling cost it is necessary to translate the predicted tool life, L_T, into Z_{Major}, which represents the number of major micro tools used per plate. Referring to **Equation (24)**, in Section 4.3.7, L_T is given in terms of volume of material removed *(mm^3)* and is a function of the cutting parameters, namely cutting speed *(v),* feed per tooth *(f_t)* and depth of cut *(d)*. Therefore, the number of tools used per plate can be defined as follows:

$$Z_{Major} = \frac{N_{ch\ major} \times L_{ch\ major}}{{L_T}/{d \times D}} \qquad \textbf{(39)}$$

where $N_{ch\ major}$ *= number of major micro channels for both sides of the plate,* $L_{ch\ major}$ *= length of major micro channels (mm),* L_T *= expected tool life (mm^3/tool), d = depth of cut (mm)* and *D = major micro tool diameter (mm).*

6.1.3.2 Translating Minor Micro Tool Life

To determine the minor micro tool cost, it is necessary to translate the predicted tool life L_T, into Z_{Minor}, which represents the number of minor micro tools used per plate. Referring again to **Equation (24)** in Section 4.3.7, L_T is defined as the predicted tool life, as function of the cutting parameters. Also, L_T is defined for a specific tool diameter. That is, the diameter of the major micro channels (0.7 mm). The minor micro channels are 0.5 mm, as is the minor micro tool diameter. It is, therefore, necessary to extrapolate the original model to be able to characterise the tool life of other sized tools.

Typically, extrapolation of an empirical model is ill advised because statistical confidence is lost in doing so. In addition, the further the new values move from the original experimental range, the less certain the predicted results become.

However, since the minor micro channels make up only a small proportion of the total machining time, a loss in statistical confidence in the tool life estimation will not affect the final cost model too severely. Additional experiments were carried out to test the accuracy of an extrapolated model.

Further, two translation equations were tested to compare the predicted tool life to the actual recorded tool life. These equations are presented in **Table 15** below.

Table 15 – Methods of Translating the Tool Life Model for Diameters other than 0.7 mm

Method 1	Method 2
$L_T^* = L_T \times \frac{D^*}{D}$	$L_T^* = L_T \times (\frac{D^*}{D})^2$

where L_T* = adjusted tool life (mm^3), L_T = original tool life for 0.7 mm tool diameter (mm^3), D* = new tool diameter* and *D = original tool diameter (D = 0.7 mm)*. Method 1 represents a linear scaling and method 2 represents a quadratic scaling. These methods follow on logically from one another, using the factor $\frac{D^*}{D}$.

Six additional experiments were carried out. For three of these experiments a tool of diameter 0.5588 mm was used. For the remaining three a tool of diameter 0.7248 mm was used. The tool life of each additional experiment was recorded, using the procedure described in Section 4.2.2.3, and compared to the predicted values for both methods of prediction. The summarised results, shown in **Table 16** below, indicate the average values for the absolute deviation of the predicted tool life to the actual recorded tool life.

Table 16 – Summarised Results of Additional Experiments

	Average Absolute Deviation
Method 1	14.64%
Method 2	30.94%

It was found that, on average, method 1 yields significantly better prediction accuracies than method 2. Method 1 was, therefore, accepted for the purpose of this cost model.

There is no absolute justification for the appropriateness of this transformation apart for the fact that the term $\frac{D^*}{D}$ adjusts the tool life accordingly. That is, a smaller diameter will have a proportionally smaller tool life due to the more fragile nature of smaller tools (and vice versa).

The author does not propose this as a formalised adjustment method. Rather, it is a 'quick-and-dirty' method for estimating the tool life of other sized tools. The results of the additional experiments to validate this method are shown in Appendix B.

The number of minor micro tools used per plate can then be defined as follows:

$$Z_{Minor} = \frac{N_{ch\_minor} \times L_{ch\_minor}}{(L_T \times \frac{D_{minor}}{D})/(d_{minor} \times D_{minor})} \quad \textbf{(40)}$$

where N_{ch_minor} = number of minor micro channels for both sides of the plate, L_{ch_minor} = length of minor micro channels (mm), L_T = tool life (mm^3/tool) of the original tool diameter, D_{minor} = minor micro tool diameter (mm), D = major micro tool diameter and *d_{minor} = depth of cut of minor micro tools (mm).*

6.1.3.3 Translating Peripheral Features Tool Life

In Section 4, it was explained why Taylor's tool life model is not applicable to micro tools. Essentially, it is because micro tools are smaller and more vulnerable to catastrophic failure, which is not accounted for by Taylor's model.

Conversely, larger tools can be modelled by Taylor's method because these tools are larger and less vulnerable to breakage. As such, these tools tend to fail by gradual wear on the tool flank. Therefore, peripheral features tool life can be defined according to the following:

$$L_{T\_peripheral} = \left(\frac{C}{v_{peripheral}}\right)^{\frac{1}{n_T}} \quad \textbf{(41)}$$

where *$v_{peripheral}$ = cutting speed (m/min), $L_{T\_peripheral}$ = peripheral tool life (min/tool)* and *n_T* and *C* are empirically determined constants whose values depend on the other cutting parameters, work material, type of tool and the tool life criterion used. The constants *C* and *n_T* must be determined experimentally for a specific set of conditions. Fortunately, *C* and *n_T* have been empirically determined by Lee, et al. (2007), to be *170* and *0.14* respectively for the machining of a similar graphite composite material used in bipolar plates. A distinction between Taylor's model and the empirical model developed in Section 4 is the way in which tool life is defined. Taylor defines tool life in terms of cutting time *(min)* whereas the empirical model developed in this project defines tool life in terms of volume of material removed *(mm^3).* The number of tools used per plate, according to Taylor's model, can then be defined as follows:

$$Z_{peripheral} = \frac{\frac{L_{outline} + 2 \times L_{peripheral\ features}}{F_{R\ peripheral}}}{L_{T\_peripheral}} \quad \textbf{(42)}$$

where *$Z_{peripheral}$ = number of peripheral features tools used per plate, $L_{outline}$ = length of the plate outline profile (mm), $L_{peripheral\ features}$ = effective cutting length of peripheral plate features (mm), $F_{R\ peripheral}$ = peripheral feed rate (mm/min)* and *$L_{T\_peripheral}$ = peripheral tool life (min)*.

6.1.4 Equipment Cost, $C_{Equipment}$

Equipment cost accounts for the cost of equipment such as machinery, workpiece holding systems, import cost, installations, etc that make up the initial capital cost. Typically, a company will not pay a lump sum amount to cover this capital cost. Rather, they will take out a loan to cover this cost and repay this loan on a monthly or annual basis. Therefore, the cost of equipment, $C_{Equipment}$, is seen as a capital recovery cost. That is, the contribution per plate towards repaying the initial capital cost.

For the purpose of this cost model, it was decided to define the overhead allocation base in terms of production units. This is defined as follows:

$$C_{Equipment} = \frac{ACR}{AP_{mach} \times N_{mach}} \quad \textbf{(43)}$$

where *ACR = annual capital recovery (R/year),* AP_{mach} *= annual production per machine (plates/machine-year)* and N_{mach} *= number of micro milling machines*. This type of overhead absorption rate is known as a 'blanket' overhead rate and is appropriate when a company produces only one product (Gowthorpe 2005). For the purpose of this project, it is assumed that this is the case.

Gowthorpe (2005), makes a noteworthy point. Management accounting information must be available in a timely manner in order to be useful. For this reason, overhead absorption is done on budgeted values and not on actual values, which are only available at the end of a financial period. The term $AP_{mach,}$ in **Equation (43)** above is really a forecasted value because the true volume of product is only known at the end of the period. What is useful about this method, however, is that a type of break-even analysis can be performed. For example, a break-even volume can easily be determined for a given financial period.

The annual production per machine, AP_{mach}, is a forecasted value and a key parameter in this cost model. This is because AP_{mach} is chosen as the allocation base for the equipment overhead cost (and other overhead costs). It is possible to define the overhead allocation base in terms of labour hours or machine hours. In doing so, however, it would be necessary to specify the total machine or labour hours that would be used in the year. This brings the analysis back to the question of the expected annual production because one can only machine as many plates as the market demands.

Annual capital recovery (*ACR*) is the equivalent annual cost of owning the asset. The annual capital recovery is a function of the initial capital value, *IV*, the number of years of operation of the equipment, n_{Years}, the effective annual interest rate, *i,* and the future salvage value of the equipment, *SV*, at the end of, n_{Years}. It should be noted here that *IV* and *SV* also depend on the number of machines purchased. *ACR* is then calculated as follows:

$$ACR = IV\left(A\middle|P, i, n_{years}\right) - SV(A|F, i, n_{years}) \quad \textbf{(44)}$$

where $(A|P,\ i,\ n_{years})$ is known as the capital recovery factor and is used to convert the initial amount, *IV*, into an equivalent uniform payment for n_{years} at an effective annual interest rate of *i*. This is defined as follows (Blank and Tarquin, 2005):

$$\left(A\middle|P, i, n_{years}\right) = \frac{i(1+i)^{n_{years}}}{(1+i)^{n_{years}} - 1} \quad \textbf{(45)}$$

The factor $(A|F, i, n_{years})$ is known as a sinking fund factor and is used to convert a future dated value, *SV,* into an equivalent annual amount *over* n_{years}. This is defined as follows:

$$(A|F, i, n_{Years}) = \frac{i}{(1+i)^{n_{years}} - 1} \quad \textbf{(46)}$$

The cost of equipment, $C_{Equipment}$, strictly speaking, is an overhead expense. Therefore, it could be argued that it should rather be aggregated with other overhead expenses. It is, however, included in the cost breakdown as an individual item for the following reason. If alternative manufacturing methods are to be compared, it is preferable to see the effect of the cost of equipment on individual unit costs. This would make the cost comparison of alternative equipment or manufacturing methods more intuitive. Further, $C_{Equipment}$ is defined as a function of annual production to demonstrate the effect of production volume on equipment and total cost.

6.1.5 Sundry Overhead Cost, $C_{Overhead}$

The approach taken in defining the sundry overhead cost per unit is similar to that taken in $C_{Equipment}$. That is, a blanket overhead rate is defined which describes the contribution, per unit of production, towards covering sundry overheads, excluding the cost of equipment. This is defined as follows:

$$C_{Overheads} = \frac{TO}{N_{mach} \times AP_{mach}} \quad \textbf{(47)}$$

where *TO = total sundry overhead (R/year),* N_{mach} *= number of similar machines* and AP_{mach} *= annual production per machine (plates/machine-year)*.

6.2 Applying the Manufacturing Cost Model

For the purpose of illustration, it is necessary to compile an initial cost estimate, using the cost model described in Section 6.1. This section details how the cost model input parameters are estimated and applied to the cost model. It should be noted here, that some of these input parameters are chosen arbitrarily for the purpose of illustration. The process of selecting the optimal or near optimal parameters is detailed in Section 7.

6.2.1 Material Cost

In order to estimate the material cost, the following parameters must be quantified:

- C_{Plate}
- $C_{Delivery}$

where C_{Plate} represents the price per plate, quoted by Schunk Kohlenstofftechnik GmbH, and $C_{Delivery}$ represents the cost to import the plates to South Africa. It should be noted here that both costs are quoted in Euro and are, therefore, subject to the Rand/Euro exchange rate.

Given that Schunk quoted *390 €* for *10 plates* (of the required specifications) and the exchange rate is *10.184 (R/€)*, as on 30/8/2011, C_{Plate} *= R397.18 per plate*. Further, the delivery cost plate, $C_{Delivery}$ *= R10 per plate*. It should be noted here that the delivery cost per plate is not fixed, but a function of the number of plates ordered. It should also be noted that the cost per plate is not necessarily fixed, but a function of the quantity ordered, according to general economy of scale theory. However, this needs to be confirmed and negotiated with Schunk.

6.2.2 Labour Cost

In order to estimate labour cost, the following parameters must be estimated:

- *LR*
- $N_{mach/worker}$

The labour rate, *LR*, is determined by the organisation and is dependent on the skill level of the machine operator. The value to use here is left up to the model user or decision maker. However, for the purpose of analysis, it is necessary approximate a value. Zanele Mlambo of the Department of Trade and Industry (personal communication, 15 August 2011) has provided average annual remuneration figures for employees working in the manufacturing sector in 2010. This was *R142 651 per year*. Then, with *252 working days* in 2010, at *8 hours per day*,

$$LR = \frac{R142\ 651}{252days \times 8hrs/day} \approx R71/hr \quad \textbf{(48)}$$

The number of machines operated by one worker, $N_{mach/worker}$, is difficult to estimate because it requires some in depth analysis to determine the optimal value. In addition, this parameter depends on the ratio of setup time (non-productive time) to machining time (productive time). This is because it is assumed that an operator can operate two or more machines in parallel, if and only if, no activities of one plate delays any activity of another plate. Therefore, the setup of one machine must be done within the machining time of another plate. The following constraint can then be placed on the number of machines operated by one employee. That is:

$$N_{mach/worker} \leq \frac{T_M}{T_S} \quad \textbf{(49)}$$

where T_M *= total machining time for one plate* and T_S *is the setup time per plate*. Further, T_M is the sum of major channels, minor channels, outline and peripheral machining times.

From a practical perspective, the author believes it is ill advised to assign more than one machine per worker. Due to the nature of it, machining requires constant monitoring to ensure that everything remains in order. This is especially true in micro machining where tool failure can occur catastrophically and suddenly. Not responding in a timely manner to tool failure will result in decreased productivity. Therefore, for the purpose of this section, and the analysis following in Section 7, it is assumed that $N_{mach/worker} = 1$.

6.2.3 Estimating Tooling Cost Parameters

Referring to the synthesis of tooling cost presented in Section 6.1.3, the following parameters must be estimated:

- $C_{Major\ Tool}$
- $C_{Minor\ Tool}$
- $C_{Peripheral\ Tool}$

where the above parameters represent the cost per tool (R/tool) for major channel, minor channel and peripheral feature tools respectively. The cost of these tools is easy enough to estimate because the prices are readily available on supplier websites. For the purpose of this project PMT (Performance Micro Tool) was used as the supplier. Prices for the major channel *(0.7 mm)*, minor channel *(0.5 mm)* and peripheral *(2.5 mm)* tools, as on 30/8/2011 are *$11.65, $13.65* and *$10.65* respectively. Since these tools are imported, a delivery cost must be added to the price to arrive at a final tool cost. Thus, an amount of *R5/tool* is attached for importing costs. Further, an exchange rate of 7.06(R/$), as on 31/8/2011, is used. This results in prices of R87.29, R101.37 and R80.19 for the major channel, minor channel and peripheral tools respectively.

6.2.4 Estimating Equipment Cost Parameters

In order to estimate the contribution per plate towards capital recovery, the following parameters must be estimated:

- *IV*
- n_{years}
- *SV*
- *i*
- AP_{mach}
- N_{mach}

where *IV = initial cost of equipment (R), i = effective annual interest rate (%),* n_{years} *= number of years of operation of the equipment, SV = salvage value of the equipment after* n_{years} *(R),* AP_{mach} *= annual production per machine (plates/machine-year)* and N_{mach} *= number of machines in operation.*

The initial cost equipment, *IV,* accounts for the total cost to install all the equipment needed to begin manufacturing. This includes the micro milling frame, high-speed spindle, work-piece holding mechanism, controller, machine housing, software and sundry accessories for all of the required micro milling machines. Import and installation costs are also included in the equipment cost. An itemised cost breakdown is shown in Appendix C. The combined estimated cost for all the equipment necessary is *$23 965* per machine. With a current *(31/8/2011)* exchange rate of *7.06 (R/$)*, the estimated initial cost is *R 169 196* per machine. For the purpose of this initial cost estimation, it is assumed that $N_{mach} = 1$.

The number of years of operation, n_{years}, is limited by one of two factors. Either, the machine reaches the end of its useful life, in which case a new machine must be acquired, or the program reaches the end of its life. For the purpose of generating an initial manufacturing cost estimate, n_{years} is assumed to be *5 years*.

The salvage value, as a rule of thumb, is assumed to be 10% of the initial value at the end of n_{years} years. Therefore, SV is *R16 920*.

The effective annual interest rate, *i*, is subject to the conditions of the loan agreement between the lender and the borrower. For this purpose, it is assumed to be 9%, which is the current (31/8/2011) prime interest rate.

As explained in Section 6.1.4, AP_{mach} is a forecasted value and is intended to be the subject of a demand sensitivity analysis. Since this value is defined in terms of production per machine, it is constrained by the available time per machine. The annual production per machine can be formalised as follows:

$$AP_{mach} = \frac{\frac{working\ days}{year} \times \frac{hours}{day} \times u}{\frac{T_M}{60}} \quad \textbf{(50)}$$

where T_M *= the total machining time (min)* and *u = machine utilisation*. Machine utilisation, in this case, is defined as the proportion of operational time to total available time. If a machine were to run at full capacity, with no down time, it would be running at maximum utilisation. This could be calculated as $u_{max} = \frac{T_M}{T_p}$. Maximum utilisation is a hypothetical scenario that is not realistic. However, it can be used to determine the theoretical maximum annual production per machine. Therefore,

$$AP_{mach} \leq \frac{\frac{working\ days}{year} \times \frac{hours}{day} \times u_{max}}{\frac{T_M}{60}} \quad \textbf{(51)}$$

With *250 working days per year*, *8 working hours per day*, a *total machining time of 21.041 minutes per plate* and a *total manufacturing time of 40.25 minutes per plate* (from Section 5.2.3 on page 91), $AP_{mach} \leq 2981$ *plates per year*. In reality, AP_{mach} will be much smaller. Even if supported by market demand, it is highly unlikely that a machine will have no non-productive time. For the purpose of this initial cost estimation, it will be assumed that AP_{mach} *= 1000 plates/machine-year*.

6.2.5 Estimating Overhead Cost Parameters

In order to estimate the contribution per plate towards sundry overheads, the following parameters need to be estimated:

- *TO*
- AP_{mach}

where *TO = total annual sundry overheads (R/year)* and AP_{mach} *= annual production (plates/machine-year)*. The total sundry overheads per year, *TO*, account for all indirect costs apart from machine equipment. These include, but are not limited to, administrative salaries, maintenance, utilities and factory rental. The value to use here is company specific.

For the purpose of this cost estimation, it is assumed that *TO = R100 000*.

The annual production per machine, AP_{mach}, is dealt with in Section 6.2.4. It should be noted here that there is a connection between the total production per year, the annual production per machine and the number of machines. This relationship can be formalised as follows:

$$AP_{mach} = \frac{Total\ Production}{N_{mach}} \quad \textbf{(52)}$$

where total production is prescribed by market demand. By including this equation in the cost model, the optimal number of machines can be determined for a certain predicted demand.

6.2.6 Initial Cost Model Results

The initial cost estimate per plate, for the manufacture of one bipolar plate under the described conditions is shown in **Table 17** below.

Table 17 – Initial Cost Estimate

Material	**R 408.00**
Labour	**R 47.67**
Tooling	**R 111.96**
Equipment	**R 40.67**
Overhead	**R 50.00**
Total	**R 658.30**

The results presented above conclude the development and initial application of the manufacturing cost model built for the purpose of this project. The remainder of this project deals with the analysis of this cost model and drawing conclusions from the results.

7. Cost Model Analysis

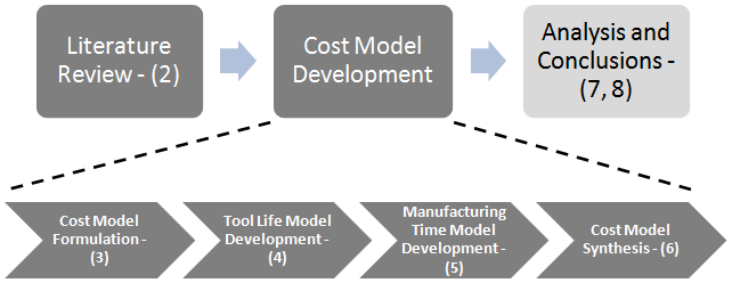

The work done in the previous sections contains the framework to be able to evaluate manufacturing performance in terms of time and cost. Further, this cost model is intended to provide the flexibility to be able to evaluate any feasible combination of input parameters. The reason being that the economic world is a dynamic one with prices and available technology ever-changing. Consequently, static results are only temporarily valid. Rather, it is more important to build a flexible framework that is able to evaluate manufacturing performance quickly and for any combination of input variables.

Nonetheless, given a suitable framework, it is not always a simple matter of applying it. This is especially true when there is complex interplay between the variables, as is the case here. This section attempts to overcome this issue by demonstrating the application of the cost model with suitable examples.

The cost model developed for the purpose of this project contains 42 input variables. Ideally, it would be useful to fully understand the influence of each of these variables on manufacturing performance. However, given the time constraints, this is outside the scope of this project. Rather, more pertinent questions are answered. These are seen as the immediate information requirements from HySA, who are responsible for the development of the capability to manufacture hydrogen fuel cells in South Africa. These questions are:

- What cutting parameters should be used when machining bipolar plates?
- How will design changes influence manufacturing performance?
- How does the potential market size influence cost?

This section addresses each of these questions in two ways. Firstly, the approach taken in answering them is discussed. This enables a future user to replicate the analysis for different underlying circumstances. Secondly, the analysis is performed under certain assumptions to illustrate the influence of input variables on manufacturing performance.

7.1 Finding Near-Optimal Cutting Parameters

In this section, cutting parameters are considered. This is because these parameters have a significant effect on manufacturing performance, in terms of both time and cost. Furthermore, the cutting parameters are probably the easiest to change from the machine operator or decision maker's point of view. That is, cutting parameters are set by adjusting the feed rate and rotational velocity on the machine.

Since the cutting parameters are easily adjustable and they significantly influence the manufacturing performance, it is worthwhile evaluating their effect. In doing so, it is possible to determine the best combination of cutting parameters. It should be noted here that, for the purpose of this section, the cutting parameter analysis is limited to those pertaining to the major channel machining. This is because, this type of machining accounts for approximately 78% of actual machining time and 82% of the machining cost.

In order to understand the effect of cutting parameters on manufacturing performance it is necessary to first formulate the problem. Since this formulation only pertains to the machining of the major micro channels, it is necessary to adapt the original time and cost formulation slightly. That is, it is not necessary to include the entire cost model. Rather, only the cost directly associated with the machining of the major channels needs to be considered.

7.1.1 Formulating the Problem

In evaluating manufacturing performance, few measures receive as much attention as manufacturing cost. Manufacturing cost is, therefore, the primary focus of this project. However, in terms of the time-cost-quality paradigm, time and quality are also important. In a competitive environment, it is necessary to be able to manufacture goods quickly and at good quality, over and above being able to manufacture them at a reasonable cost. The degree to which each of these measures needs to be met depends on the particular industry and strategy of the manufacturer.

Following this, it is necessary to consider other measures of manufacturing performance when formulating this problem. The quality aspect is assumed to be non-negotiable. Referring to the tool life model of Section 4; in building this model, a critical amount of tool wear was chosen upon which tool life was defined, such that an 'acceptable' standard of quality is maintained. This is described in detail in Section 4.2.2.2 on page 60.

Therefore, for the purpose of this problem, the time-cost relationship is described. The time objective, which is an adaption of **Equation (28)**, can be formalised as follows:

$$T_{CM\_major} = \frac{N_{ch\_major} \times L_{ch\_major}}{F_R} + \frac{wp(N-1)}{F_R} + (T_{tc} + T_{refz})z_{major} \quad \textbf{(53)}$$

where T_{CM_major} = *major channels machining time (min/plate)*, N_{ch_major} = number of major micro channels on both plate sides, L_{ch} = *average length of channels*, F_R = *feed rate (mm/min)*, *wp = plate width (mm), N = number of plates machined at a time,* T_{tc} = *tool changing time,* T_{refz} = *z-axis referencing time* and z_{major} = *tool life multiplier*.

Further, the cost objective can be formalised as follows:

$$C_{CM\_major} = T_{CM\_major} \times LR + C_{MajorTooling} \quad \textbf{(54)}$$

where C_{CM_major} = *cost associated with machining the major micro channels (R/plate), LR = operator labour rate (R/hour)* and $C_{MajorTooling}$ = the major micro end mill tooling cost (R/plate), as already described in Section 6.1.3, but presented here again for convenience. $C_{MajorTooling}$ is described by the following formula:

$$C_{Major\ Tooling} = C_{Major\ Tool} \times Z_{major} \quad \textbf{(55)}$$

where, $C_{MajorTool}$ = *cost per major micro end mill (R/tool)* and

$$Z_{major} = \frac{2 \times N_{ch\_major} \times L_{ch\_major}}{L_T \Big/ d_{major} \times D_{major}} \quad \textbf{(56)}$$

where L_T is derived from the tool life (mm^3/tool) model of Section 4.3.7 on page 73 and Z_{major} represents the *number of tools used per plate (tools/plate).*

The above time and cost objectives are constrained by the capability of the machine in use. That is, the objectives are constrained by the maximum rotational velocity (n) and feed rate (F_R) achievable by the machine. This can be represented as follows:

$$\frac{v_{major} \times 1000}{\pi \times D_{major}} = n \leq n_{Max} \quad \textbf{(57)}$$

and

$$\frac{v_{major} \times f_{t\,\mathrm{major}} \times 2}{\pi \times \mathrm{D_{major}}} = \mathrm{F_R} \leq F_{R\,Max} \quad \textbf{(58)}$$

All of the input parameters, except the cutting parameters, have previously been assigned values based on certain assumptions described in Section 5.2.1. Following this, only the cutting speed (v_{major}) and feed per tooth ($f_{t\ major}$) need to be set. Essentially what remains in this case are two objectives, namely T_{CM_major} and C_{CM_major}, which are represented as a function of the cutting parameters. The stage is, therefore, set to apply an optimisation algorithm to find the combination of cutting parameters that yields the best result in terms of time and cost.

An optimisation algorithm operates like an intelligent search of the solution space, where the solution space is made up of all possible combinations of the input variables. More specifically, an optimisation algorithm assesses candidate solutions relative to one another and uses predefined logic to systematically find the best solutions on a trial and error type basis. For this particular application, the optimisation algorithm is intended to systematically find the combination of cutting parameters that yield the best manufacturing performance in terms of time and cost.

7.1.2 Solving the Problem

The solution space for the problem formulated above is infinite because it is characterised by all possible combinations of the cutting parameters, which are all bounded continuous variables. The problem is further complicated with the inclusion of two non-linear objectives.

7.1.2.1 The Solution Approach

The nature of the problem described above suggests the use of a metaheuristic to solve it. Although using a metaheuristic is not the only feasible approach to solving this problem, it is one of the most versatile.

According to Talbi (2009), metaheuristics represent a family of approximate optimisation techniques. These techniques are approximate because they do not guarantee exact optimal solutions. However, metaheuristics have gained much popularity over the last two decades, according to Talbi (2009), because they do provide 'acceptable' solutions in a reasonable amount of time. Further, their use in a variety of applications such as engineering design and supply chain management, demonstrate their efficiency and effectiveness in solving complex problems (Talbi 2009).

The use of a metaheuristic to optimise cutting parameters in micro milling has been seen previously in literature. One such example was done by Sreeram, et al. (2006). They used a genetic algorithm to optimise tool life and, in effect, machining cost by finding the best combination of cutting parameters for a particular component. Their results indicated that the optimal cutting parameters were different from those recommended by the supplier, especially the depth of cut parameter. Further, Sreeram, et al. (2006), showed that the use of an optimisation algorithm could increase

machining efficiency and reduce production costs through the correct selection of cutting parameters. This is due to the effect of cutting parameters on tool life and machining time, two significant cost drivers in micro milling.

The solution developed for the purpose of this section is derived from the simulated annealing algorithm. Simulated annealing gets its name from the process of cooling molten metal; also known as annealing. If a metal is heated and then cooled rapidly, the highly agitated atoms are forced to settle into a random structure. If, however, the temperature is decreased slowly, allowing the atoms enough time to settle, a strong crystal lattice structure is formed (Talbi 2009). This process is analogous to an optimisation problem in the sense that the search pattern needs to shift slowly and carefully from a wide-ranging pattern to a localised pattern.

Further, the algorithm built for the purpose of this section is based on the generic algorithm for multi-objective simulated annealing presented by Nam and Hoon Park (2010).

7.1.2.2 Building the Solution

The algorithm built for the purpose of this section is represented by its pseudo code shown in **Figure 36**. A description of this algorithm follows presently.

Lines 1 – 4 define a few variables used in the algorithm. These are as follows:

- *F* stores a set of feasible solutions for the problem. Although *F* is initially empty, it will, as the algorithm progresses, be transformed into a set of non-dominated solutions. This is otherwise known as the pareto front. The concept of dominated and non-dominated solutions is an important one in multi-objective optimisation. By definition, a solution, *A*, pareto dominates another solution *B* if *A* is at least as good as *B* for all objectives and better than *B* for one objective.
- T_0 stores the initial 'temperature' of the annealing process. This represents the starting value for T_k from **Equation (59)** below.
- k_{lim} defines the number of iterations in the process.
- *a* is defined as the rate of cooling in the annealing process when it is considered in the equation below (where *k* is the iteration counter of the algorithm). Further elaboration on this and its influence in the algorithm is presented in section 7.1.2.3.

$$T_k = a^k \times T_0 \quad \textbf{(59)}$$

Line 5 populates S with an initial candidate solution chosen randomly from within the solution space. The candidate solution *S* is coded as a vector containing the input parameters (*v*, f_t and *d*) values as well as the objective values (T_{CM_major} and C_{CM_major}) corresponding to those inputs. Similarly, *F* is coded as an array containing a set of *S-type* vectors.

Line 6 is the initiation of the main loop running for k_{lim} iterations with *k* being the iteration counter.

Line 7 calculates the 'temperature' for that iteration. This is a function of the cooling rate *a*, the iteration number *k* and the initial temperature T_0 as indicated in **Equation (59)**. The role of this elaborated on in Section 7.1.2.3.

```
1.  F = Initial Set of random Solutions          % This will be the pareto front
2.  T0 = Initial Temperature                     % Starting point in the annealing process
3.  klim = # of iterations in the annealing process
4.  a = cooling rate
5.  S = initial candidate solution
6.  while k ≤ klim                               % Run for klim iterations
7.      Tk = a^k T0
8.      R = Tweak(S, (1 − k/klim)^(1/x) )        % Tweak S by multiplying bounded range of
                                                 % inputs by 2nd term
9.      If R pareto dominates S then
10.         S = R;
11.     else if S pareto dominates R then
12.         If rand(0,1) < P then                % Where P = e^((Quality(R) − Quality(S))/Tk)
13.             S = R
14.         end if
15.     else
16.         S = R                                % If neither S nor R dominate each other, then accept
                                                 % new solution
17.     end if

% Now that we have a new Candidate solution 'S', we can add it to the Solutions in F, and
then remove any %pareto dominated solutions or in other words, update the front
population.

18.     Add solution S to F
19.     if modulus of k/100 = 0                  %Every 100 iterations
20.         F = ParetoUpdate(F)                  % Keep only Pareto Dominant solutions in F
21.     end if
22.     k = k+1                                  %Counter for main while loop
23.     plot (F)                                 Plot the solutions in F
24.end while
```

Figure 36 - Simulated Annealing Algorithm

Line 8 determines the new candidate solution *R* by tweaking the current candidate solution *S*. The second input term in the *Tweak* function controls the maximum half-range noise to be added to each variable in the tweaking process according to the following formula (where *t* is the second term):

$$Maximum\ Half\ Range\ Noise = [Upperbound - Lowerbound] * t \quad \textbf{(60)}$$

Usually, the range of uniform noise is fixed at a predefined value by setting t to a fixed value. However, for the purpose of this thesis the range of uniform noise is decreased slowly as the simulated annealing algorithm progresses. This is achieved by the following formula.

$$t = (1 - {}^{k}/_{k_{lim}})^{1/x} \quad \textbf{(61)}$$

Further elaboration on the formula above is presented in Section 7.1.2.3. This tweaking method is derived from the *Bounded Uniform Convolution method* described by Luke (2010). The *Tweak* function further ensures that the new candidate solution satisfies the problem constraints as prescribed by the machine capacity, according to **Equations (57)** and **(58)**.

Lines 9 – 17 form the heart of the simulated annealing algorithm. They decide whether to accept the new candidate solution *R.* This is done by replacing the old solution *S* with the new solution *R*. The decision is made based on the following criteria:

- If *R* pareto dominates *S,* then replace *S* with *R.*
- Otherwise, if *S* pareto dominates *R*, then replace *S* with *R* with probability *P*. Essentially, this allows the algorithm to occasionally move 'downhill'. The probability, *P*, with which this occurs is controlled by **Equation (63)** and explained in Section 7.1.2.3.
- Finally, if neither *S* nor *R* dominates each other, then *S* is replaced with *R*. This ensures that the algorithm does not stagnate on a reasonably 'good' solution but is willing to jump to an alternative solution if neither one dominates the other.

The probability *P*, which largely controls the behaviour of the algorithm, is a function of the *quality* of the solutions *S* and *R*. Quality is derived from Luke (2010) and is measured relative to a set of solutions. Firstly, *strength* is defined as the number of solutions in a set that the original solution dominates. Quality is then determined according to the following:

$$Quality(B) = \frac{1}{1 + \sum_{\substack{g \in G \text{ that Pareto} \\ Dominates\ B}} Strength(g)} \quad \textbf{(62)}$$

Quality is thus defined as the inverse of the sum of all the solutions in the set that pareto dominates the original solution. This method provides an objective way of defining the value of a solution relative to a set of solutions.

Line 18 adds the new candidate solution *S* to the existing front *F.*

Lines 19 – 21 Every 100 iterations, the pareto front is updated by removing any dominated solutions. This allows a short search history to be kept, which, if plotted, affords the user some insight into where and how the algorithm is searching in the solution space.

Lines 22 – 24 are the closing of the main *while* loop where the counter *k* is increased and the current solutions in the set *F* are plotted.

7.1.2.3 Controlling the Behaviour of the Algorithm

An important feature in any metaheuristic is the algorithm behaviour in terms of exploration versus exploitation. It is preferable to encourage more exploration in the early stages of an algorithm while later stages should be geared more towards exploitation. This allows for proper identification (via exploration) and clarification (via exploitation) of near-optimal solutions in the solution space. The behaviour of the algorithm should, therefore, shift from exploration to exploitation as the algorithm progresses. The ideal changing behaviour of the algorithm is illustrated by **Figure 37** below.

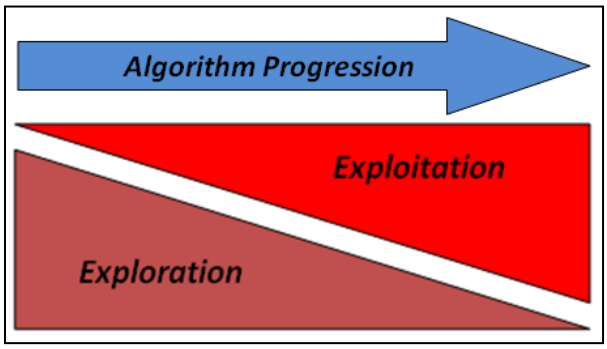

Figure 37 – Changing Behaviour of the Algorithm

The rate that the search algorithm shifts from exploration to exploitation is the key to customising a metaheuristic to a particular problem. Two mechanisms have been identified to control the shifting rate for this application. These are the *probability, P* in terms of *a* and the *half range noise, Rd* in terms of *x*. These are discussed presently.

The probability, *P,* is defined by the formulae:

$$P = e^{\frac{Quality(R) - Quality(S)}{T_k}} \quad \textbf{(63)}$$

and

$$T_k = a^k * T_0 \quad \textbf{(64)}$$

The parameter *P* determines the probability that a worse solution will be accepted over a better solution. This, effectively, controls the amount of exploration in the search by allowing the algorithm to occasionally accept a worse solution over a better one. In a traditional hill search, this would be equivalent to allowing the algorithm to move 'downhill' on occasion. The higher the value of *P*, the more exploration in the algorithm, while the lower the value of *P*, the more exploitation. The parameter, T_0 (set to a value of 10), represents the approximate starting value for T_k when $k = 0$.

The parameter, *a*, in **Equation (64)** above controls the rate at which *P* decreases. In the context of simulated annealing, *a* is known as the 'cooling rate'. It should be noted here that the parameter *k* refers to the algorithm iteration counter, as described in Section 7.1.2.2. Choosing a larger value for *a*, allows *P* to decrease at a slower rate, effectively allowing more exploration in the algorithm.

Conversely, choosing a smaller value for *a,* allows *P* to decrease at a faster rate, affording more exploitation to the algorithm.

The half range noise *Rd* is defined in terms of *x* according to the formula

$$Rd = [Upper\ Bound - Lower\ Bound] * \left(1 - {}^{k}/_{k_{lim}}\right)^{1/x} \quad \textbf{(65)}$$

where *Upper Bound* and *Lower Bound* represent the upper and lower bounds for each input variable respectively. Further, *k* and k_{lim} represent the iteration counter and maximum number of iterations respectively.

The half range noise, *Rd*, is the maximum amount that any input variable can change when tweaking a candidate solution. The greater the value of *Rd*, the more noise can be added to input variables and, consequently, the more the output variables can jump around in the solution space.

The parameter *x* controls the rate at which *Rd* decreases. Choosing a larger value for *x* allows *Rd* to decrease more rapidly and, in so doing, affords more exploitation to the algorithm. Conversely, choosing a smaller value for *x* slows down the decrease of Rd, thereby, affording more exploration to the algorithm.

Following the arguments above, the behaviour of the algorithm, in terms of exploration and exploitation, is controlled by the selection of parameter values for *a* and *x*. The correct values for these parameters are determined by experimentation and the user's judgement. For the purpose of this problem, values of *10* and *0.997* for *x* and *a* respectively, were found to yield good results for 3000 iterations (k = 3000).

7.1.3 Algorithm Results

The previous section saw a discussion of the development and operation of the optimisation algorithm. In this section, this optimisation algorithm is used to optimise two manufacturing performance objectives, namely machining time and cost. Further, these objectives have been described as a function of the cutting parameters and are, therefore, optimised as such.

7.1.3.1 Initial Results and Analysis

In order to gain understanding into the nature of the time-cost relationship, various configurations were tested. By configurations it is meant that different values for the constraints represented by **Equations (57)** and **(58)** are applied to the algorithm and the results recorded. Recall that these constraints represent the maximum capability of the machine in use. This is a useful exercise because it illustrates the effect that machine limitations have on the best possible time and cost

solutions and the relationship between them. For the purpose of this document, three alternative configurations and the corresponding results are presented.

For the first configuration, typical machine constraints are considered. That is, maximum rotational velocity (n_{Max}) and maximum feed rates (F_{R_Max}) are ***60 000 rev/min*** and ***1 500 mm/min*** respectively. Using these constraints, the simulated annealing algorithm was run and the results plotted in **Figure 38**. The figure plots the resulting solutions on a Cartesian plane with machining time and cost on the x and y-axes respectively. The best possible (near-optimal) solutions are shown in blue, while the green dots indicate non-optimal solutions found by the algorithm. The arrangement of the solutions plotted in **Figure 38** indicates that the algorithm tends towards one optimal solution in terms of both time and cost. This is counter to initial expectations that the problem contains a set of optimal solutions that trade-off time and cost. Essentially, what this means is that cutting parameters that yield the solution with the lowest cost also yield the solution with the shortest time. The objectives for this algorithm configuration are, therefore, non-conflicting.

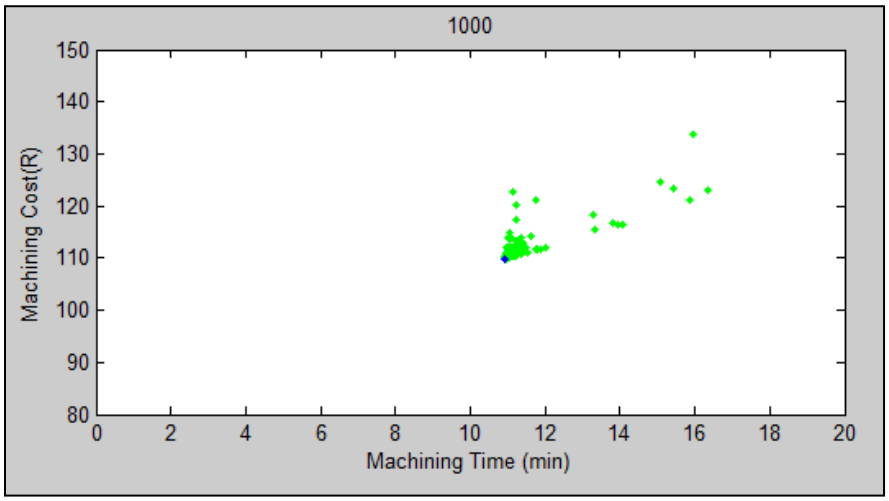

Figure 38 – Configuration 1, n_{Max} = 60 000 rev/min, F_{R_Max} = 1 500 mm/min

For the second configuration, a lower maximum rotational velocity is applied to the algorithm. The constraints applied are, therefore, ***30 000 rev/min*** and ***1 500 mm/min*** for the maximum rotational velocity and feed rate respectively. The results are plotted on a Cartesian plane with machining time and cost on the x- and y-axes respectively, shown in **Figure 39**. The near-optimal (non-dominated) solutions are plotted in blue while the non-optimal (dominated) solutions found during the progression of the algorithm are plotted in green.

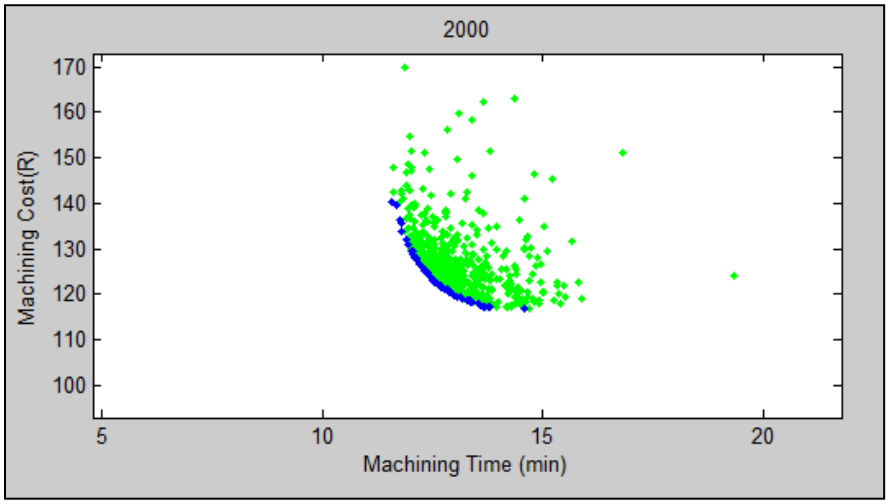

Figure 39 - Configuration 2, n_{Max} = 30 000 rev/min, F_{R_Max} = 1 500 mm/min

Contrary to the first configuration, **Figure 39** indicates a set of near-optimal solutions, represented by the blue curve. This is characteristic of objectives which are conflicting in nature. That is, an improvement in one objective will require deterioration in another. Hence, the objectives are traded-off with one another. It is interesting to note here that the nature of the time-cost relationship changes with changing constraints.

Finally, for the third configuration, values of ***60 000 rev/min*** and ***5 000 mm/min*** were applied to the maximum rotational velocity and feed rate constraints respectively. Similarly, **Figure 40** indicates the results. Once again, the configuration resulted in a set of near-optimal solutions suggesting that the objectives are conflicting.

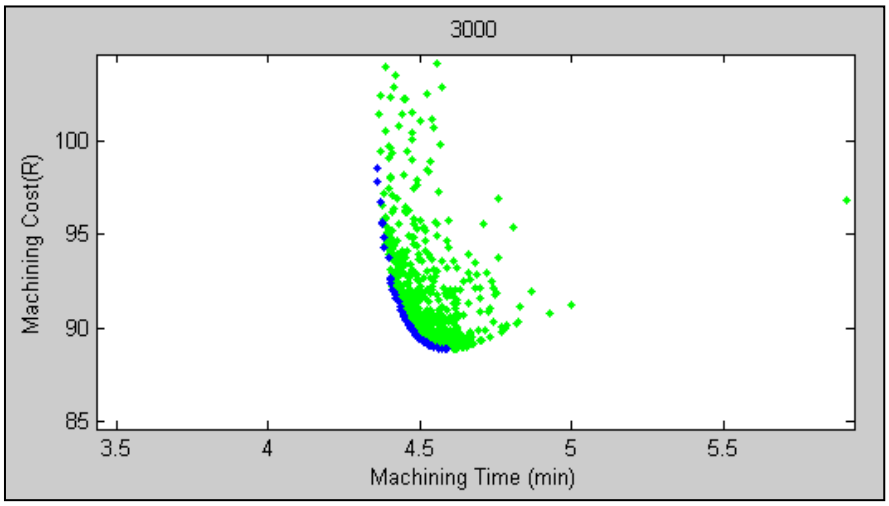

Figure 40 – Configuration 3, n_{Max} = 60 000 rev/min, F_{R_Max} = 5000 mm/min

The changing nature of the time-cost relationship is an interesting phenomenon and has to do with the way in which tool life is defined. Consider the form of the tool life model, shown below. As described in Section 4, L_T represents the predicted *volume of material removed (mm^3)* as a function

of cutting parameters, where *v = cutting speed (m/min), f_t = feed per tooth (µm)* and *d = depth of cut (mm)*.

$$L_T = e^{5.842+5.275d-0.000348v^2-0.00506{f_t}^2-1.724\,d^2+0.00270vf_t} \quad \textbf{(66)}$$

The cutting parameters *v, ft* and *d* also determine the speed of machining according to the feed rate formula:

$$F_R = \frac{v \times f_t \times 2}{\pi \times 0.7} \quad \textbf{(67)}$$

where F_R *= feed rate (mm/min)*. The values *2* and *0.7* above represent the number of flutes/cutting edges and tool diameter respectively. It should be noted here that feed rate is always increasing for an increase in cutting speed and feed per tooth. It should also be noted that the objectives of machining time and cost are largely driven by tool life and feed rate. A low machining time is associated with a high feed rate and a high tool life while a low machining cost is similarly associated with a high tool life and a high feed rate. Therefore, the time vs. cost trade-off is really a feed rate vs. tool life trade-off, with near-optimal solutions having a high feed rate and high tool life.

The question then is whether the objectives of feed rate and tool life are conflicting or non-conflicting. From the formulation of these objectives above in terms of cutting parameters, it is not so obvious. The pareto front analysis performed previously suggests that these objectives are at times conflicting and at times non-conflicting, depending on the range within which the cutting parameters are selected.

Consider **Figure 41** below. It shows a plot of *tool life (L_T*, on the z-axis) as a function of *cutting speed (v,* on the y-axis) and *feed per tooth (f_t,* on the x-axis*)*, for a constant *depth of cut (d)*. The changing colour represents the changing expected tool life with dark blue being a low tool life and red being a high tool life. Now consider the behaviour of tool life within the narrow parameter range, demarcated by the rectangle, versus the behaviour of tool life over the whole parameter spectrum. Within the narrow range, tool life always increases for an increase in feed per tooth and cutting speed. However, this is not always true over the whole spectrum. Tool life can both increase and decrease for an increase in cutting speed and feed per tooth, depending on the location in the solution space.

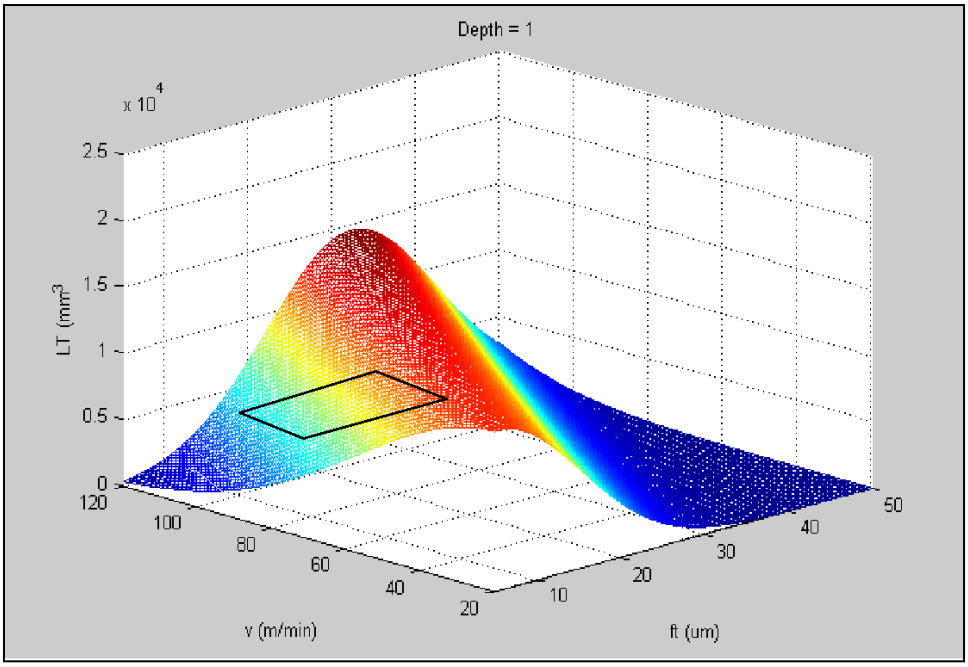

Figure 41 - Tool Life Plot - Fixed Depth of Cut

The inconsistency in the behaviour of tool life in terms of the cutting parameters is the reason for the changing nature of the time-cost relationship. That is, the change from a non-conflicting to a conflicting relationship as the solution space is broadened. This is essentially done by setting the algorithm constraints, namely n_{Max} and F_{R_Max}. A summary of the results of the three configurations is shown in **Table 18**.

Table 18 – Configurations Results Summary

Configuration	*Algorithm Constraints*		Values Achieved			
	n_{Max} (rev/min)	F_{R_Max} (mm/min)	Average n achieved (rev/min)	Average F_R achieved (mm/min)	Limiting constraint	Nature of Objectives
1	60 000	1 500	36 061	1 499.99	F_{R_Max}	Non-Conflicting
2	30 000	1500	29 969	1 272	n_{Max}	Conflicting
3	60 000	5000	59 974	4 451	n_{Max}	Conflicting

For configuration 1 and 3, the limiting constraint is the maximum allowable rotational velocity, n_{Max}. By limiting constraint it is meant the constraint which actually limits the values that the cutting parameters can achieve. This is indicated by the value of the average rotational velocity, n, achieved for all the near-optimal solutions found versus the maximum allowable rotational velocity. Notice further, that for configuration 1 the limiting constraint is the maximum allowable feed rate, F_{R_Max}. It

can, therefore, be concluded that when the burden of constraint is placed on the maximum allowable rotational velocity, the objectives are conflicting and vice versa.

This is an interesting and important consideration in terms of choosing which micro milling machine to purchase. Typically, the spindle (controls n_{Max}) and worktable drive motors (controls F_{R_Max}) are customisable. That is, their capability can be specified.

Micro milling operations are typically characterised by high spindle speeds and low feed rates. This is because the tools used are small and require higher rotational speeds and lower feed rates to maintain acceptable cutting parameters. Therefore, in the context of micro milling, it is unlikely that the burden of constraint will be on the rotational velocity due to the nature of the problem. Rather, the burden will be on the achievable feed rate. That is, the feed rate capacity of the machine will most likely determine how cheaply the plates can be machined. Also, because the time and cost objectives are non-conflicting when the feed rate carries the burden of constraint, this will also determine how quickly the plates can be machined.

7.1.3.2 Feed Rate Sensitivity

Following the argument above, it will be useful from a management perspective, to quantify the effect that increased feed rate capacity will have on the near-optimal machining time and cost. This is because increasing the feed rate capacity will improve the achievable time and cost; two important considerations for managers and decision makers.

To address this, the simulated annealing algorithm was run for several configurations. For each configuration, the maximum rotational velocity was held constant while the maximum feed rate was increased. Further, the best possibe solution, in terms of both time and cost, was recorded and plotted, shown in **Figure 42** below, as a function of the maximum allowable feed rate. The relationship between the near-optimal time and cost and maximum allowable feed rate can be more formally expressed by **Equations (68)** and **(69)** below, which were obtained by fitting a regression line through the resulting solutions. They are as follows:

$$T_{CM\_major} = 6 \times 10^{-06} {F_{R\,Max}}^2 - 0.0242\, F_{R\,Max} + 33.806 \quad \textbf{(68)}$$

and

$$C_{CM\_major} = 7 \times 10^{-06} {F_{R\,Max}}^2 - 0.0333\, F_{R\,Max} + 144.6 \quad \textbf{(69)}$$

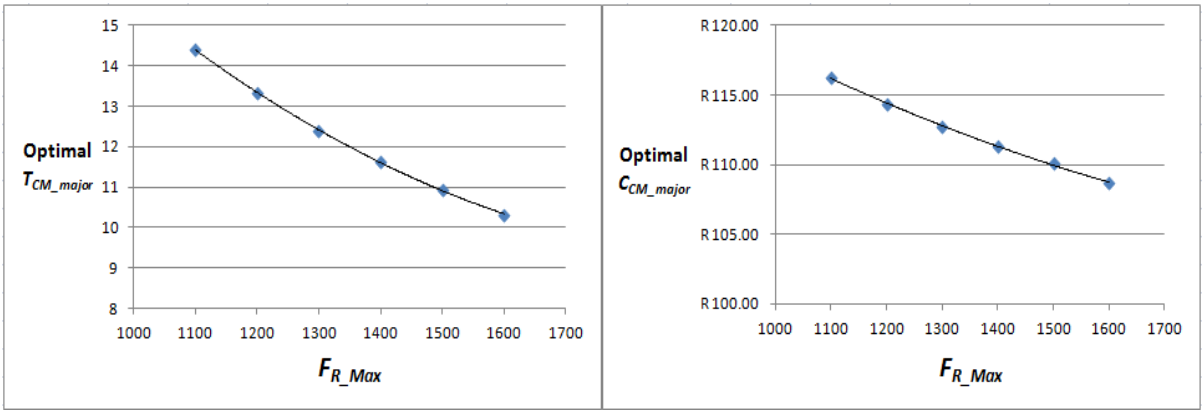

Figure 42 – Feed Rate Sensitivity Analysis

It should be noted here that even though improving feed rate capacity will improve both machining time and cost, it is not necessarily a wise decision. This is because the cost objective dealt with in this analysis is the cost associated with the major micro channel machining operations, and not the complete manufacturing cost. That is, it does not include the cost of equipment, which will typically be increased if the feed rate capacity is increased. Therefore, the additional cost of equipment (per plate) must also be considered. This is not done for the purpose of this analysis because it would be necessary to evaluate all the ways of increasing feed rate capacity of micro milling machines and accurately estimating the costs associated with doing so. This is outside the scope of this project.

This section is concluded with a presentation of the results of the optimisation algorithm. **Table 19** below presents the cutting parameters, which yield near-optimal solutions in terms of time and cost for different machine constraints.

Table 19 – Cutting Parameters for Near-Optimal Solutions under Machine Constraints

Machine Constraints	Cutting Parameters				Near-Optimal Solutions		Achieved Machine Values	
F_{R_Max}	n_{Max}	$v_{\_major}$	f_{t_major}	$d_{\_major}$	T_{CM_major}	C_{CM_major}	Achieved n	Achieved F_R
1100	60000	68.34	17.70	0.7	14.41	R 116.23	31074.37	1099.86
1200	60000	71.08	18.56	0.7	13.32	R 114.37	32322.55	1199.81
1300	60000	73.87	19.34	0.7	12.41	R 112.74	33591.92	1299.30
1400	60000	76.14	20.22	0.7	11.61	R 111.28	34621.25	1399.85
1500	60000	80.52	20.48	0.7	10.93	R 110.10	36616.73	1499.70
1600	60000	81.94	21.47	0.7	10.33	R 108.65	37258.99	1599.77

7.2 Effect of Design Changes on Manufacturing Cost

Another important consideration from a management perspective, and as indicated by HySA, is the effect of design changes on the manufacturing cost. This section attempts to address this issue by evaluating slightly different designs in terms of their effect on the overall manufacturing cost. By design changes, it is not meant a completely different design. Rather design changes, in this context, refers to changes in the number or size of micro channels, since this is the primary feature of the bipolar plate.

The question remains: why should alternate designs be evaluated? The answer to this question lies in the development progress of bipolar plates, from concept to production. As of the date of this project, the flow field design type has been decided, where flow field design type refers to either serpentine, parallel or parallel serpentine channels. An elaboration of this can be found in Section 2.2.2. However, the exact specifications, in terms of the characteristics of the channels, have not been decided yet. This is because even small changes in the number or size of channels can significantly influence the performance of the plate. This performance influence must, therefore, be understood before the design can be optimised and the final design specified.

Consequently, the cost model developed for this project must incorporate the flexibility to be able to evaluate different designs in terms of cost. This section addresses the aforementioned issue, firstly, by describing how to evaluate different designs and, secondly, by evaluating possible design changes. The reason for evaluating design changes is mostly to illustrate the process, but also to highlight the effect that typical changes could have on the manufacturing cost.

7.2.1 How to Evaluate Design Changes

The procedure to evaluate alternative designs is relatively simple. One complication, however, arises in the evaluation of designs whose channel widths do not equal *0.7 mm*. Recall here, from Section 4, that the tool life model developed applies to micro end mills of diameter *0.7 mm*. Nonetheless, it is necessary to be able to estimate the tool life of other sized tools, larger or smaller. This is to be able to evaluate designs, in terms of cost, whose channel widths are not equal to *0.7 mm*. The need, therefore, exists to be able to adjust the original tool life model to suit other sized tools.

This need was addressed in Section 6.1.3.2, where two alternative methods of adjusting the original tool life model were assessed. It was found that the following method yields the best accuracy:

$$L_T^* = L_T \times \frac{D^*}{D} \qquad \textbf{(70)}$$

where L_T* = adjusted tool life (mm^3), L_T = original tool life for 0.7 mm tool diameter (mm^3), D* = new tool diameter* and *D = original tool diameter (D = 0.7 mm)*. It should be noted here that statistical confidence is lost in translating the original tool life model in this manner.

The adjusted tool life model should be incorporated into the cost model when evaluating alternate designs, especially those that have different channel widths to that of the original design. In addition to this, certain restrictions are placed on other channel characteristics. These characteristics relate to the size of the flow field area. Assuming the area is square, which it is in the original design, the size of the flow field can then be represented by the length of one side, L_F. The length of channels, L_{Ch}, is then limited by the following inequality:

$$L_{Ch\_major} \leq 3 \times L_F \tag{71}$$

provided the number of turns in the flow field pattern remain constant. In this case, the number of turns is three. Furthermore, the number of channels, N_{Ch_major}, can be limited by the following inequality:

$$N_{Ch\_major} \leq \frac{L_F}{3(D_{major} + W_L)} \tag{72}$$

where D_{major} = *diameter of the major micro tool*, which equates to the channel width and W_L = *width of the land* (gap between channels). The above inequality is necessitated by the physical space available on the flow field area.

As long as these spacing limitations are not violated, evaluating changes to the design parameters is as easy as inputting alternate values and comparing the results.

7.2.2 Evaluating Alternative Designs

For the purpose of this section, three alternate designs are compared. These designs are all of the same type and pattern. The only difference is the channel width and number of channels. If narrower channels are used, it would naturally be possible to fit more channels into the same area. The inverse is also true for wider channels. The question is then: if the flow field area is kept constant, what effect would smaller or larger channel sizes have on the manufacturing time and cost?

To answer this question, three alternate designs are considered, the details of which are shown in **Table 20** below.

Table 20 – Flow Field Design Alternatives

Alternative	L_{Ch}	D_{major}	W_L	*Theoretical Maximum* N_{ch}	N_{ch}	$\frac{Channel\ Area}{Total\ Area}$
1	309	0.7	0.7	24.52	23	0.469
2	309	0.5	0.5	34.33	32	0.466
3	309	0.9	0.9	19.07	18	0.472

Alternative 1 represents the nominal case. That is, the current design of the bipolar plate. Alternatives 2 and 3 represent situations where slightly narrower and wider channels are used respectively. Further, correspondingly more or fewer channels are used. Still further, it is assumed that the land width is equal to the channel width. The number of channels chosen is done in such a manner so as to maintain the ratio of channel area to total flow field area. It is important to maintain the same ratio of channel area to land area for bipolar plate performance reasons. Section 2.2 details this issue.

There is a complication in applying alternatives 2 and 3 above. The near-optimal cutting parameters that were found in Section 7.1 apply to tools of diameter *0.7 mm*. If the same cutting parameters were applied to a smaller tool diameter (*0.5 mm* for example) the feed rate constraint would be violated. Conversely, if the same cutting parameters were applied to a larger tool diameter, sub-optimal performance would result. This is because, the smaller the diameter, the higher the feed rate necessary to maintain the same cutting parameters. To address this issue, the procedure followed in Section 7.1, is followed for the other sized tool diameters. That is, near-optimal cutting parameters are found, under certain machine constraints, for tools of size *0.5 mm* and *0.9 mm*. This is done using the simulated annealing algorithm. The results are presented in **Table 21** and **Table 22** for tools of diameter *0.5 mm* and *0.9 mm* respectively.

Table 21 – Cutting Parameters for Near-Optimal Solutions (D_{major} = 0.5 mm)

Machine Constraints		Cutting Parameters			Near-Optimal Solutions		Achieved Machine Values	
F_{R_Max}	n_{Max}	$v_{\_major}$	f_{t_major}	$d_{\_major}$	T_{CM_major}	C_{CM_major}	Achieved n	Achieved F_R
1100	60000	57.09	15.13	0.7	14.44	R 118.01	36343.92	1099.56
1200	60000	60.14	15.67	0.7	13.35	R 116.31	38283.26	1199.77
1300	60000	62.29	16.35	0.7	12.46	R 114.86	39657.72	1297.04

Machine Constraints		Cutting Parameters			Near-Optimal Solutions		Achieved Machine Values	
1400	60000	64.91	16.94	0.7	11.64	R 113.49	41322.16	1399.90
1500	60000	66.52	17.71	0.7	10.96	R 112.32	42350.88	1499.80
1600	60000	69.34	18.12	0.7	10.36	R 111.19	44141.18	1599.80

Table 22 – Cutting Parameters for Near-Optimal Solutions (D_{major} = 0.9 mm)

Machine Constraints		Cutting Parameters			Near-Optimal Solutions		Achieved Machine Values	
F_{R_Max}	n_{Max}	$v_{\_major}$	f_{t_major}	$d_{\_major}$	T_{CM_major}	C_{CM_major}	Achieved n	Achieved F_R
1100	60000	76.98	20.20	0.7	14.38	R 114.45	27226.03	1099.98
1200	60000	80.40	21.10	0.7	13.29	R 112.47	28435.90	1199.81
1300	60000	83.67	21.96	0.7	12.37	R 110.69	29592.49	1299.82
1400	60000	86.69	22.83	0.7	11.58	R 109.06	30661.55	1399.96
1500	60000	89.79	23.62	0.7	10.89	R 107.57	31757.64	1499.98
1600	60000	93.17	24.28	0.7	10.29	R 106.19	32953.38	1599.91

The different flow field designs, represented by alternative 1, 2 and 3 in **Table 20** above, can now be evaluated in terms of time and cost. Using the near-optimal cutting parameters, for each tool diameter, and assuming that the feed rate constraint is 1100 mm/min, the results shown in **Table 23** are obtained.

It can be seen from **Table 23** that the total manufacturing time is less for larger sized tool diameters. This is because larger tool diameters means that fewer channels can fit into the flow field area. In addition, the optimisation algorithm yields cutting parameters that try to maximise feed rate, regardless of the tool size. This results in the same feed rate being used for each design alternative.

In terms of manufacturing cost, it is intuitive that only labour and tooling cost are affected by design changes, considering how the cost model is formulated. The results shown in **Figure 43** indicate clear advantages in terms of labour and tooling costs when using larger tool diameters. Recall here that larger tool diameters correspond to wider channels. This essentially means that fewer channels can fit into the flow field area, evident by the effect on labour cost, in **Figure 43**.

Table 23 – Effect of Design Changes on Manufacturing Time and Cost

		Alternative		
		1	2	3
Alternative Parameters	v_{major}	68.34	57.09	76.98
	f_{t_major}	17.7	15.13	20.2
	D_{major}	0.7	0.5	0.9
	N_{ch}	23	32	18
Alternative Results	Material	R 408.00	R 408.00	R 408.00
	Labour	R 45.23	R 51.95	R 41.50
	Tooling	R 105.31	R 146.55	R 82.38
	Equipment	R 40.67	R 40.67	R 40.67
	Overheads	R 50.00	R 50.00	R 50.00
	Total Manufacturing Cost	R 649.21	R 697.16	R 622.56
	Total Manufacturing Time (min)	38.22	43.90	35.07

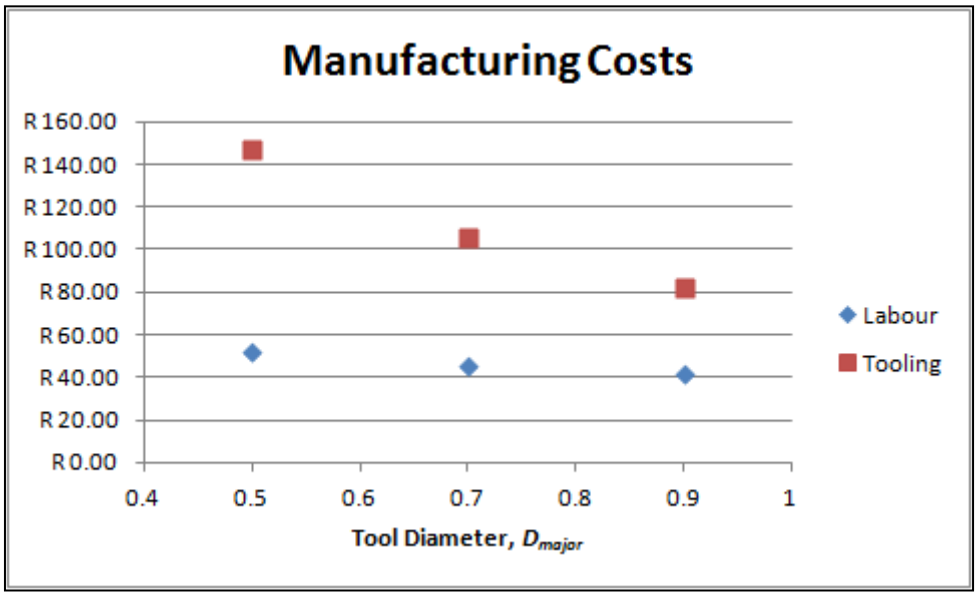

Figure 43 – Effect of Design Changes on Manufacturing Costs

The effect on tooling cost is especially significant. This is due to two main reasons. Firstly, if larger tool diameters are used then fewer channels need to be machined. Secondly, larger tools have a higher tool life, according to the tool life adjusting method, shown in **Equation (70)**.

From the analysis presented in this section, it can be concluded that employing the use of wider (and fewer) channels in the bipolar plate design can result in significantly improved manufacturing performance, in terms of both time and cost. However, as with all things, a holistic approach needs to be taken. What this analysis fails to address is the effect of wider channels on the operating performance of bipolar plates. This must also be considered before finalising the plate design.

7.3 Effect of Annual Production Volumes

In an ideal world, the bottleneck in a supply chain would not lie in the market. That is, a market would remain unsaturated and companies could sell as much as they can produce. In a competitive industry, however, market size dictates throughput. That is, companies can only sell as much as the market allows. Consequently, companies can (or should) only produce as much as they can sell.

In this regard, an analysis of the effect of production volumes on cost is really an analysis of the external market size on cost. This is a useful analysis because, following the explanation above, market size is one external factor that significantly influences manufacturing cost.

This section addresses this issue by modelling the effect of annual production volumes on unit production cost. This is done in two steps. Firstly, the approach taken in doing so is described. Secondly, the analysis is done using typical input parameters.

7.3.1 Production Volumes Analysis Approach

For the purpose of this analysis, two parameters are identified. These are AP_{total} and AP_{mach_max} where the former represents the total annual production for all machines combined and the latter represents the maximum annual production allowable per machine.

AP_{total} is dictated by the market demand, following the explanation above. An actual prediction of this value would involve a thorough market analysis and is outside the scope of this project. Rather, this section aims to perform a sensitivity analysis on this parameter by plotting its effect on manufacturing cost.

AP_{mach_max} is estimated subjectively by the manufacturer. This parameter represents the burden that the manufacturer is willing to put on any single machine. In Section 6.2.4, the theoretical maximum number of plates producible per machine was determined to be *2981 per year*. However, this value makes no allowance for maintenance down time (scheduled or unscheduled). Hence, a subjective value must be estimated for the maximum number of plates producible per machine. For the purpose of this analysis, three typical values are considered.

From AP_{total} and AP_{mach_max}, the number of machines required, N_{mach}, and actual number of plates per machine, AP_{mach}, can be determined as follows:

$$N_{mach} = \left\lceil \frac{AP_{total}}{N_{mach\_max}} \right\rceil \quad \textbf{(73)}$$

$$AP_{mach} = \frac{AP_{total}}{N_{mach}} \quad \textbf{(74)}$$

In traditional manufacturing economy theory, a similar approach can be taken to labour, whereby the number of employees required is a function of the annual production. As such the labour cost

would then be a stepped fixed cost, increasing when the requirements exceed the capacity. However, for the purpose of this cost model, this approach is not taken. This is because human resources are too versatile to assume that they have nothing to do if there is no immediate machining need. For example, if at any given time, there are workers who do not have any machining to do, they can direct their attentions to planned maintenance activities. In this case, the labour cost for this time must be assigned to maintenance cost and not manufacturing labour cost.

7.3.2 Production Volumes Analysis Results

For the purpose of this analysis, three separate values for N_{mach_max} are considered. These are 500, 1000 and 1500 and the results are shown in **Figure 44**, **Figure 45** and **Figure 46** respectively.

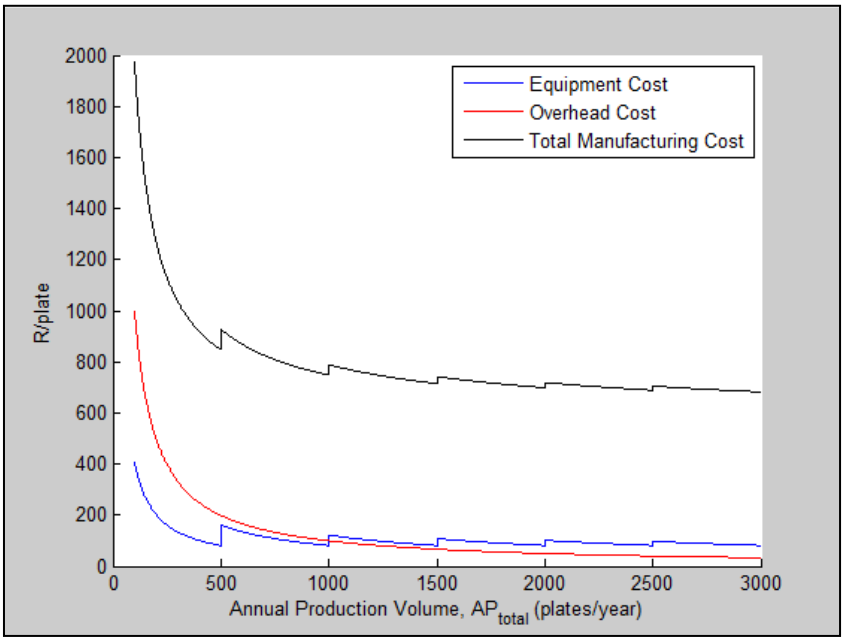

Figure 44 – Production Volumes Analysis, N_{mach_max} = 500

The figure above plots manufacturing costs as a function of annual production volumes with equipment cost indicated in blue, overhead cost indicated in red and total manufacturing cost in black. If $N_{mach\_max} = 500$, it essentially means that if production volume surpasses *500*, an additional machine is required. This provides the 'stepped' feature of the figures.

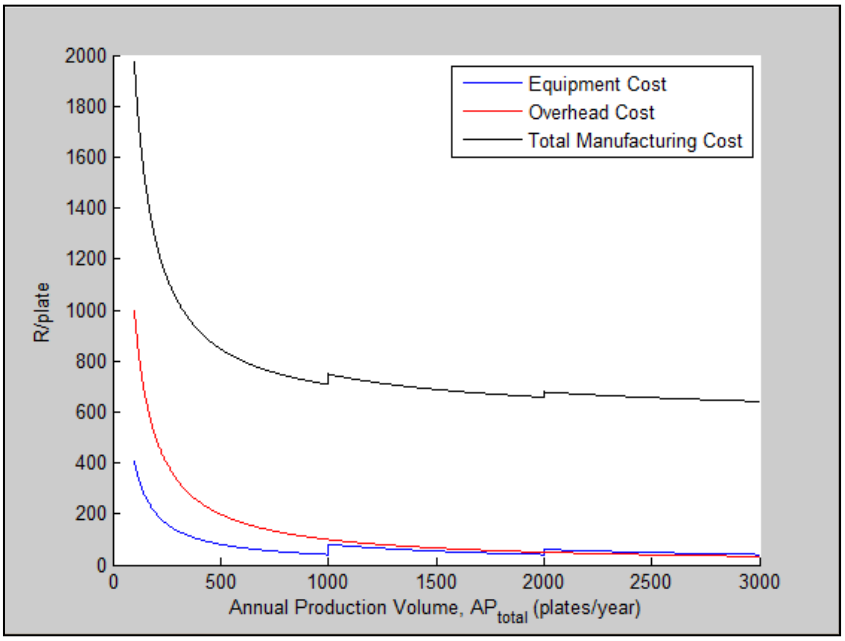

Figure 45 - Production Volumes Analysis, N_{mach_max} = 1000

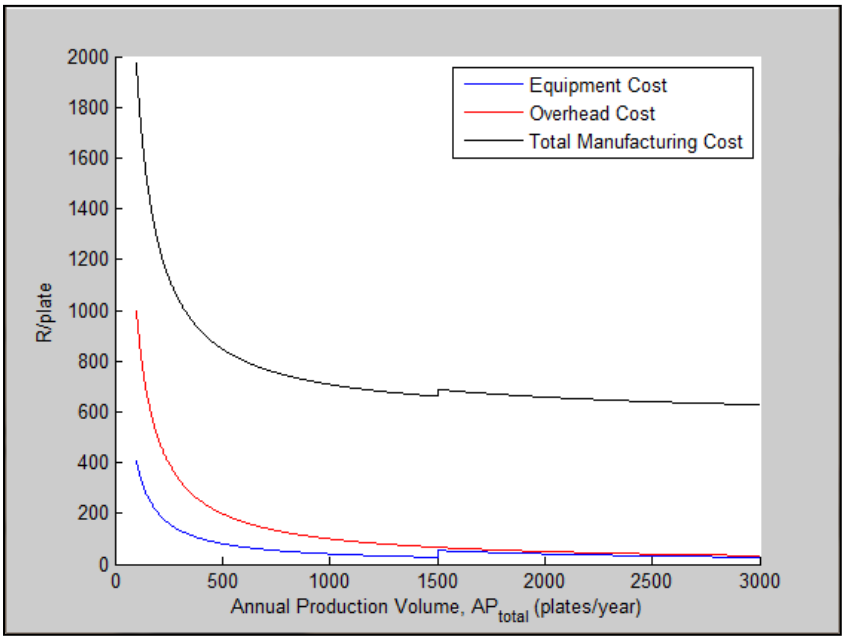

Figure 46 - Production Volumes Analysis, N_{mach_max} = 1500

The results of this analysis all indicate a similar downward trend in overall manufacturing cost as production volumes are increased. However, it does appear to be beneficial to make N_{mach_max} as large as possible. That is, to manufacture as many plates as possible on one machine, before requiring another machine. On the other hand, doing so creates additional burden on the micro milling machines. This could prove unwise in the long term depending on the maintenance characteristics of the machines.

8. Conclusions

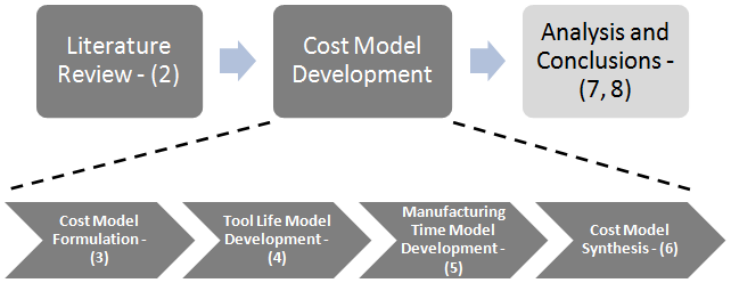

This section briefly summarises the work done in this project and provides some general insights based on the initial cost estimation results. Further, this section highlights the intrinsic and extrinsic value added. Still further, some limitations of the cost model are described after which possible future work is suggested based on the limitations described.

In South Africa, there is a strategic imperative to develop the capability to manufacture hydrogen fuel cell stacks locally. This comes in anticipation of a growing global hydrogen economy and South Africa's advantageous position as the leading platinum group metals supplier.

This project contributes to this need by building a framework to evaluate the manufacturing performance of the machining of bipolar plates; a major cost contributor in fuel cell stack production. This framework, otherwise known as a manufacturing cost model, allows the manufacturing performance in terms of time and cost, to be evaluated for a number of scenarios. These scenarios include, but are not limited to, alternative designs, machining technologies and annual production volumes.

The formulation of traditional cost models is data driven. That is, historical cost data are used to define cost estimating relationships which are collated into a cost model. This model, however, is not afforded this luxury because no historical manufacturing data is available. The approach taken was, therefore, a more fundamental one. That is, fundamental manufacturing knowledge and experimentation were used to develop cost estimating relationships, which in turn were collated into a cost model.

The result of this effort is a manufacturing cost model, which relates relevant input values to manufacturing times and costs.

As has been stated previously (several times) this project primarily provides the framework for future cost estimation. However, in building this framework and populating it with preliminary cost estimates, a general preliminary impression can be derived.

Considering the preliminary manufacturing cost results, from **Table 17** on page 104, it is plain to see that the main cost contributor is the material cost, $C_{Material}$, accounting for approximately *62%* of the

total manufacturing cost. For the purpose of this project, the material cost component has largely gone unaddressed. This is because its value is primarily influenced by external factors such as the exchange rate and the price charged by Schunk. Therefore, little can be done in terms of adjusting operational conditions to reduce this cost.

The reason for the relatively large material cost is that these blank plates must be compression moulded by Schunk. Therefore, all costs (and profits) associated with this process are absorbed into the price of these blank plates.

In theory, there should be little time difference between moulding the blank plates and moulding the complete plates with channels and peripheral features included. Therefore, the variable cost, excluding the cost to manufacture the compression mould, should be similar for the blank and complete components. This then begs the question: will it not be more cost effective to compression mould the complete plate locally? The answer to this question lies in the comparison of compression moulding and machining cost models. It is expected that machining will be more cost effective for small batch sizes while for mass-production type operations, compression moulding should be more effective. However, it should also be noted here that manufacturing a compression mould for blank plates is far easier and cheaper than a compression mould for complete plates.

Another consideration is the price discount that could be achieved if blank plates are ordered from Schunk in larger volumes. The material cost estimate used in this project is based on a small volume order (40 plates). Considering general economy-of-scale theory, it should be possible to reduce the material cost per plate by ordering larger volumes. However, this must be confirmed and negotiated with Schunk.

The value of the work completed in this project can be seen from both a practical and academic perspective. The academic value of this project is evidenced by its contribution to the literature. Consider the following:

- The work completed in Section 4, namely the tool life model development has been compacted into an article and accepted for publication in internationally reviewed conference proceedings. See Dirkse van Schalkwyk and Essmann (2011).
- In addition, the work completed in Section 7.1, is an adaptation of an article that has also been accepted for publication in peer-reviewed conference proceedings, although these proceedings have not yet been published (as on 30/1112011). See Essmann and Visser (2011).

The practical value of this project must be assessed in terms of its contribution to its underlying goal. That is, its contribution to the development of the capability to manufacture hydrogen fuel cells

locally. In developing the capability to do this; a few things remain to be discovered. These include but are not limited to:

- Knowledge of the correct manufacturing method to use.
- Knowledge of the effect of external factors on manufacturing performance for a given manufacturing method.

This project partly addresses both of these issues by the development of a cost evaluation tool. This tool is developed for one manufacturing method, which shows promise for this purpose, namely micro milling. Within the micro milling context, this cost model serves several purposes. The main purposes are as follows:

- It allows micro milling to be compared to other methods in terms of manufacturing performance for similar external influences. For example, provided a similar cost model exists for compression moulding, the total manufacturing cost for micro milling can be compared to that of compression moulding for a certain expected annual production. Since micro milling is expected to be preferential for small production volumes, this analysis would either confirm and quantify this theory or reject it all together.
- In addition, this model allows for the near-optimisation of the manufacturing performance for given operational conditions. This issue is addressed in part in Section 7.1. Further, for near-optimal performance, this model allows for a sensitivity analysis to be done, where the effect of other factors on manufacturing performance is quantified.

The approach taken in building this cost model is, to some extent, non-traditional since it is not based on historical cost data. Rather, this cost model is built from fundamental manufacturing knowledge and experimentation. The fact that this approach is non-traditional begs the question of the quality of it.

Following this, no statistical significance can yet be attached to the results of this cost model, This is because it is not based on historical cost data and no current cost data exists either. This is not an ideal situation because a lack of statistical significance means that no certainty is provided of the accuracy of the solution. The approach taken here, however, is the best that the author believes can be done without a pre-existing production setup where time studies can be performed and cost data collected.

Another consideration regarding the limitations of the model is the ‘manual’ nature of it. By this it is meant that cost inputs need to be entered manually. In an ideal situation, this model could be integrated with a costing system where changes to input costs could be updated automatically.

Careful attention needs to be paid to the cost input variables, because failure to account for changes to these values could distort the model output.

Another issue exists that could be considered a limitation of this project. This project is intended to form a cost model and not a comprehensive manufacturability study. Although the two are not exactly the same, there are elements which overlap. As such, cost models are often seen as partial manufacturability studies, as described by Schreve, et al. (1999), and mentioned in Section 3. What is lacking from this study, which one would expect from a comprehensive manufacturability study, is detailed analysis of how the plate will be manufactured and what quality level can be expected from this process. One example of this is found in the details of the tool life model, developed in Section 4. It should be recalled here, this model accounts for two types of tool failure, namely catastrophic and gradual. Catastrophic failure is easy to determined in-process by visual inspection. Gradual failure on the other hand is not. This type of failure occurs slowly and would typically require special equipment to monitor the tool status and detect failure upon occurrence.

Following the argument above, a comprehensive manufacturability study would follow naturally from the completion of this research. This study should address issues relating to quality, tool wear monitoring and workpiece holding in greater detail.

Another natural follow-on study from the completion of this work is a manufacturing methods comparison. More specifically, a comparison between compression moulding and micro milling should be undertaken. Using this cost model and a compression moulding equivalent, this study should address manufacturing performance in term of time and cost. In addition, the manufacturability of bipolar plates should be compared for each method.

9. References

Altintas, Y. (2000) *Manufacturing Automation: Metal Cutting Mechanics, Machine Tool Vibrations and CNC Design*. Cambridge: Cambridge University Press

Blank, L. and Tarquin, A. (2005). *Engineering Economy.* New York: McGraw Hill.

Boothroyd, G., Dewhurst, P. and Knight, W. (2002). *Product Design for Manufacture and Assembly 2nd ed.* New York: M Dekker.

Chae, J., Park, S.S. and Freiheit, T. (2005). Investigation of micro-cutting operations. *International Journal of Machine Tools and Manufacture Design, Research and Application*, 46 (3-4): 313-332.

Cho, E.A., Jeon, U.S., Ha, H.Y., Hong, S.A. and Oh, I.H. (2004) Characteristics of composite bipolar plates for polymer electrolyte membrane fuel cells. *Journal of Power Sources* 125: 178-182.

Coetzee, R, et al. (2007). *Strategy: micro-manufacturing strategy for south africa.* Advanced Manufacturing Technology Strategy.

Crow, K. (2000). *Achieving target cost/design-to-cost objectives.* [Online]. [Cited August 19, 2010]. http://www.npd-solutions.com/dtc.html

Curran, R., Raghunathan, S. and Price, M. (2004). Review of aerospace engineering cost modelling: the genetic causal approach. *Progress in Aerospace Sciences 40:* 487-534.

Dirkse van Schalkwyk, T., and Essmann E.C. (2011). The micro milling of bipolar plates - a tool life model. *ISEM 2011 Proceedings:* 102-1 - 102-13.

Dirkse van Schalkwyk, T., and Dimitrov, D. (2007). Mapping of repeatability, accuracy and energy use of a micro-milling machine in building a business case. *Proceedings of the 2nd International Conference on Micro-Manufacturing*: 314-317.

eFunda, Inc. (2010). *Milling.* [Online]. [Cited June 29, 2010]. http://www.efunda.com/processes/machining/mill.cfm

Ehmann, K.F., et al. (2004). I*nternational assessment of research and development in micro manufacturing*. World Technology Evaluation Centre (WTEC), Inc.

Essmann, E.C. and Visser, T.E. (2011). Solving a muli-objective micro milling problem using metaheuristics. *Proceedings of the 40th Annual Conference of the Operations Research Society of South Africa:* 124 - 136

Filiz, S., Conley, C.M., Wassermn, M.B. and Ozdoganlar, O.B. (2007). An experimental investigation of micro-machinibilty of copper 101 using tungsten carbide micro-end mills. *International Journal of Machine Tools & Manufacture*: 1088-1100.

Freivalds, A. (2009). *Niebel's Methods Standards, and Work Design12th ed.* New York: McGraw-Hill Companies.

Fuel Cell Markets. (2002). A*dvantages & benefits of hydrogen and fuel cell technologies.* [Online]. [Cited February 11, 2011]. http://www.fuelcellmarkets.com/fuel_cell_markets/5,1,1,663.html

Giebel, M. (2010). *Introduction to Target Costing.* Course material. Stellenbosch.

Gowthorpe, C. (2005). *Business Accounting and Finance for Non-Specialists, 2nd edition.* London: Thomson Learning.

Groover, M. (2008). *Automation, Produciton Systems and Computer-Integrated Manufacturing.* New Jersey: Pearson Education Incorporated.

Hermann, A., Chaudhuri, T. and Spagnol, P. (2005). Bipolar plates for PEM fuel cells: A review. *International Journal of Hydrogen Energy,* 30(12): 1297 – 1302.

HySA. (2009). *Hydrogen & Fuel Cell Technologies Research, Development & Innovation Strategy.* [Online]. [Cited February 9, 2011]. http://hydrogen.qsens.net/

HySA Systems. *HySA Systems*. (2009). [Online]. [Cited February 9, 2011]. http://hydrogen.qsens.net/centers-of-competence/hysa-systems

Larminie, J. and Dicks, A. (2002). Fuel Cells Systems Explained, Second Edition. West Sussex: John Wiley and Sons.

Lee, H.S., Chu, W.S., Kang, Y.C. and Ahn, S.H. (2007). Comparison of fabrication cost of composite bipolar plates made by compression molding an by machining. *International Conference on Computational and Experimental Engineering and Sciences,* 4(3): 195 - 200.

Li, H., Lai, X., Chengfeng, L., Feng, J. and Ni, J. (2007). Modelling and experimental analysis of the effects of tool wear, minimum chip thickness and micro tool geometry on the surface roughness in micro-end-milling. *Journal of Micromechanics and Microengineering*: 1-12.

Li, X, and Sabir, I. (2005). Review of bipolar plates in PEM fuel cells: Flow-field designs. *International Journal of Hydrogen Energy*, 30: 359-371.

Liu, X, DeVor, R.E., Kapoor, S.G. and Ehman, K.F. (2004). The mechanics of machining at the micro scale: assessment of the current state of the science. *Journal of Manufacturing Science and Engineering,* 126: 666-678.

Liow, J.L. (2009). Mechanical micromachining: a sustainable micro-device manufacturing approach. *Journal of Cleaner Production,* 17: 662-667.

Luke, S. (2010). *Essentials of Metaheuristics.*

Matsubabara, A., Kakino, Y., Ogawa, T., Nakagawa, H. and Sato, T. (200). Monitoring of cutting forces on end-milling for intelligent machine tools. *Proceedings of the 5th Internaltional Conference on Progress of Machining Technology*: 615.

Mayor, J.R. and Sodermann, A.A. (2009). *Investigation of the parameter space for enhanced tool life in high aspect-ratio full-slot micromilling of copper.* Unpublished manuscript.

McConnel, V.P. (2009). High-temperature PEM fuel cells: hotter, simpler, cheaper. *Fuel Cells Bulletin*.

Middleman, E., Kout, W., Vogelaar, B., Lenssen, J. and de Waal, E. (2003). Bipolar plates for PEM fuel cells. *Journal of Power Sources,* 118: 44-46.

Minitech Machine Corporation. *Products.* 2011. [Online]. [accessed October 30, 2011] http://www.minitech.com/mill.php?step=Step+1

Montgomery, D.C. and Runger, G.C. (2007). *Applied Statistics and Probability for Engineers 4th ed.* John Wiley & Sons.

Myers, R.H., Montgomery, D.C. and Anderson-Cook, C.M. (2009). *Response Surface Methodology: Process and Product Optimisation Using Designed Experiments, 3rd ed.* New Jersey: John Wiley and Sons.

Nam, D. and Hoon Park, C. (2010). *Multi-objective simulated annealing: a comparative study to evolutionary algorithms.* Unpublished manuscript.

Pellegri, A., and Spaziante, P.M. (1980). *Bipolar separator for electrochemical cells and method of preparation thereof*. United States of America Patent. 4197178.

PhysOrg.com™. (2008). *NIU engineers make micro-milling affordable*. [Online]. [Cited May 30, 2011]. http://www.physorg.com/news135436262.html

Prakash, J.R.S., Rahman, M. Senthil Kumar, A. and Lim, S.C. (2002). Model for predicting tool life in micro milling of copper. *Chinese Journal of Mechanical Engineering,* 15 sup: 115-120.

Prinsloo, L. (2011). *New think tank Mistra to probe potential benefits of fuel cell for SA*. [Online] [Accessed 18 March 2011]. http://www.engineeringnews.co.za/article/new-think-tank-mistra-to-investigate-benefits-that-sa-could-reap-from-fuel-cell-market-2011-03-18

Qin, Y. (2010). *Micro-Manufacturing Engineering and Technology*. Oxford: Elsevier.

Rahman, M., Senthil Kumar, A. and Prakash, J.R.S. (2001). Micro milling of pure copper. *Journal of Materials Processing Technology*: 39-43.

Schreve, K., Schuster, H.R. and Basson, A.H. (1999). Manufactruing cost estimation during design of fabricated parts. *Proceedings of the Institution of Mechanical Engieers,* 201(B): 731 - 735.

Schunk Kohlenstofftechnik GmbH. *Machined and Blank Plates.* (2011). [Online]. [Cited October 31, 2011]. http://www.schunk-group.com/en/sgroup/Blank-Plates-Machined-Plates/schunk01.c.42455.en

Shaw, M.C. (1995). Precision finishing. *Annuals of CIRP,* 44: 343 - 348.

Society of Manufacturing Engineers (SME). (1983). *Tool and Manufacturing Engineers Handbook, volume 1, Machining.* Dearborn: McGraw-Hill Book Co.

Sreeram, S., Senthil Kumer, A., Rahman, M. and Zaman, M.T. (2006). Optimization of cutting parameters in micro end milling operations under dry cutting conditions using genetic algorithms. *International Journal of Advanced Manufacturing Technology, 30*: 1030-1039.

Steward, R.D., Wyskida, R.M. and Johannes, J.D. (1995). *Cost Estimator's Reference Manual.* New York: Wiley and Sons.

Talbi, G. (2009). *Metaheuristics: From Design to Implementation.* New Jersey: John Wiley & Sons.

Tansel, I., Rodriguez, O. Trujillo, M. Paz, E. and Li, W. (1998). Micro end milling - I. Wear and breakage. *International Journal of Machine Tools & Manufacture,* 38: 1419-1436.

Tsuchiya, H. and Kobayashi, O. (2004). Mass production cost of PEM fuel cell by learning curve. *International Journal of Hydrogen Energy,* 29(10): 985 - 990.

Verseput, R. (2000). *Digging into DOE*. [Online] [accessed May 4, 2011] http://www.qualitydigest.com/june01/html/doe.html

Watkins, D.S., Dircks, K.W. and Epp, D.G. (1991). *Novel fuel cell fluid flow field plate*. United States of America Patent. 4988583.

Watkins, D.S., Dircks, K.W. and Epp, D.G. (1992). *Fuel cell fluid flow field plate*. United States of Ameria Patent. 5108849.

Williams, E.D., Ayres, R.U. and Heller, M. (2002). The 1.7 kilogram microchip: Energy and material use in the production of semiconductor devices. Environmental Science and Technology, 36: 5504 - 5510.

Zaman, M.T., Rahman, M., Kumar, A.S. and Sreeram, S. (2004). Effect of engagement arc of tool life in micro end miling operations. *Proceedings of the 3rd International Conference in Advanced Manufacturing Technology,* 49.

Appendix A Material Properties for FU 4369 HT

The following data sheet is provided courtesy of Schunk Kohlenstofftechnik GmbH (2011)

Grade FU 4369 HT

Data Sheet

Schunk Kohlenstofftechnik GmbH
Rodheimer Strasse 59
35452 Heuchelheim, Germany
research.skt@schunk-group.com
www.schunk-group.com

Bulk density	(g/cm³)	1.90
Flexural strength	(MPa)	40
Compressive strength	(MPa)	50
Young's modulus dynamic flexural	(GPa)	 24 10
Hardness Rockwell HR10/40		100
Thermal conductivity	(W/mK)	55
Coefficient of thermal expansion α 20 - 140 °C (70 - 285 °F) xy in plane z through plane	(10^{-6}/K)	 15 38
Specific electrical resistance xy in plane z through plane	(µΩm)	 90 190
Heat deflection temperature	(°C / °F)	210 °C / 410 °F

bos 04.08

The data shown above are not guaranteed, but typical values based on our experience. It should be understood that a spread of results can occur due to variations in materials and production processes.

Please find the standards for the determination of our material properties at
www.schunk-group.com/skt/dm

schunk Group

Appendix B Additional Tool Life Experiment Results

This appendix presents the results of the additional tool life experimentation performed for the purpose of this project. The idea with the additional experiments was to determine a method of transforming the original tool life model (valid for tools of a 0.7 mm diameter) into one that is valid for other sized tool diameters. Two methods were tested to compare the predicted tool life to the actual recorded tool life. These methods are as follows:

Method 1	**Method 2**
$L_T^* = L_T \times \frac{D^*}{D}$	$L_T^* = L_T \times (\frac{D^*}{D})^2$

where L_T^* *= adjusted tool life (mm^3),* L_T *= original tool life for 0.7mm tool diameter (mm^3),* D^* *= new tool diameter* and D *= original tool diameter (D = 0.7 mm)*.

Six additional experiments were carried out. Three of which using a tool of diameter 0.5588 mm and three using a tool of diameter 0.7248 mm. The tool life of each additional experiment was recorded, using the procedure described in Section 4.2.2.3, and compared to the predicted values for both methods of prediction. It can be determined that Method 1 yields the better result.

Method 1: LT* = LTx(D*/D)

Run	Cutting Speed (v)	Feed/tooth (ft)	Depth (d)	Diameter = 0.5588				Diameter = 0.79248			
				Point Prediction	Actual TL CL	Actual TL VMR	% Difference	Point Prediction	Actual TL CL	Actual TL VMR	% Difference
1	56.621	13.040	0.565	3139.660	8377.550	2644.307	15.78%	4452.609	8644.528	3869.617	13.09%
11	70.000	10.000	1.100	8105.546	12097.590	7436.147	8.26%	11495.138	5136.745	9412.470	18.12%
13	70.000	17.500	0.200	769.486	8328.598	930.804	-20.96%	1091.271	6085.952	964.599	11.61%

Method 2: LT* = LTx(D^2)

Run	Cutting Speed (v)	Feed/tooth (ft)	Depth (d)	Diameter = 0.5588				Diameter = 0.79248			
				Point Prediction	Actual TL CL	Actual TL VMR	% Difference	Point Prediction	Actual TL CL	Actual TL VMR	% Difference
1	56.621	13.040	0.565	2466.876	8377.550	2644.307	-7.19%	4961.478	8644.528	3869.617	22.01%
11	70.000	10.000	1.100	6368.643	12097.590	7436.147	-16.76%	12808.868	5136.745	4477.844	65.04%
13	70.000	17.500	0.200	604.596	8328.598	930.804	-53.95%	1215.988	6085.952	964.599	20.67%

C

Appendix C Detailed Cost Breakdown for Initial Equipment Cost Estimate

This Appendix presents the itemised cost breakdown for the initial equipment cost estimate of Section 6.2.4. This breakdown is as follows:

Item	**Description**	**Price (USD)**
Frame	Mini-Mill/3	12,000
Spindle	NSK 3000	4,300
Workpiece Holding	Vacuum Table System	1,016
Controller	Cntrl 4	1,450
Accessories	Enclosure 3/GX	2,800
Software	VisualMill Std	999
Import and Install	-	1,400
Total Equipment		23,965

These items and prices, apart from the workpiece holding and import and assemble costs, are obtained from Minitech Machine Corporation (2011) on 30/10/2011. The workpiece holding and import and installation cost are estimated from the author's experience.

D

Appendix D Visual Representation of the Tool Life Model

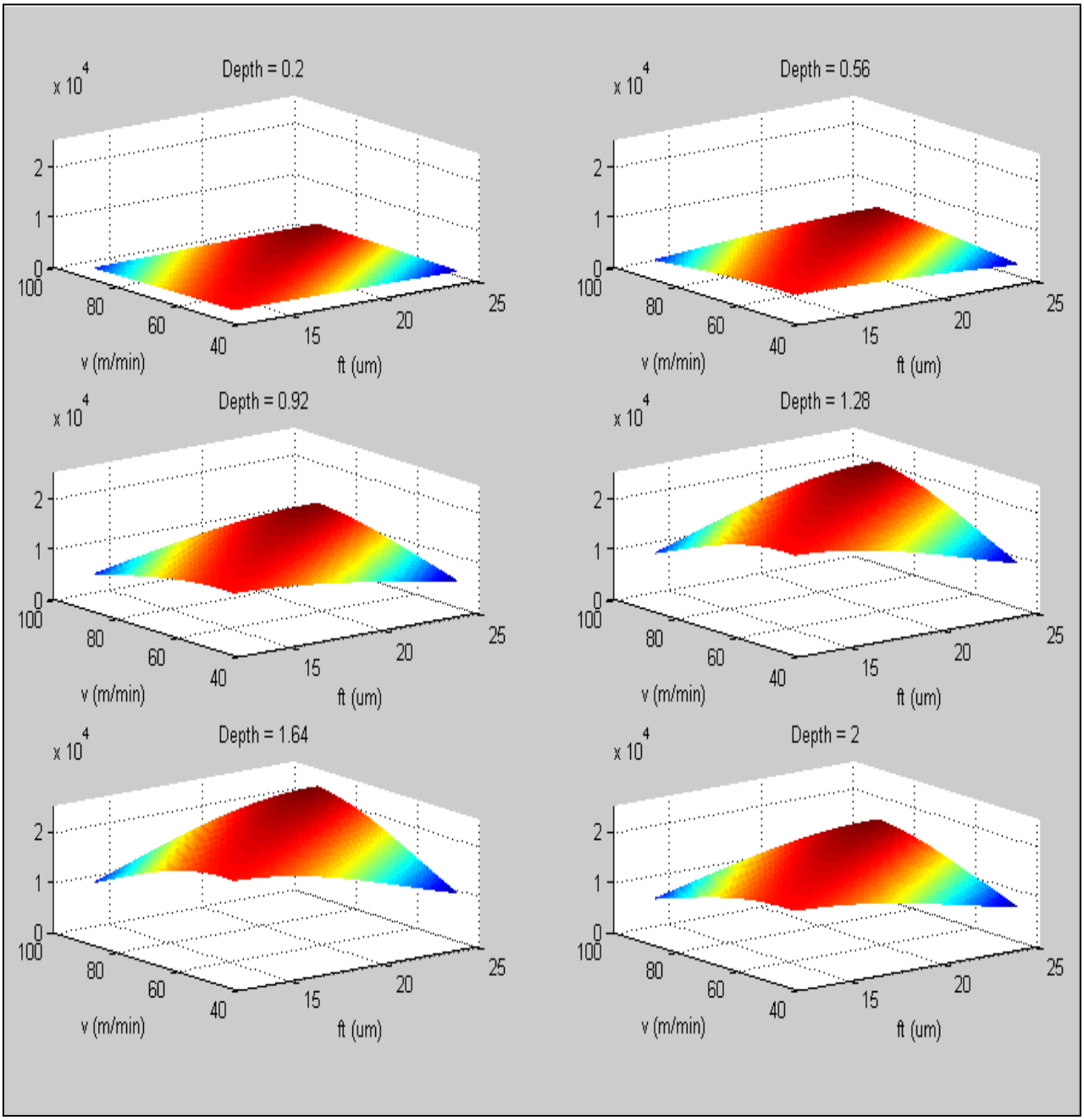
Depth = 0.2
Depth = 0.56
Depth = 0.92
Depth = 1.28
Depth = 1.64
Depth = 2
x 10^4
v (m/min)
ft (um)

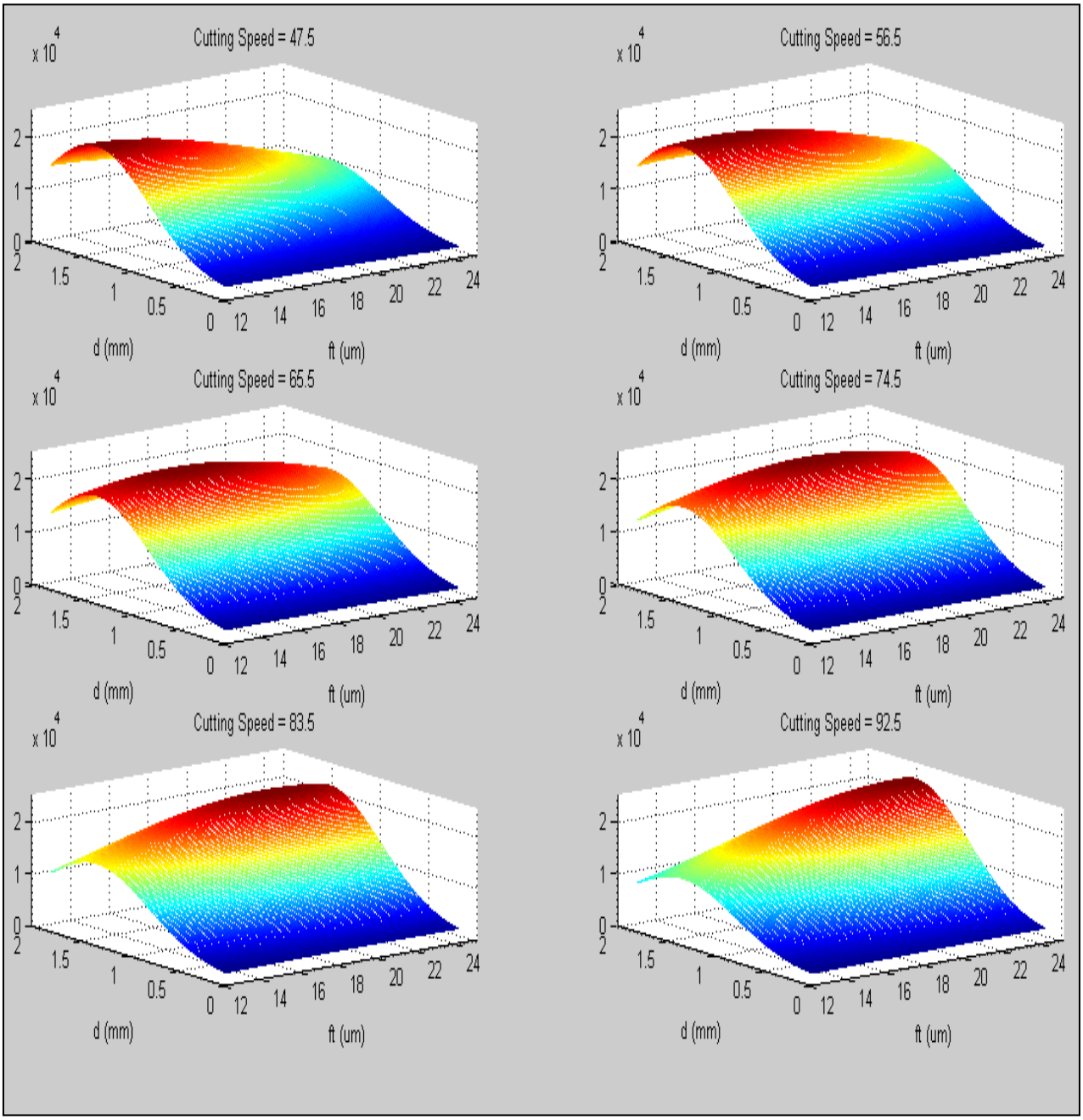
Cutting Speed = 47.5
Cutting Speed = 56.5
Cutting Speed = 65.5
Cutting Speed = 74.5
Cutting Speed = 83.5
Cutting Speed = 92.5
x 10^4
d (mm)
ft (um)

E

Appendix E Personal Note

The application of a number of concepts and techniques was necessitated by the natural progression of this project. It was, therefore, necessary to research, learn about and understand these concepts before they could be applied. To describe the steps involved in doing so would require an additional thesis. Rather, short descriptions of the main lessons learned are discussed presently:

- The literature review, of Section 2, sees an overview of seemingly unrelated fields of interest. In researching these, much was learned. Perhaps the most pertinent lesson is that every piece of research, whether it is in the form of an article or handbook, must be driven by an underlying business need. Without this, the financial incentive to further the research would be absent. Therefore, identifying lucrative research fields of the future is really an exercise in identifying future market needs and business drivers.
- In formulating the cost model, in Section 3, it was necessary to define the structure of the eventual cost model. In approaching this task typical manufacturing cost breakdowns were investigated. Evident from this investigation was the effect that different breakdowns had on the estimated cost. That is, the way in which cost is calculated can, at times, significantly affect the estimated cost. As a result, good business judgement must be used in determining the appropriate cost breakdown structure.
- The tool life model of Section 4 came with many and difficult challenges. These ranged from choosing the appropriate experimental design to correctly defining and measuring tool life. Perhaps the most important lesson in this regard was that with enough focused thought and research, all challenges can be overcome, whether they are practical or academic.
- Section 5 involved abstract thinking and modelling to build the manufacturing time model. This again relates to the absence of an existing production line. Therefore, theoretical time models needed to be developed that represent the way in which bipolar plates would typically be machined.
- Synthesizing the cost model, as done in Section 6, saw the coming together of the previous work. This required taking a systems approach in integrating various sub-models/formulae.
- Finally, the analysis performed in Section 7 required the application of certain, sometimes complex, techniques, which needed to be researched and understood before doing so. This, too, was a steep learning curve.

Overall, perhaps the most valuable lesson was that of the *'donut principle'.* That is, the principle that it is necessary to understand the w*hole* as well as the *hole* of the donut. Only in understanding both of these aspects can one fully grasp the complexity of a donut.

Similarly, this project required understanding of a range of aspects with varying levels of abstraction. These included understanding the 'ins' and 'outs' of the separate components such as the tool life

model, the encapsulation of these components into a cost model as well as the role of the cost model in its broader context. This idea speaks to the very core of industrial engineering thinking. That is, the combination of analytical and systems thinking.